9-1-2016

The Role of Citrullination and the Type III Intermediate Filaments in Retinal Gliosis

John Wizeman
University of Connecticut, wizeman@uchc.edu

The Role of Citrullination and the Type III Intermediate Filaments in Retinal Gliosis

John William Wizeman, Ph.D.

University of Connecticut, [2016]

Abstract: Visual disorders are a massive economic and personal burden. Two leading causes of blindness in the United States, Glaucoma and Age-Related Macular Degeneration (AMD), currently have no cure [1, 2]. A major secondary issue in these diseases, often untreated, is the development and ongoing presence of scars in the eye [2, 3, 4]. While scarring is a byproduct of the wound healing process [5], this scarring in the eye can lead to blindness [6, 7]. In the retina the scarring process is a result of ongoing retinal gliosis, mediated by the structural Müller glial cells [8, 9, 10]. Two well-characterized markers of this process are the cytoskeletal Intermediate Filament (IF) proteins vimentin and the glial fibrillary acidic protein (GFAP), which become overexpressed as a stress response [11, 12]. Importantly, interfering with the soluble, non-cytoskeletal forms of these two proteins with the small molecule withaferin A (WFA) has anti-proliferative [13] and anti-migratory effects [14, 15], two cellular processes integral to scarring [16, 17, 18]. As with many other proteins, GFAP and vimentin can be regulated by a number of different post-translational modifications (PTM). One PTM which the IF proteins are subjected to is citrullination [19].

Here, I have identified citrullination as an injury-induced response in the retina. Increases in citrullination are seen as early as 1 day after injury. This citrullination occurs along GFAP and vimentin filaments. I have identified two sites on GFAP that are citrullinated after retinal injury. The enzyme responsible for this injury-induced citrullination in the retina was PAD4. The citrullinated form of GFAP was targeted initially in a retinal explant system by the pan-PAD inhibitor Cl-amidine using an intravitreal injection model. The treatment decreased the levels of GFAP protein indicating a reduction of the gliotic phenotype. These findings mimicked what was seen in a mouse model of glaucoma, the DBA/2J mouse line. In this system, changes in citrullination within the glaucomatous eyes preceded changes in GFAP protein levels. These findings identify citrullination of GFAP as a major response to

injury in the retina, mimicking the disease pathology of glaucoma. The ability to target these proteins within the retina, initially, and in the whole eye with an intravitreal injection to reduce a major gliotic marker has implications for the future development of therapeutics for treating the often undiagnosed gliosis associated with retinal disorders.

The Role of Citrullination and the Type III Intermediate Filaments in Retinal Gliosis

John William Wizeman, Ph.D.

B.S., Saint Michael's College, [2008]

A Dissertation

Submitted in Partial Fulfillment of the

Requirements for the Degree of

Doctor of Philosophy

at the

University of Connecticut

[2016]

APPROVAL PAGE

Doctor of Philosophy Dissertation

The Role of Citrullination and the Type III Intermediate Filaments in Retinal Gliosis

Presented by

John William Wizeman, Ph.D.

Major Advisor _____

Royce Mohan, Ph.D.

Associate Advisor _____

Elisa Barbarese, Ph.D.

Associate Advisor _____

Stephen J. Crocker, Ph.D.

Associate Advisor _____

Betty A. Eipper, Ph.D.

Associate Advisor _____

Zhao-Wen Wang, Ph.D.

University of Connecticut

[2016]

Acknowledgements

I would first and foremost like to thank my thesis advisor, Dr. Royce Mohan, for his unending support throughout my time in his lab. I have learned an incredible amount from him. In five years, we have had discussions and debates about every aspect of life, from science and training to politics and culture and beyond. His guidance has helped me in not only honing my scientific skills but in time management and helping me to learn how to focus properly in more ways than I can recount on paper. From our first conversation at recruitment weekend to our last in the lab, it was always good to have someone whose interest in science could drive interesting and lively discussion about new ideas, and helped remind me why I wanted to undertake this process. I also want to thank Dr. Paola Bargagna- Mohan, with whom I have been fortunate to share a lab space for the past five years. Paola has always been willing to discuss scientific techniques and tips, as well as many other topics during my time in the lab. Paola and Royce have been my lab family for a long time, and their ever-present guidance and support will be missed as I move on in my career. I hope to make them proud as a scientist.

I would also like to thank the members of my thesis committee who helped me in shaping a more focused project from a more broad initial interest early in graduate school. Dr. Elisa Barbarese, Dr. Stephen Crocker, Dr. Betty Eipper, and Dr. Zhao-Wen Wang were instrumental in keeping the efforts for this project on task and clear, and for that I am extremely grateful. I was also fortunate to do a rotation with Dr. Barbarese, and would also like to thank her for guidance during that time.

I would also like to thank the Neuroscience Department at UConn Health, including Dr. Mains, for support throughout my time here. The office, including Jody Gridley, Anna Sagan, Diana Mikulak and Mary Nordgren have been extremely helpful in answering what I'm sure at times felt like an endless onslaught of questions. I also want to thank the Biomedical Science Ph.D. program at UConn, specifically Dr. Barbara Kream and Dr. Lynn Puddington, who were helpful during my time on the GSO. I also want to thank Stephanie Rauch and Dorothy Linhoff for their help during this time.

Of course, I would like to thank my wife, Kate Ely Wizeman, for her support. For five years she has gracefully helped me through many different trials. Through sleepless nights, anxiety and fear,

frustration, and a number of hours where I could only stare at the computer screen, she has helped keep me tethered to the world beyond graduate school. I have known her for 12 years, and during this time I have yet to meet someone more selfless, more caring, more loving, more devoted than her. She has always had more patience than anybody, and that was indescribably important to me as I finished graduate school. We have been fortunate to be married for four of the five years in this time, bought a house, got a dog, and will soon welcome our first child into the world. I cannot think of anyone I could possibly hold in higher esteem, or love more, than Kate. I am genuinely lucky to have met and married such a wonderful person.

I want to thank my immediate family for their support during this time, including their understanding when I was short or irritated after long and frustrating days of experiments in the lab. My mother has been supportive through my entire life, and I think that sometimes she does not understand how important she has been to me. I can only hope the work in this thesis will have made her proud. I am also lucky to have two sisters who have been supportive over the past five years (and more). Whether through making meals, or through simple conversations, they have been invaluable throughout graduate school. I also have three nephews, Tate, Cooper, and Gordon, who I was thrilled to help welcome into the world. I met the oldest the day before I started graduate school, and celebrated his fifth birthday the day after I defended this thesis. They have been a joyful part of my life in that time. Lastly, I want to thank my father, who unfortunately passed a few short months before this thesis was completed from multiple glioblastoma. Although he was not able to see its completion, his passing reminds me daily that although sometimes our bench research may not seem to be making headline grabbing breakthroughs, everything we do is to benefit the sick, the dying, those losing hope. Every small victory at the bench is a major step in relieving that pain, frustration and fear that those facing untreatable illnesses face daily.

I want to also thank my in-laws, Dr. Matthew Ely and Susan Ely, for their tremendous support and help throughout graduate school. Kate and I could not have possibly gotten through the past five years without their help, including their generosity in opening their home to us as we moved back to

Connecticut from Boston. From watching the dog, to helping with meals, to everything else they have given us, I am extremely grateful for their positive influence on my life.

I would lastly like to thank the friends who I have been fortunate to share both triumphs and troubles with during my time in graduate school. This includes many students in the graduate program, as well as the students of the neuroscience graduate program, who often share a sense of camaraderie. Specifically, Kyle Denton, Maegan Gross, and Bhavita Walia have been very good friends for the past 5 years, and I look forward to even better times beyond graduate school as we all move on in our careers.

Table of Contents

List of Figures

List of Abbreviations

AD – Alexander Disease
AMD – Age-Related Macular Degeneration
CNS – Central Nervous System
DAPI – 4',6-Diamidino-2-Phenylindole
ERK – Extracellular Signal Regulated Kinase
EAE – Experimental Autoimmune Encephalomyelitis
GCL – Ganglion Cell Layer
GFAP – Glial Fibrillary Acidic Protein
IF – Intermediate Filament
IOP – Intraocular Pressure
INL – Inner Nuclear Layer
IPL – Inner Plexiform Layer
MBP – Myelin Basic Protein
MS – Multiple Sclerosis
NFL – Nerve Fiber Layer
ONL – Outer Nuclear Layer
OPL – Outer Plexiform Layer
PAD – Peptidylarginine Deiminase
PTM – Post-Translational Modification
RA – Rheumatoid Arthritis
TGF-β2 – Transforming Growth Factor Beta 2
UPP – Ubiquitin Proteasome Pathway
Vim – Vimentin
WFA – Withaferin A

Chapter 1

Introduction

1.1 Overview

Visual disorders are a massive economic and personal burden. Two of the leading causes of blindness in the United States, Glaucoma and Age-Related Macular Degeneration (AMD), currently have no cure [1, 2]. A major secondary issue in these diseases, often untreated, is the development and ongoing presence of scars in the eye [2, 3, 4]. While scarring is a byproduct of the wound healing process [5], this scarring in the eye can lead to blindness [6, 7]. It can occur in the cornea and the retina, and closely resembles the scarring seen after injury to these tissues [20]. In the retina the scarring process is a result of ongoing retinal gliosis, mediated by the structural Müller glial cells [8, 9, 10].

Müller cells are the major glial cells in the retina [8, 21]. Müller cells stretch the entire width of the retina, come into contact with all neuronal subtypes [22], and are the reactive cells in retinal gliosis [8]. Two well-characterized markers of this process are the cytoskeletal Intermediate Filament (IF) proteins vimentin and the glial fibrillary acidic protein (GFAP), which become overexpressed as a stress response [11, 12]. The absence [23, 24, 25, 26, 27] or overabundance [28] of these two proteins in glial cells alters overall tissue health in response to injury the CNS. Importantly, interfering with the soluble, non-cytoskeletal forms of these two proteins with the small molecule withaferin A (WFA) has anti- proliferative [13] and anti-migratory effects [14, 15], two cellular processes integral to scarring [16, 17, 18].

The function of the soluble forms of these IF proteins and what roles they have in scarring highlight the importance of understanding the multiple ways this pool of IF proteins is regulated. As with many other proteins, GFAP and vimentin can be regulated by a number of different post-translational modifications (PTM). While phosphorylation of the IF proteins has been studied extensively [29, 30, 31] and is known to be important in controlling the levels of soluble and cytoskeletal IF protein [32], it is only one of several PTMs that can alter this balance [31]. Another PTM which the IF proteins are subjected to

is citrullination [19]. Citrullination is a relatively understudied PTM that functionally removes a positive charge and disrupts the polymerization of GFAP and vimentin [33].

Citrullination is becoming known as a disease related process [34]. Increased levels of citrullinated GFAP are present in brains of Multiple Sclerosis (MS) [35, 36] and Alzheimer's Disease (AD) patients [19], and citrullinated vimentin is a major biomarker of rheumatoid arthritis severity [37]. Interestingly, total levels of citrullinated proteins are increased in both AMD [38] and glaucomatous eyes [39]. This increase of disease related citrullination in ocular disorders which can include a scarring pathology [4, 40] and the effect that citrullination has on the solubility of the IF proteins [33] is not known. In my thesis, I will demonstrate that citrullination occurs on the intermediate filaments in the retina during retinal gliosis, and identify the specific enzyme(s) responsible for citrullination of GFAP. Finally, using small molecule inhibitors, I will demonstrate that citrullination can be reduced in an injury model.

1.2 Visual Disorders and Scarring

Visual disorders encompass a broad range of conditions that interfere with the ability of the eye to sense light and transmit signals to the brain (Fig. 1-1). They also represent a large economic burden, and dramatically diminish the quality of life in the people they affect, often irreversibly [41, 42]. These disorders can affect numerous different parts of the eye. For instance, Age-Related Macular Degeneration (AMD) is a deterioration of the macula, the major light-sensing region of the retina [43], while glaucoma is a condition damaging the optic nerve that is often due to disruptions in the normal maintenance of pressure in the eye [44]. The cornea, at the anterior aspect of the eye, is also subject to a number of different types of injuries. These injuries, such as chemical injuries [45] can penetrate different tissues and, by causing the cornea to lose its transparency, prevent light from reaching the retina. The retina is also subject to injuries, whether secondary to corneal injury [45, 46] or directly to the retina as in blast injury [20, 47]. Unfortunately, each of these injuries can lead to an irreversible blindness.

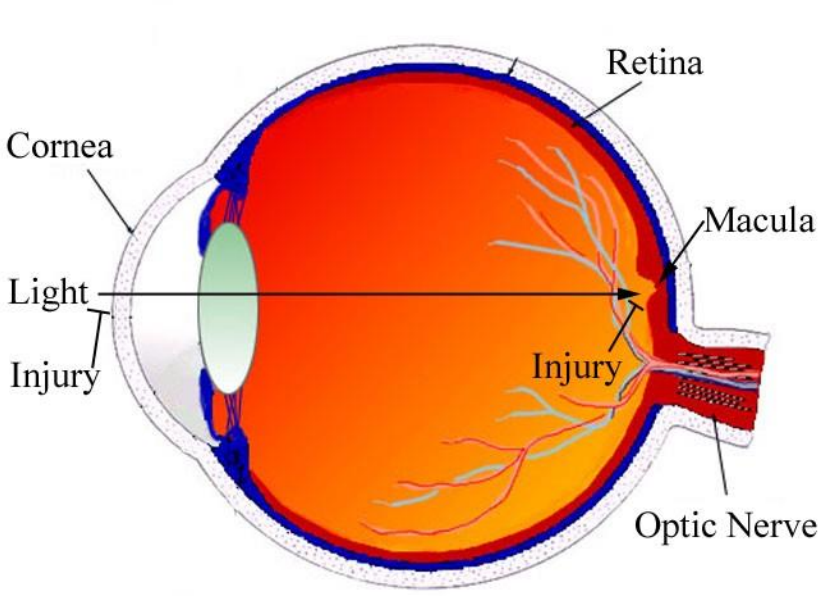

Figure 1-1. The Path of Light through the Eye

Light travels through the cornea and ultimately becomes focused onto the macula, within the retina. Light is converted to an electrical signal and transmitted to the brain through the optic nerve. Injury at the cornea obstructs the path of light to the retina. Injury to the retina or optic nerve can either obstruct light reception in the retina or prevents transmission of electrical signals to the brain. Modified from [48].

In these ocular conditions, a major secondary factor is the development of a chronic debilitating scar [4, 40]. This scarring is a progressive pathological consequence of cells attempting to heal the injury site to provide support to surviving cells and prevent the spread of damage [49]. In the cornea and retina this scarring can lead to the prevention of normal ocular function [6, 7]. In the cornea, this scarring is a result of fibrotic processes that leaves the cornea opaque and incapable of properly transmitting light. In this process, corneal keratocytes develop into fibroblasts to be able to fill the wound left from injury, and eventually differentiate into myofibroblasts, which cause the opacity that can lead to blindness [50].

In the retina, scarring can occur in several different locations depending on the pathological trigger. Scars can be caused by proliferation of Müller cells into the subretinal space, leading to a subretinal scar (Fig. 1-2). These subretinal scars occur between the neural retina and the retinal pigment epithelium (RPE), which in turn can lead to retinal detachments similar to those seen in proliferative vitreoretinopathy (PVR) [51]. These detachments can be treated surgically, but have a high rate of recurrence [51]. At the site of interaction between the vitreous and the retina, the vitreoretinal surface, scars are often formed by process extension along the retinal surface and into the vitreal space [40, 52] (Fig.1-2). These cell processes are extensions of Müller glial endfeet, normally a part of the inner limiting membrane of the retina in the layer of axons that connect the retina to the brain. The process extension is driven by increases in GFAP and vimentin expression within the cell. These vitreal scars, called epiretinal membranes, are also found in the aging eye, with their presence more frequent and their size increased in patients with AMD. As new data suggest that Müller glia may also work as a kind of "optical fiber" to deliver light correctly to the photoreceptors [53], such scars on the vitreal surface not only disrupt the normal architecture of the retina but can also alter the path light takes through to the photoreceptors.

Both subretinal and epiretinal scars are generated through Müller glial reactivity [17, 40]. While the Müller glia are responsible for maintaining normal retinal homeostasis, their reactive nature in injury and disease creates problems leading to blindness. This reactivity, called retinal gliosis, is an attempt to stabilize the retina after injury, but frequently leads to disruptions of normal retinal function when gliosis

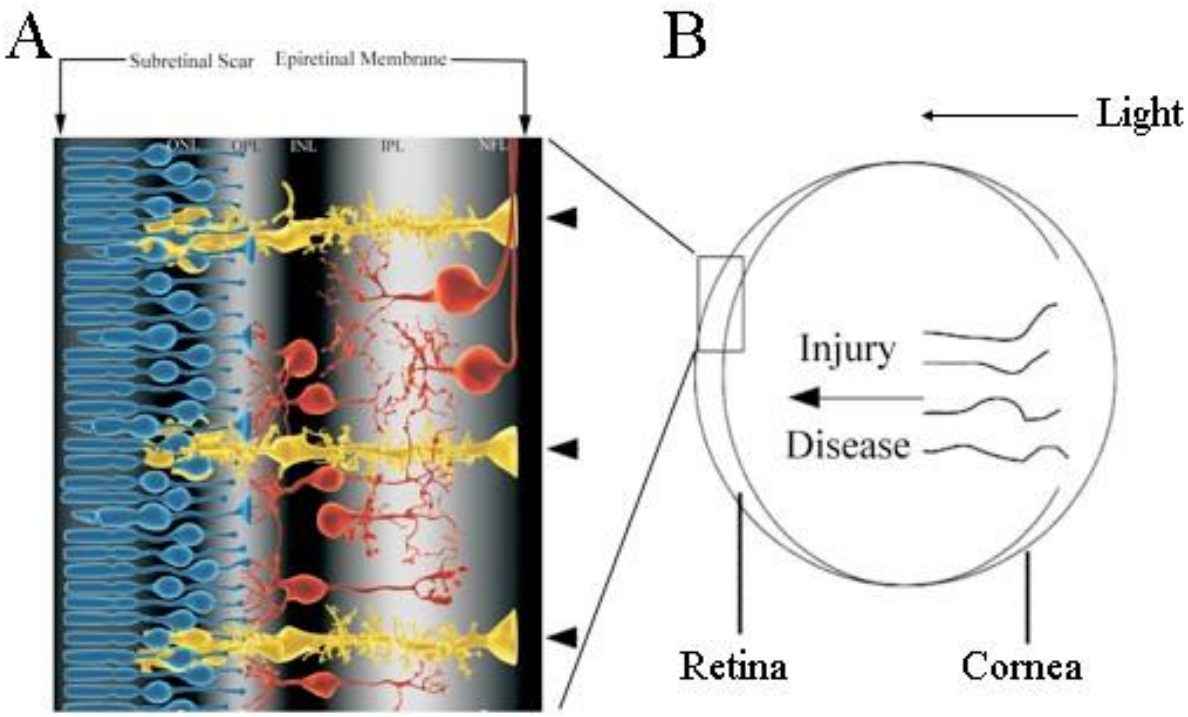

Fig. 1-2. Anatomy of Retina and Location of Scars.

(A) Muller glial cells (yellow) come into contact with all neuronal subtypes (red) and photoreceptors (blue) to provide support. (B) In injury or during disease, the cornea and the retina react and can form scars. Muller glial cells can proliferate to form subretinal scars or extend processes to form epiretinal membranes, impeding the transmission of light to the photoreceptors. Modified from [54].

becomes chronic. Controlling the negative aspects of chronic gliosis could lead to therapeutic improvements [13].

1.3 Retinal Gliosis and IF Proteins in Müller Glial Cells

The majority of visual disorders affecting the retina have an underlying gliosis [22]. This process is very similar to the gliosis seen in the rest of the central nervous system. While reactive astrocytes are responsible for gliosis in the brain [55], in the retina the majority of the reactivity is due to the Müller glial cell. Müller glia are the structural cells of the retina, spanning the entire width of the retina and coming into contact with every neuronal cell type. In an uninjured state, the Müller glia provide homeostatic support to all the neuronal subtypes [22]. They contribute to the maintenance of the blood- retinal barrier, control retinal pH, and are thought to be involved in the cone visual cycle [22, 56]. In response to pathological changes in the retina, the Müller glia become reactive. This reactivity involves both general and specific changes. The general changes are present regardless of the type of pathology, and include the upregulation of vimentin and GFAP in Müller cells. The specific changes depend on the type of insult to the retina, but also result in alterations to normal Müller cell function.

Experimental models to study Müller cell reactivity include chemical injuries, mechanical manipulations, laser and light injuries, and genetic models [17, 57, 58, 59, 60]. In experimental retinal detachments, retinas injected with an experimental marker for Müller cell nuclei were proliferative, with nuclei migrating along vimentin filaments towards the photoreceptors, where they presumably go on to form glial scars [17]. In a genetic mouse model in which Müller glial cells overexpress human Bcl2 [57], Müller cells undergo increased and early apoptosis. In this apoptotic retina, photoreceptors become detached from the RPE. Subsequently, the photoreceptors begin to die after Müller glial cells die, highlighting the importance of the Müller glia for the maintenance and health of photoreceptors. In a genetic mouse model of glaucoma (DBA/2J mice), several iris proteins are mutated, resulting in increased

intraocular pressure and damage to the optic nerve [58, 59]. This model system shows Müller reactivity, indicated by increased GFAP expression early in pathology [60]

Retinal gliosis has recently been identified an associated process in chemical injuries, such as experimental corneal alkali injury [13]. This mimics the clinical condition [45], which is also accompanied by increases in intraocular pressure (IOP) [61]. In this system, regulators of Müller glial cell cycle are altered to allow for proliferation. Cyclin D3 and PCNA are increased, while p27kip1 is decreased following injury [62, 13]. The use of withaferin A (WFA) in the alkali injury model, a small molecule known to bind soluble forms of the IF proteins, returned the expression of these markers to patterns seen in the uninjured eye as visualized by immunohistochemistry, in a vimentin-dependent manner. Importantly in this model both the cornea and the retina undergo scarring, and the use of WFA is able to show clinically relevant improvements to both tissues, emphasizing the importance of the intermediate filament proteins [13, 15]

1.4 IF Proteins in Scarring and Fibrosis

The intermediate filaments are a large class of proteins that are categorized by their sequence similarity [63, 29]. They are the type I and type II keratins, the type III IFs including GFAP, vimentin, desmin, syncoilin and peripherin, the type IV lamins, the type V neurofilaments and the type VI proteins, restricted to the lens [for review 63, 64]. GFAP and vimentin are the main IF and cytoskeletal proteins in glial cells of the central nervous system. Both proteins are present in reactive Müller glia.

GFAP and vimentin are known to play major roles in the normal scarring. The role of the IF proteins in scarring is becoming increasingly important in retinal health, and insights into these roles frequently come from knockout mice. Vimentin and GFAP knockout mice show no apparent phenotype in an uninjured state and develop normally [25]. However, these mice show changes in injury response. Fibroblasts from vimentin knockout (vim-KO) mice [65] are impaired in their ability to fill in a scratch wound in culture, and contract collagen more slowly, in part due to a disrupted actin cytoskeleton. In the

adult vim-KO mice subject to full-thickness dermal injury, fibroblasts exhibit a delayed differentiation into myofibroblasts, again showing a disruption in the actin cytoskeleton compared to similarly injured wild-type mice [66]. In GFAP and vimentin double knockout mice subjected to stab wound in the brain, glial scars were significantly less dense and bled more frequently than seen in wild type mice. In lesioned hippocampal sections, IF protein double knockout mice also displayed significantly shorter process extension compared to wild type controls, and this absence of intermediate filaments in astrocytes resulted in the greater loss of synapses after lesion [27].

In the retina, the absence of GFAP and vimentin in experimentally detached retinas frequently led to tearing near the vitreoretinal surface, and these retinas were subject to more tearing during normal handling [23, 24]. Retinas deficient in GFAP and vimentin are also more accepting of transplanted retinal cells. When retinal cells from P0 mice were injected into wild type adult mice, the cells did not migrate away from the injection site and showed limited neurite growth, while reactive gliosis was observed within the weeks following transplantation. In the IF protein double knockout mice, however, retinal cell precursors migrated and were able to extend neurites, occasionally as far as the optic nerve [26]. The integration and extension of neurites in this knockout system places an emphasis not only on experimental methods that could be employed to control IF proteins, but identifies the regulation of these proteins as integral injury response to any clinical attempt to regenerate retinas with vision loss.

While the formation of glial scars and the integration of neuronal precursors seems to be dependent on the cytoskeletal form of the IF proteins in these systems, recent work has identified the soluble, non-cytoskeletal form of these proteins as an integral target for clinically relevant improvements. Previous findings discovered that targeting soluble vimentin with WFA improves outcomes in several clinically relevant model systems representing injury to the eye. In addition to the improvement in retinal gliosis observed by WFA binding in the alkali injury model mentioned above [13], WFA was able to target vimentin in both a corneal fibrosis model and a glaucoma model of fibrosis [67]. In the corneal fibrosis model, treatment with WFA decreased levels of smooth muscle actin, as a marker of myofibroblast differentiation and conversion to a fibrotic phenotype. It also improved corneal

transparency, a key feature of overall corneal health [15]. In a rabbit glaucoma model, treatment with WFA led to a decrease in cell proliferation, and altered the survival of aqueous filtration blebs, displaying improved drainage of fluid in the eye in glaucoma [67]. The discovery that soluble forms of the IF proteins are targets for clinically relevant improvements in these systems, and that WFA can bind these soluble forms, highlights the importance of understanding the soluble IF proteins. Recent research has identified novel roles for these soluble IF proteins, which is discussed below.

1.5 Roles of Soluble IF Proteins

Biochemical examination of GFAP and vimentin was initially difficult, as they are often considered insoluble under normal physiological conditions. Many of their physical properties can be altered by different conditions, such as salt concentration or pH. High salt concentrations and high pH (>8.4) drives polymerization [68] of the IF proteins. For this reason, the insoluble, long filaments were the best studied for a long time. The traditional solubilization of the intermediate filaments requires the use of 8M urea, with lower concentrations leading to dimerization and tetramerization and the inability to isolate filamentous forms [69, 70, 71].

The ability to extract soluble IFs using a low salt buffer [72] led to the identification of tetrameric vimentin as a basic vimentin subunit in normal cells. It also allowed for the approximation of the ratio of soluble to insoluble in a non-pathological state. Approximately 90-95% of the pool of these proteins falls into the insoluble fraction in a physiological state [72], while 5-10% is soluble. Importantly, the extraction of soluble forms of vimentin has led to important discoveries about how the soluble pool is regulated differently from the insoluble fraction. The difficulty of investigating the soluble form of IF proteins in isolation from the cytoskeletal forms has only recently been overcome through the use of molecular biology tools [73, 74]

Soluble vimentin has several important functions that are non-cytoskeletal. Closely related function to its role in the cytoskeleton, soluble vimentin is extremely important for lammellipodia

formation [73] by forming the leading edge of processes in fibroblasts. In lamellipodia of fibroblasts there is a distinct lack of filamentous vimentin, while small vimentin particles can be clearly seen. Additionally, when vimentin filaments were forcibly broken down after the addition of a mimetic peptide, which inhibits vimentin filament assembly [73, 75], lamellipodia like structures were increased. Soluble vimentin also plays a very important role as a chaperone for the transport of kinases to the nucleus. Soluble vimentin in injured neurons was shown to transport the activated form of extracellular signal- regulated kinase (ERK) to the nucleus 76] through direct binding to importin-β and transport toward the nucleus through interaction with dynein. Recent work has also shown that in vimentin knockout mice, translocation of pERK to the nucleus was impaired [77]. Additionally, vimentin is differentially phosphorylated in corneal myofibroblasts, and they maintain higher levels of vimentin in the soluble pool compared to fibroblasts [77]. This phosphorylation makes vimentin more sensitive to WFA treatment than the unphosphorylated form. This interplay also affects the interaction of vimentin with ERK, and as a result, WFA also blocks ERK nuclear translocation. Ultimately, these changes in phosphorylation of vimentin impaired cell spreading in these cells as a result of the disrupted interaction between soluble vimentin and the focal adhesions necessary for rearrangement during the spreading process, an important finding with regards to cell migration. Vimentin may also serve as a scaffold for other signaling transduction molecules, as β-3-adrenergic receptor signaling was significantly reduced following breakdown of vimentin filaments [78]. Mutated soluble GFAP binds portions of the proteasome to disrupt normal proteolytic function [79], often leading to GFAP containing aggregates. As discussed above, the use of WFA to bind soluble GFAP in retinal gliosis led to improvements in tissue health at 7 days [13].

The functions of soluble IF proteins are often overlooked in favor of the cytoskeletal functions when examining reactive conditions such as gliosis. With increasing knowledge about the roles of the soluble IF proteins and the impact they have on tissue health, however, the production, maintenance, and regulation of this soluble pool become important avenues of research for therapeutic developments, specifically in ocular health.

1.6 IF Protein Regulation

Filaments are highly conserved in structure, with all IFs containing an N-terminal head domain, a C-terminal tail, and an alpha-helical rod domain. While the head and tail domains can differ greatly, the rod domain is very highly conserved [80]. This rod domain is further structured into coiled-coil and linker domains [81]. The rod domain is critical to the filamentous structure of the protein, as the rod domains interact to hold together polymers of intermediate filaments [82]. All type III IFs have a conserved cysteine [13], which is believed to be important as a sensor of the cellular environment. When vimentin was incubated with zinc, polymeric structures were able to form, while blocking this cysteine resulted in an increase in soluble vimentin [83]. Additionally, when vimentin deficient cells were transfected with a construct modifying cysteine to serine, filamentous networks were incapable of forming. Corroborating evidence from experiments with WFA, disruption of this cysteine decreased cell spreading, as measured by cytoplasmic area. Interestingly, magnesium was seen to compete with zinc in vimentin binding, with zinc being preferentially bound, even at levels too low to induce polymerization. This implies a role of this cysteine, and its control by zinc, in the maintenance of homeostatic levels of soluble vimentin as well as in the polymerization into filaments.

The head and tail domains of vimentin are known to modulate other interactions, including the diameter of the filament and its formation beyond dimers and tetramers, as seen by electron microscopy [69]. When the head domain was deleted, only aggregates of dimers and tetramers were found, despite the use of polymerizing conditions. Deletion of the tail domain displayed IFs of mixed diameter, mostly larger than normal. This interaction of the tail likely helps to compact the filaments to 10 nm through interactions with the rod domains between antiparallel dimers [84]. The head and tail domains are also responsible for interactions with other proteins [85].

The highly conserved nature of the IF structure is important for the interactions which regulate the formation of the filamentous forms of the IF proteins. As outlined in figure 3, the IFs GFAP and vimentin are translated as monomers (1-3A) and quickly form parallel dimers (1-3B), directly interacting

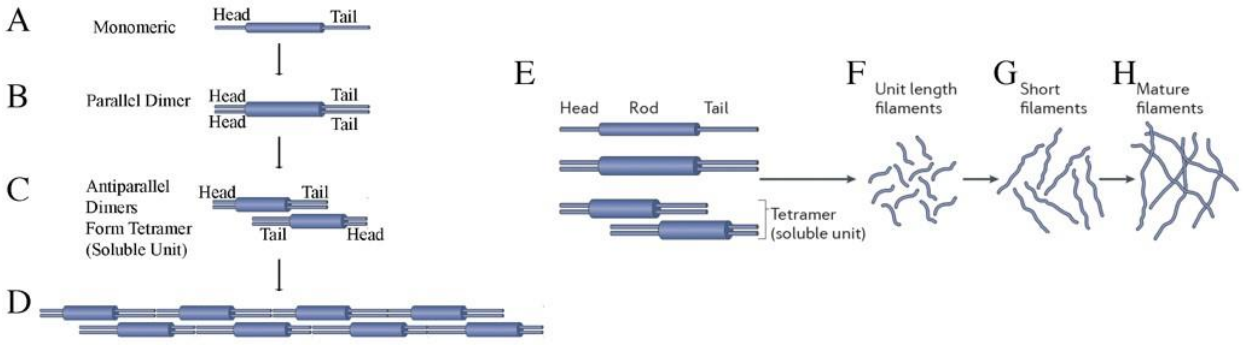

Figure 1-3. Formation and Assembly of Intermediate Filament Polymers

The assembly of intermediate filaments takes place in a stepwise fashion. Initially polarized monomers are translated (A), and quickly form parallel dimers (B). Two dimers then interact in an anti-parallel fashion to form a tetramer, the basic soluble subunit under physiological conditions (C, E). 8 dimers interact to form a unit length filament (D, F). These unit length filaments go on to form short filaments, or "squiggles" (G) and long polymers to form the cytoskeleton (H). Modified from [31].

through their rod domains. This dimer then interacts in an anti-parallel fashion with another dimer to form a tetramer (1-3C, E). This tetramer is considered a soluble unit, as it is the most basic unit that exists in the physiological state. Eight tetramers form a unit length filament (1-3D,F) [31], which can interact with other unit length filaments to form short filaments which appear as "squiggles" (1-3G) [86] or the long, 10nm thick filaments that have been described in most studies (1-3H). Unlike the polar addition of subunits to actin and tubulin cytoskeletons, the intermediate filament cytoskeletons can incorporate subunits bilaterally along their length [81].

While the production of the IF proteins is controlled at the transcriptional and translational level and their turnover is controlled by several processes, the formation of filaments and the maintenance of the soluble pool of IF proteins, as well as the balance between these two, is regulated by a number of different post-translational modifications [31, 77, 32].

The majority of studies into the transcriptional regulation of GFAP and vimentin have focused on the alternative splicing and isoforms of GFAP [87]. Vimentin transcription and translation is thought to involve only one mRNA product from the vimentin gene [88]. While vimentin and GFAP both have major isoforms (Fig. 1-4, 1-5), GFAP is alternatively spliced into at least 8 different isoforms, with different developmental distributions (Table 1) [87]. Studies into the localized translation of GFAP [89] are limited, although there is some evidence that mRNA can be localized to astrocytic processes. Specifically, it is known that the GFAP alpha isoform can be found in the processes [90]. Studies about the upregulation of GFAP and vimentin protein in disease states usually refers to the canonical isoforms of each IF family member, although the isoforms are also further subjected to post-translational modifications. The major GFAP isoform, GFAP alpha, is the isoform of interest in this thesis.

The intermediate filaments are subject to several types of proteolytic processing, including caspase and calpain cleavage, as well as ubiquitination. The calpain cleavage fragments are often seen in western blots, as it creates a distinct degradation pattern [92]. Caspase cleavage can cause GFAP fragments that promote aggregation [93]. As with many other proteins, IFs are also degraded by the ubiquitin proteasome pathway (UPP), and therefore ubiquitination is one mechanism by which IFs are

Table 1. Intermediate filament proteins in astrocytes and reactive gliosis. Modified from [91]

Astrocyte IF protein	Expression in reactive astrocytes	Protein length (aa)		Transcript
	Mouse/human	Mouse	Human	
GFAPα	Increased/increased	430	432	Exon 1–9 (canonical)
GFAPβ	Increased/increased	Unknown[#]	Unknown[#]	Alternative upstream start site
GFAPγ	Increased/[***]not expressed	Unknown[#]	Unknown[#]	Lacks exon 1, includes the last 126 bp of intron 1
GFAPδ[*]	Increased/increased	428	431	Exon 1–7a
GFAPκ	Increased/increased	433	438	Exon 1–7b
GFAPξ	Increased/increased	Unknown[#]	Unknown[#]	Includes last 284 bp of intron 8–9
GFAPΔ135[**]	Below detection/increased	385	387	Part exon 6 deleted
GFAPΔ164[**]	Not expressed/not clear	368	366	Part exon 6 and exon 7 deleted
GFAPΔexon6[**]	Below detection/not clear	341	347	Exon 6 deleted
GFAPΔexon7[**]	Increased/increased	400	406	Exon 7 deleted

[*] GFAPδ is also known as GFAPε.

[**] Splice forms were expressed, full length sequences were not experimentally determined but were based on *in silico* cloning.

[#] Only partial but specific mRNA sequences were quantified, full length is unknown.

regulated in cells. Mutated GFAP interacts frequently with portions of the UPP, altering the proteasomal ability to degrade proteins [79]. Interestingly, this is not the only interaction between IFs and the UPP that can disrupt normal function. The E3 ligase responsible for tagging the IFs for proteasomal degradation is gigaxonin [94]. Mutations in gigaxonin cause giant axonal neuropathy, and it was found that IF degradation is found to be impaired in this situation [74]. Similarly, the E3 ligase parkin is the most common mutated protein in inherited forms of Parkinson's Disease [95], indicating that the UPP and its normal function, which can be altered by dysregulated IFs, can be a factor in a number of neurodegenerative conditions.

The intermediate filaments are subject to a large number of post-translational modifications. The best studied of these is phosphorylation [96], but they are also subject to ubiquitination, farnesylation, sumoylation, and acetylation [31]. IF proteins are also increasingly identified with the disease related PTM citrullination. Each of these PTMs is a form of regulation that alters the dynamics of the IF proteins in the cell. Studies of phosphorylation have highlighted the importance of these modifications on the function of the IFs.

Phosphorylation of the intermediate filaments is very well studied, and is an important regulator of the assembly of the long polymeric filaments that make up the cytoskeleton [32, 77, 77, 97]. A number of different sites on both GFAP and vimentin are specifically phosphorylated [77, 97] (Fig. 1-4, 1-5). Two vimentin phosphorylation sites, Ser-38 and Ser-72, are known to inhibit the polymerization of vimentin when phosphorylated [32, 77]. Vimentin is phoshporylated by a number of different kinases, including Protein Kinase A [98, 33], Protein Kinase C [99, 33] Calcium/Calmodulin-dependent kinase II [100], among others. Phosphorylation in the head domain of GFAP protects against protein turnover [97]. Phosphorylation of vimentin at Ser-38 also sensitizes myofibroblasts to treatment with the IF targeting molecule WFA. In the ocular system, phosphorylation of vimentin controls the regulation of lens growth, as mice with vimentin phosphorylation sites mutated showed cataract like symptoms and a dramatic reduction in lens volume [101].

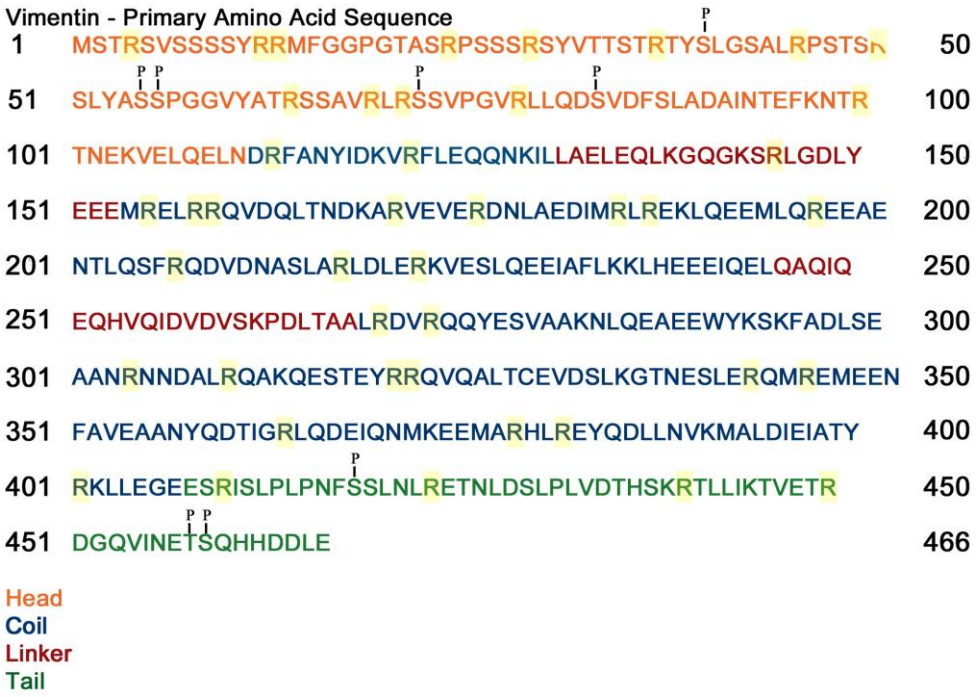

Figure 1-4 Primary Amino Acid Sequence of Human Vimentin

The primary amino acid sequence of human vimentin. Arginines are highlighted in yellow as potential citrullination sites. Several phosphorylation sites involved in filament assembly are identified (P-). Residues within the head domain are represented in orange, residues in the rod domain are represented in blue and red, and residues in the tail domain are represented in green.

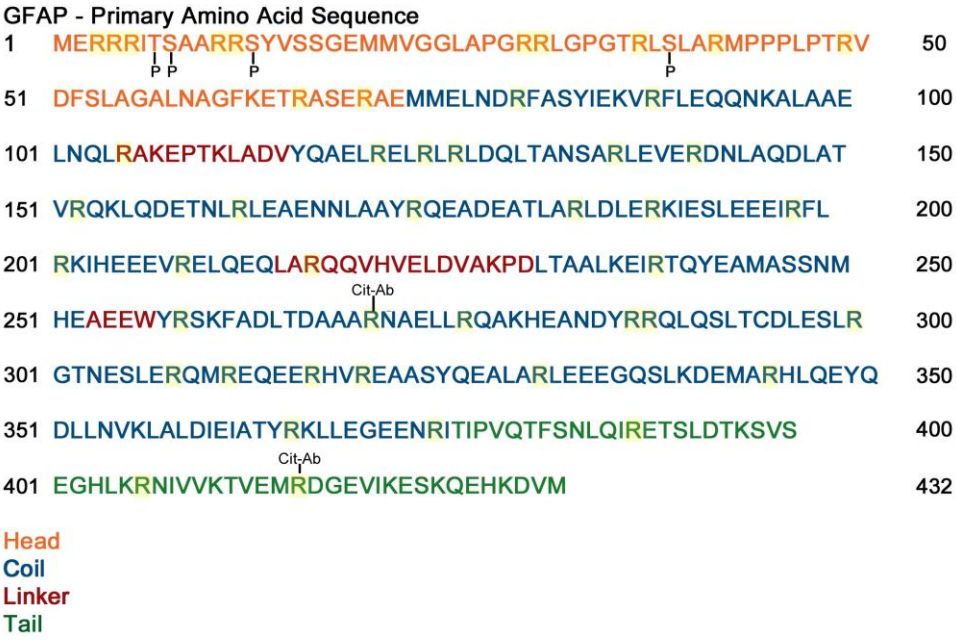

Figure 1-5 Primary Amino Acid Sequence of Human GFAP Alpha

The primary amino acid sequence of human GFAP alpha isoform. Arginines are highlighted in yellow as potential citrullination sites. Several phosphorylation sites involved in filament assembly are identified (P-). R270 and R416 are recognized by antibody CTGF-1221. Residues within the head domain are represented in orange, residues in the rod domain are represented in blue and red, and residues in the tail domain are represented in green.

Although phosphorylation is the best studied PTM with regards to the IF proteins, citrullination of the intermediate filaments is becoming acknowledged as important as an increasing number of neurodegenerative diseases are discovered to be associated with citrullinated GFAP and vimentin. Although there are relatively few studies identifying distinct effects of this PTM on GFAP and vimentin, insights from the modification itself, the enzymes responsible, and inhibitors of those enzymes have established methods to study the role of citrullination in injury and disease.

1.7 Citrullination and the IF proteins

Citrullination

Citrullination, or deimination, is a post-translational modification targeting peptidylarginine. So named due to its original isolation from *Citrullus lanatus* (watermelon) [102], citrulline is a non-standard amino acid for which there is no corresponding tRNA [34]. It can be found as either free citrulline as a byproduct of nitric oxide production, or as peptidylcitrulline after conversion by a family of enzymes known as peptidylarginine deiminases, referred to as PADs. Citrullination of peptidylarginine is a hydrolytic process that requires calcium as a cofactor and creates ammonia as a byproduct (Fig. 1-6). In mammals, the process is carried out by five members of the same enzyme family. These are PADs1-4 and PAD6. For all active PADs, the level of calcium required for activity is significantly higher than physiological levels [103].

PAD enzymes

The PADs are a family of five closely related and conserved enzymes that vary in their activity and tissue expression [34, 103]. Their presence is conserved among mammals, but other vertebrates have varying levels of PAD genes present [103]. They are all found in the same gene cluster [105], but have different tissue expression.

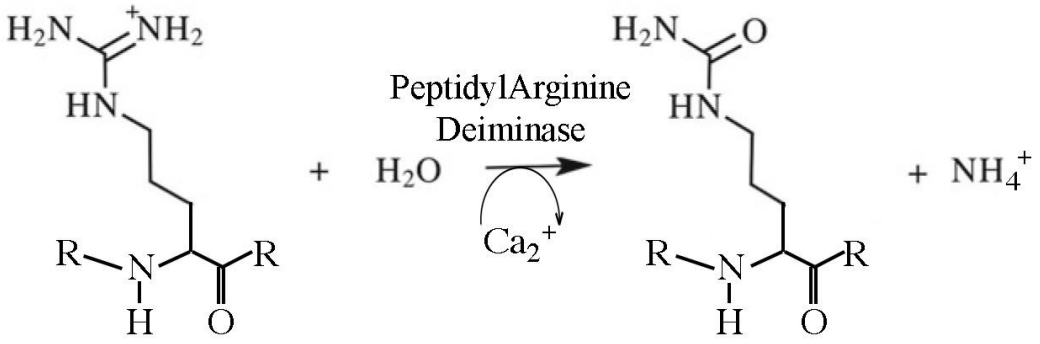

Figure 1-6. The Citrullination Reaction

Citrullination is the process by which peptidylarginine is converted, through the calcium-dependent family of enzymes known as PADs, into peptidylcitrulline, releasing ammonia as a byproduct. Peptidylcitrulline has a net neutral charge compared to the net positive charge of peptidylarginine.

PAD1 is found most abundant in the layers of the epidermis [106]. It has been most well studied in regards to its function in keratinocytes [107], where it is thought to citrullinate the keratin K1 [106], and is thought to play a role in psoriasis [108]. Studies into other tissues, such as spleen, kidney, and CNS tissues have not shown PAD1 expression, indicating its expression and function is limited to the epidermis and uterus and limiting interest in models of CNS disease and injury.

PAD2 is often considered the most broadly expressed PAD enzyme, being found in a number of different tissues. It was originally isolated from skeletal muscle, pancreas, and spinal cord [107]. It has since been identified in brain [109, 110, 19, 111], spleen and kidney [112]. PAD2 expression is also found in the retina, and is increased in Age-related Macular Degeneration eyes [38]. Importantly, it is known to citrullinate vimentin [113] and myelin basic protein (MBP) [114]. PAD2 knock-out mice [112] appear to show no difference in the multiple sclerosis (MS) mouse model of experimental autoimmune encephalomyelitis (EAE) [115] when clinical scores were compared to wild-type, even though PAD2 appeared to be responsible for the citrullination of proteins in this system. Some controversy exists as to the responsibility of PAD2 in this system, as some citrullinated MBP was reported when checked by a second group [116]. Other methods of PAD knockdown have shown changes in this system, discussed below. Overexpression of PAD2 [117] caused a severe phenotype in skin, with lesions that were positive for a number of tumor markers, including increased IL6 and IL8 levels. Interestingly, PAD2 overexpression increased levels of vimentin within a skin cancer cell line as well. Similarly, it was found in a breast cancer cell line to have bound histones and play a role in gene regulation [118].

PAD3 is often found in skin and hair [106, 119], as well as in mammary glands [120] and peripheral nerves 121]. In the epidermis it is thought to citrullinate several proteins [106, 122, 119]. Recently, it has been found in human neural stem cells [123], where it was shown to inhibit neural stem cell growth and disrupt the vimentin cytoskeleton. This was reversed with the use of the pan-PAD inhibitor Cl-amidine.

PAD4 is found often in immune cells, such as macrophages, lymphocytes and neutrophils. There, it is involved in the mass citrullination of histones to release chromatin [124]. This is possible because

PAD4 is the only PAD with a known nuclear localization sequence, although PAD2 has also been localized to nuclei [118]. Several PAD4 knockout and PAD4 low strains have been developed [112, 125, 126]. Mice survive, indicating that PAD4 absence is not embryonic lethal, but PAD4 may have some embryonic role, as PAD4 mice are thought to be slightly less viable [125]. This is supported by the fact that mice deficient in PAD4 show an increase in proliferation of haematopoietic cells [127]. Known to be present in a number of different tumor types [128, 129], and directly interact with the p53 protein [130], PAD4 likely has a role in regulation of angiogenesis. A human PAD4 was originally called PAD5, but was later identified as a homologue of murine PAD4 [103]. This leads to the naming convention, in which there is PAD1-4 and PAD6.

PAD6 is often considered inactive, as it has not been shown to have activity *in vitro.* It is mainly found in mammalian oocytes [105, 131]. Studies have shown PAD6 knockout mouse lines are embryonic lethal at the two cell stage [132]. mRNA has been found in a number of different tissues, but protein has only been reported in ovaries and oocytes [105, 133]. Like PAD1, PAD6 is not a major candidate for deimination in the retina.

Targets of Citrullination

While citrullination can theoretically occur on any peptidylarginine, the list of proteins known to be citrullinated *in vivo* is small. This indicates that there is likely a specific motif that the PAD enzymes preferably interact with, although research into this area is still limited. The list of empirically discovered citrullinated proteins includes several of the intermediate filaments, such as GFAP [19, 35, 134, 135], vimentin [19, 33, 136], desmin [33], and the keratins [122, 137]. A major target of citrullination research is the histones, as they can be citrullinated to control gene expression. Other proteins, such as Myelin Basic Protein [138] and others [122, 139, 140, 1141, 142] are also targeted by PADs.

The citrullination of GFAP and vimentin has been identified both *in vivo* and *in vitro* [111, 35, 135, 33]. Citrullinated proteins are upregulated in a number of different diseases. An *in vitro* study has

identified the impact of citrullination on the assembly, disassembly, and interaction of the intermediate filaments with phosphorylation. After incubation with PAD, there was a lack of long, filamentous structures and an increased presence of soluble subunits. The citrullination of the IFs also leads to the prevention of IF phosphorylation [33], which leads to disrupted IF assembly. Unfortunately, it is not known whether citrullination prevents filament formation or induces filament breakdown.

There have been a number of studies that have identified the presence or increase of citrullinated proteins in the CNS in disease or injury. For instance, in Alzheimer's [19, 134, 143], PAD2 and PAD4 are found in disease regions [143], citrullinated GFAP and vimentin [111] have been identified as two major targets, and citrullinated proteins are found in astrocytes of these patients [134]. In Parkinson's, dopaminergic neurons are found to have citrullinated proteins in both cell bodies and dendrites [134]. Elevated PAD2 has also been seen in prion diseases [144, 145].

In multiple sclerosis (MS), MBP is known to be deiminated. Citrullination in MS currently has the most well established model concerning the pathological implications of this modification as it relates to disease. Interactions between MBP and lipid bilayers are partially dependent on the multiple positive charges on MBP, and deimination is thought to decrease this interaction [146]. While the PAD2 knockout mice have shown no change in the EAE model of MS [115], in either severity or onset, the use of 2-chloroacetamidine mentioned above showed a significant change in the disease course of EAE [116].

Although the insights into functional effects of citrullination on proteins are limited, the increased presence of these species in disease makes them an interesting target for further research. The availability of several different drug tools to probe roles of citrullination on IF proteins allows for further insights into the role of citrullination on the IF proteins and the relevance of this change to disease course.

1.8 Tools for probing IF Proteins

Withaferin A

Formerly, the IF proteins were not known to be druggable targets. The discovery that the small molecule WFA targets soluble vimentin identified for the first time a novel probe for the type III IFs [14]. This was achieved by developing an affinity analog of WFA, WFA-biotin, which was employed to isolate the binding target(s) of WFA. This study also identified that the sole conserved cysteine on vimentin is the covalent binding site of WFA, as observed through mass shifts from LC/MS-MS products [14]. The epoxide group of WFA is subject to nucleophilic attack by this cysteine, forming the covalent bond that can interrupt vimentin polymerization [14] (Fig. 1-7A-B, Fig. 1-8A, C). Interestingly, this finding also indicated the likelihood of WFA binding to other type III IF family members, as this cysteine is conserved within this protein family (Fig. 1-7A, red). In subsequent studies, binding to GFAP [13] was also confirmed through this conserved cysteine, as was another type III IF protein involved in corneal injury, desmin [15]. Interestingly, this conserved cysteine residue received further interest when it was shown to act as a sensor for divalent cations. The addition of zinc [83] is known to aid in the polymerization of filaments, and mutating this cysteine residue alters the initial stages of polymer formation. As will become important in studies of retinal gliosis, the binding of WFA to vimentin is conserved among IFs, as the same binding paradigm exists within GFAP (Fig. 1-8) [13]. The effects of WFA previously described were identified at low micromolar doses, and when the conserved cysteine is mutated, a much higher dose is required for potency [147].

The use of WFA as an anti-tumor agent predates its identification as a vimentin-targeting molecule [149, 150]. Although in-depth mechanisms of action for these other uses of WFA are limited, there is research into the pathways altered at different doses of WFA. At doses above 2 µM, WFA can have apoptotic effects and affects the ubiquitin proteasome pathway, as seen by a significant increase in ubiquitinated proteins in human umbilical vein endothelial cells (HUVECs) when treated with 5 µM WFA [151]. Another well established pathway that can be affected by WFA is the NF-kB pathway,

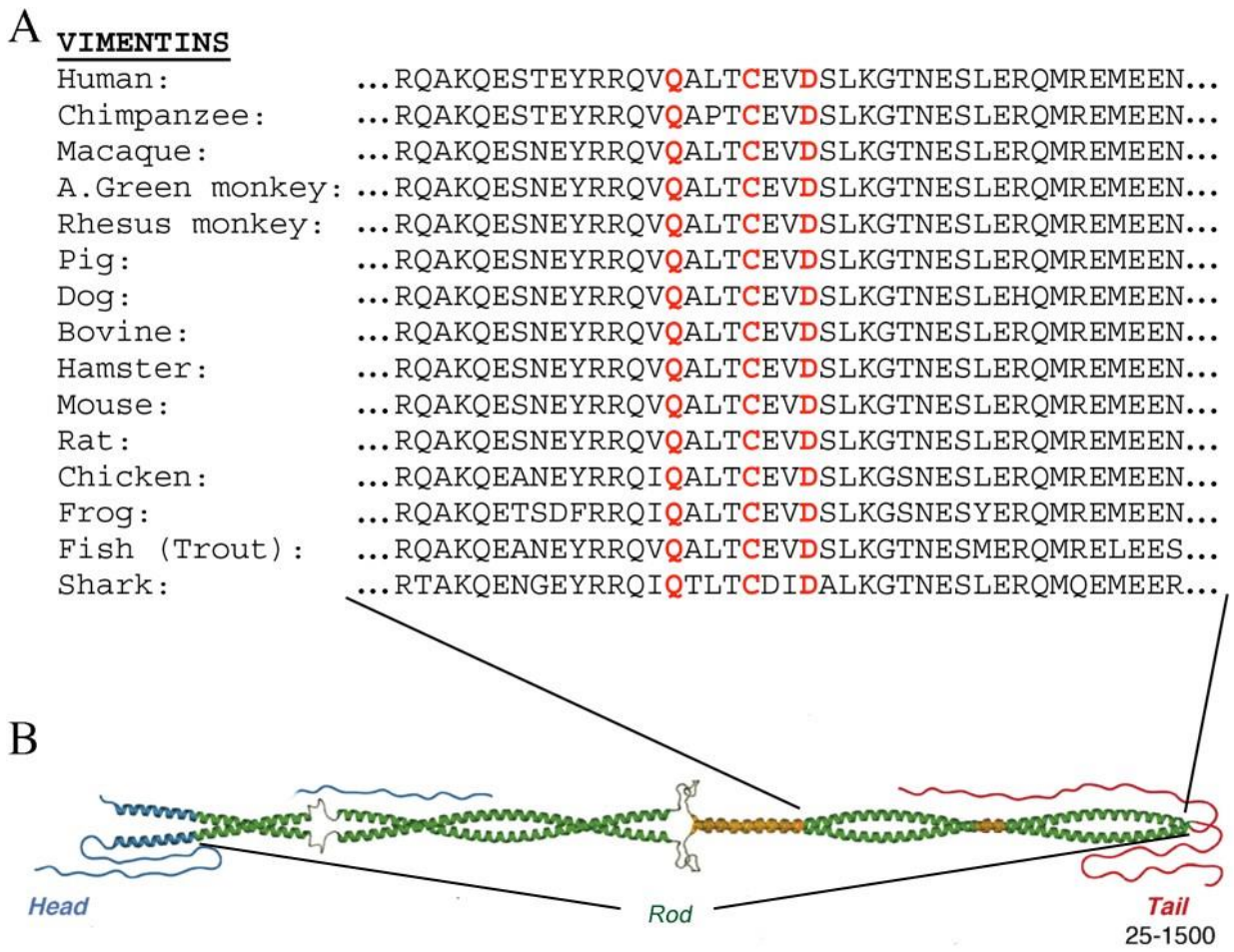

Figure 1-7. Conservation of Cysteine Residue and WFA binding Residues in Vimentin

(A) Sequence within rod 2B domain in multiple vertebrate species revealing the conservation among a number of species. In red are the residues with which WFA interacts; cysteine (covalently), Glutamine and Aspartic Acid (non-covalently). (B) Coiled-coil parallel dimer of vimentin with Head, Tail and Rod (linker and coil) regions outlined. Modified from [148, 14]

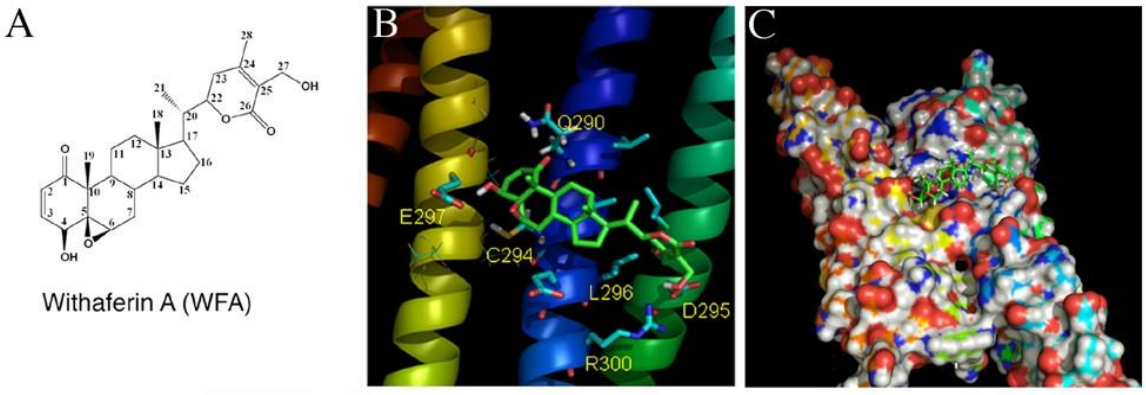

Figure 1-8. Structure and interaction of WFA with GFAP and Vimentin

(A) Chemical structure of Withaferin A (WFA). (B) Ribbon Diagram Interaction of WFA with GFAP tetramer, including interaction of WFA epoxide group with the conserved cysteine of GFAP. (C) Diagram of WFA in binding cleft of vimentin. Modified from [14, 13]

known to be associated with optic nerve head astrocytes in glaucoma [152]. WFA inhibits NF-kB at a 1 μM dose in HUVECs, through alteration of the normal degradation of phosphorylated IkB. The complex interaction of WFA in different systems, including those related to ocular health, and at varying doses, highlight the potential use of WFA in these systems in conjunction with other, known inhibitors [153].

Antibodies Recognizing Citrullinated Proteins

The early methods to recognize citrullination either relied on PAD activity or identification of a modified form of peptidylcitrulline, which could then be probed in more conventional means. An excellent review of previous methods was recently published [154], and the focus here will be on two antibodies to identify citrullinated species, F95 and CTGF-1221.

The F95 antibody is a mouse monoclonal IgM raised against a deca-citrullinated peptide [155], linked to keyhole limpet hemocyanin. It has been used for identification of citrullinated proteins in Alzheimer's [134], Multiple Sclerosis [35], and an experimental model of hypoxia [156]. Its initial confirmation was through the ability to bind highly citrullinated forms of MBP by ELISA, and has been subsequently confirmed through immunoprecipitation, mass spectrometry, and the use of a number of different inhibitors [157, Chapter 2-3]. Increased citrullination of GFAP leads to decreased antigenic reactivity to GFAP [19] antibodies. This led to the development of specific citrullinated GFAP antibodies. One of these antibodies, CTGF-1221, is raised against human GFAP citrullinated at R270 and R416 (corresponding to R267 and R413 in mouse) [19]. This antibody was capable of recognizing recombinant human GFAP *in vitro* after exposure to PAD enzymes, confirmed by mass spectrometry and western blotting. The use of these two antibodies, in both immunohistochemistry and proteomic analysis by SDS-PAGE has allowed for a greater probing of the function of IFs in a number of different systems.

PAD Inhibitors

In recent years, the ability to target and inhibit the PAD enzymes has become a subject of increasing interest, given the prevalence of this modification in disease. While insight into the functional effects that citrullination has on proteins has not advanced far, the identification and improvement of inhibitors has become a well-studied field.

Initially, taxol (paclitaxel) was used to inhibit PADs [158], and it showed an effect when used in the EAE model [159]. This is complicated by the fact that taxol not only blocks PADs, but mainly alters the dynamics of microtubules. Later, it was found that 2-chloroacetamidine, which was somewhat similar to known substrates, was a useful inhibitor [160], altering disease course in EAE [116]. A year later, an improved inhibitor called F-amidine was developed using a similar concept, namely that a compound that could covalently bind to the active site cysteine would strongly inhibit PAD activity. After this, a new inhibitor, Cl-amidine, was developed [161]. Cl-amidine has been the most widely used inhibitor so far, seeing improvements in several clinical models [162, 163, 164, 165, 166].

While the separate PAD enzymes have different responses for each of the different inhibitors, more recent work has looked into specific inhibitors for the different enzymes. Derivatives of Cl- and F- amidine are effective PAD3 inhibitors [167]. PAD4, as the enzyme that is known to be involved in a wide variety of different processes, has garnered the most interest as a target of inhibition. A novel high- throughput screen has identified streptonigrin, an antitumor antibiotic, as an extremely effective and selective inhibitor of PAD4 activity [168] that, like Cl-amidine, is irreversible. This inhibitor represents a useful research tool, although its off-target effects are likely to limit potential as a therapeutic [169, 170].

1.9 Conclusion

In a system such as the mammalian retina, which does not normally regenerate but is subject to scarring and fibrosis, the regulation of the IF proteins is a major influence on tissue health. Recent studies have highlighted the importance of the soluble forms of two IF proteins, GFAP and vimentin, on scarring and retinal health. One of the PTMs that regulate these filaments is the relatively understudied modification of citrullination. Citrullination is increasingly being recognized as a disease related process, with citrullinated GFAP and vimentin being found in a number of neurodegenerative diseases.

The roles of GFAP and vimentin in scarring remain a clinically important issue that remains a challenge. The identification of injury and disease-related mechanisms of soluble GFAP and vimentin

regulation is a key step toward understanding how one may attempt to improve recovery in pathological conditions. This thesis work hypothesizes that citrullination is an injury-induced response to injury in the eye, and that it is occurring to the IF proteins GFAP and vimentin. Further, this citrullination can be targeted in the retina by a number of different molecules in full organ and tissue systems.

Chapter 2

Citrullination of Glial Intermediate Filaments is an Early Response in Retinal Injury

John W. Wizeman[1], Anthony P. Nicholas[2], Akihito Ishigami[3], Royce Mohan[1*]

[1]Department of Neuroscience, University of Connecticut Health Center, Farmington, CT, USA;

[2]Department of Neurology, University of Alabama at Birmingham and the Birmingham VA Medical Center, Birmingham, AL, USA.

[3]Molecular Regulation of Aging, Tokyo Metropolitan Institute of Gerontology, Tokyo 173-0015, Japan

***Corresponding author**

Royce Mohan, MS., PhD.

Department of Neuroscience

University of Connecticut Health Center

263 Farmington Ave

Farmington, CT 06030-3401

Email: mohan@uchc.edu

Phone: 860 679 2020

Conflicts of Interest: The funders had no role in study design, data collection and analysis, decision to publish, or preparation of the manuscript. Royce Mohan is one of the inventors on US Patent 8283323.

Author Contribution Summary

John Wizeman: Conception and design of experiments, collection, analysis and interpretation of results, manuscript writing

Anthony Nicholas: Provided material for experiments, manuscript revision

Akihito Ishigami: Provided material for experiments, manuscript approval

Royce Mohan: Conception and design of experiments, analysis and interpretation of results, manuscript writing, financial support

This chapter has been published in the peer-reviewed journal *Molecular Vision*

2.1 Abstract

Purpose: A hallmark of retinal gliosis is the increased detection and modification of the type III intermediate filament (IF) proteins vimentin and glial fibrillary acidic protein (GFAP). Here we have investigated vimentin and GFAP in Müller glia in a mouse model of alkali injury, focusing on the post-translational modification of citrullination.

Methods: Mice were injured by corneal exposure to 1.0 N NaOH and eyes were enucleated at different time points post injury. Levels of soluble and cytoskeletal forms of IF proteins and citrullination were measured by western blots. Citrullinated GFAP was identified by immunoprecipitation followed by 2-dimensional isoelectric focusing-poly acrylamide gel electrophoresis western blotting using a specific antibody that recognizes citrullinated-GFAP. Vimentin, GFAP and citrullinated proteins were localized in the retina by immunohistochemistry (IHC). Drug treatments were investigated in retinal explant cultures of posterior eye-cups obtained from mouse eyes that were injured *in vivo*.

Results: We report that detection of GFAP in injured retinas increased over a period of 1 to 7 days, showing increase levels in both soluble and cytoskeletal forms of this IF protein. The global level of citrullinated proteins was also induced over this time period, with low-salt buffer extraction showing the most abundant early changes in citrullination. Using IHC, we found that GFAP filaments assembled at Müller glial end feet, growing in size with time through the inner layers of the retina between 1 to 3 hours post injury. Interestingly, over this early time period, levels of soluble citrullinated proteins also increased within the retina as detected by western blotting, coincident with localization of the citrullinated epitopes on growing GFAP filaments and existing vimentin filaments by 3 hours post injury. Taking advantage of the *in vivo* injury model to promote a robust gliotic response, posterior eye-cups from 7-day post-injured eyes were treated in explant cultures with the peptidyl arginine deiminase inhibitor Cl-amidine, which was found to reduce global citrullination. Surprisingly, the detection of injury-induced high molecular weight GFAP species containing citrullinated epitopes was also reduced by Cl-amidine treatment. Using a low dose of the potent type III IF drug withaferin A (WFA), we showed that Cl-amidine treatment in combination with WFA reduced global protein citrullination further, suggesting that GFAP may be a key component of pathological citrullinated targets.

Conclusions: Our findings illuminate citrullination as a potential novel target for trauma-induced retinal gliosis. We also propose that strategies for combining drugs targeting type III IFs and citrullination may potentiate tissue repair, which is an idea that needs to be validated *in vivo*.

2.2 Introduction

Gliosis is a pervasive and complex process that occurs in many central nervous system (CNS) disorders and after traumatic injury, where astroglial cells become reactive, proliferate and undergo hypertrophy [171, 172]. A major hallmark of reactive gliosis is the overabundance of the type III intermediate filament (IF) proteins vimentin and glial fibrillary acidic protein (GFAP). When stimulated by stress signals or injury, radial Müller glia, which span the entire width of the retina, initiate reactive gliosis by increasing levels of GFAP. Soluble tetrameric precursors of GFAP, along with vimentin, co-polymerize into long filamentous forms that create an elaborate cytoskeleton network [8]. Notably, heightened detection of GFAP and vimentin filaments is found in several major human retinal diseases [173, 174, 55]. As such, the pathological overabundance of GFAP and vimentin in Müller glia can drive the formation of scar tissue [175, 176]. Scar tissue exerts tractional forces on retinal membranes, distorting underlying vital cellular structures for which surgery is currently the only treatment option [177]. Corroborating such a pathological role for overabundance of type III IFs in neurodegeneration, the deficiency of vimentin and GFAP in mice is protective in several stress-related and injury contexts [178, 171], but the tissue fragility due to complete lack of filaments underscores the importance of these type III IFs in normal structural function of Müller glia [24]. The ability to regulate glial reactivity to promote wound healing and halt destructive aspects of glial overactivation could benefit from a greater understanding of how vimentin and GFAP are regulated during the injury-repair process.

Vimentin and GFAP are both regulated by multiple post-translational modifications (PTM) [33, 179, 180, 181, 182]. Among these is the PTM citrullination, also known as deimination. Citrullination is

the calcium-dependent transformation of arginine residues on proteins. This reaction is carried out by the enzyme family called peptidyl-arginine deiminases, or PADs. There are five known PAD isoforms in the mammalian genome, PAD1 to 4, and PAD6 [34]. Citrullinated GFAP and vimentin have been observed in the brains of Alzheimer's patients [111], while citrullinated GFAP is found to accumulate in the brains of Multiple Sclerosis (MS) patients [36]. In the experimental autoimmune encephalomyelitis (EAE) model of MS, a small molecule inhibitor of PAD activity was able to rescue diseased mice from clinical EAE [116]. Increased citrullination has also been recently reported in the retina and optic cup of age- related macular degeneration (AMD) donor tissues [38], as well as in the glaucomatous optic nerve [39] and in astrocytes exposed to increased ocular pressure [183]. While there have been recent insight into the mechanics of retinal injury [184, 185, 62, 186], the use of PAD inhibitors has only recently been explored in an experimental model of neurotrauma [187]. In that study, effective early downregulation of protein citrullination within hours of injury that is protective highlights the importance of molecular events that occur during the early hours following CNS injury [187]. Previous studies have suggested that citrullination may affect the formation of filaments by blocking phosphorylation sites or induce the collapse of insoluble, filamentous type III IFs [33, 188]. The in vitro investigation of these type III IFs has provided the insight that citrullination impacts type III IF polymerization/depolymerization steps, but the physiological relevance of this PTM of type III IF proteins in retinal gliosis remains unknown.

Using an alkali injury model, we previously showed that the small molecule withaferin A (WFA) targets vimentin and GFAP in Müller glia during retinal gliosis in vivo [13, 46]. WFA targets type III IFs via binding to a highly conserved rod 2B domain that is common to this class of IF protein [13, 151, 14, 15]. Given its potent effects targeting soluble forms of IFs, WFA reduces the proliferative response of Müller glial cells in gliosis, and ultimately, also perturbs the filament structure of IFs [153]. Here we have exploited the alkali injury model to investigate whether citrullination occurs during retinal gliosis. We show for the first time that citrullinated modified forms of vimentin and GFAP filaments are detected very early after injury. Using the alkali-injured mouse eyes in an explant culture model [13], we have also established that this system can robustly enhance citrullination ex vivo, providing a convenient method to

investigate the signaling axis that links reactive gliosis with citrullination using pharmacological inhibitors of citrullination and type III IFs.

2.3 Materials and Methods

Ethics Statement

All animal experiments were conducted in accordance with procedures approved by IACUC committee of the University of Connecticut Health Center. Mice were housed in specific pathogen free cages in designated laboratory animal housing facilities.

Drug Treatments in Retinal Explant Culture System

N-a-benzoyl-N5-(2-chloro-1-iminoethyl)-L-Orn amide (Cl-amidine) was purchased from EMD Millipore (#506282, Billerica, MA). WFA was purchased from Chromadex (Santa Ana, CA).

Mice and Ocular Injuries

129S6/SvEVTac mice were purchased from Taconic (Hudson, NY) and bred in house. Over 100 mice of approximately 2-3 months of age were used in this study. Corneal alkali injuries were performed in 129S6/SvEVTac (Taconic, Hudson, NY) mice of either sex as previously described [13] with a minor modification. Mice were given an intraperitoneal (i.p.) injection of Ketamine/Xylazine, and corneas were anesthetized with proparacaine eye drops. A 1 µl drop of 1N sodium hydroxide was then applied directly to the central cornea for 45 seconds. The 1N alkali strength is widely used in experimental mouse models [189] and has clinical relevance [190]. Following injury, the eye was immediately flushed extensively with sterile phosphate buffered saline (PBS) solution. The corneal epithelium was gently removed using a Tooke knife, and eyes were then treated topically with atropine, followed by tobramycin and erythromycin. For time course studies, injured mice were treated daily with topical applications of tobramycin and erythromycin for 3 days post-injury and humanely sacrificed by CO_2 inhalation at

different times. Equal numbers of male and female mice were pooled in experiments, and all mice underwent bilateral alkali injury.

Retinal Dissections

Mouse eyes were enucleated immediately after sacrifice as previously described [13]. Eyes were placed into ice-cold PBS + Antibiotic/Antimycotic (A/A) solution until dissection on ice.

Posterior Eye Cup Explant Culture

Enucleated eyes from 7 days post-injury mice were dissected under sterile conditions to separate the posterior eye-cup from the anterior aspect. The posterior eye-cups, which contain the neural retina, retinal pigment epithelium, choroid and sclera [13], were briefly rinsed in PBS and then distributed 1 eye cup per well into 750 ml DMEM/F12 (Gibco, Waltham, MA) medium +A/A (Invitrogen, Waltham, MA) solution, +10% fetal bovine serum (FBS; Atlanta Biologicals, Flowery Branch, GA) in a 24-well culture dish. The eye-cups were placed in a 5% CO_2 incubator at 37 ^{o}C and subject to drug treatments. Fresh batches of either Cl-amidine or WFA was replenished daily for a treatment period of 3 days in DMEM cell culture medium containing 10% FBS or left untreated. DMSO was used as vehicle in similar pilot experiments along with Cl-amidine concentration studies to identify an effective concentration for treatments.

Protein Extraction from Retinal Samples

Three mouse eye-cups were placed in ice-cold soluble buffer (20 mM Tris buffer, 200 mM NaCl, 1% NP-40) supplemented with a proteinase inhibitor cocktail (Roche, Indianapolis, IN) and tissue was minced into pieces on ice. Samples were left on ice for 45 minutes and then spun at 14,000 RPM for 5 minutes at 4 ^{o}C. The supernatant was removed and labeled as the “soluble” fraction (containing soluble forms of IF proteins), while the pellet was placed into 1:3 diluted β-mercaptoethanol:Laemmli buffer to extract

cytoskeletal forms of IFs and spun down at 14,000 RPM for 5 minutes at 4 ^{o}C. This protein extract was labeled as the "insoluble" cytoskeletal fraction. Both soluble and insoluble fractions were then passed repeatedly through a 26-gauge needle 10 times to shear DNA.

Immunostaining

Unfixed eyes were first frozen in OCT (Tissue-Tek, Radnor, PA) at -80 ^{o}C, before being cut on a cryostat at -24 ^{o}C. Sections were cut at 10 or 15 µm thickness, attached to Superfrost slides and stored at -80 ^{o}C until used. Slides were air dried for 30 minutes and then fixed in ice-cold methanol/acetone (5 min/1 min). Fixed slides were washed in PBS 3 times for 5 minutes, and then primary antibody was added in Dako background reducing solution (Dako, Glostrup, Denmark) at the specified concentration. Slides were incubated with primary antibody for 3 h at 37 ^{o}C and then either washed directly or moved to 4 ^{o}C overnight for further incubation and then washed 5 times for 10 minutes afterwards. Slides were then incubated with secondary antibodies at specified concentrations overnight (15 h) at room temperature in the dark, and subsequently washed 5 times for 10 minutes prior to imaging.

Western Blotting

Bicinchoninic Acid Assay (Pierce, Waltham, MA) was used for quantification of protein. Protein samples were boiled 95-100 ^{o}C for 5 to 10 minutes in Laemmli buffer and then loaded on 4-20% Tris-HCl SDS-polyacrylamide gels (Bio-Rad). Proteins were transferred onto a 0.2 µm PVDF membrane (Bio-Rad, Hercules, CA). Membranes were blocked in 5% milk in 1X Tris Buffered Saline + Tween (TBST) for 1 hour at room temperature, then incubated with primary antibody for 1 hour at room temperature or overnight at 4^{o} C. Membranes were washed 3 times for 15 minutes, then incubated with secondary antibody for 45-60 minutes at room temperature. Membranes were washed 4 times for 15 minutes and developed with Enhanced Chemiluminescence (ECL; Bio-Rad) solution. To normalize for protein loading, membranes were stripped in 10X Tris-Glycine-SDS buffer for 30 minutes at RT, then probed as

above with either glyceraldehyde 3-phosphate dehydrogenase (GAPDH) or β-actin antibodies. All figures are shown with corresponding GAPDH or β-actin control beneath.

Antibodies

Primary antibodies used in the experiments included: rabbit polyclonal anti-GFAP (Abcam, Cambridge UK, 7779 1:4,000 WB, 1:500 IHC; Abcam 7260 1:20,000 WB, 1:500 IHC), mouse-IgM monoclonal F95 (anti-peptidyl-citrulline antibody, Millipore MABN328, 1:500 WB 1:200 IHC), rabbit polyclonal GAPDH (Santa Cruz, Dallas TX sc25778 1:500 WB), rabbit polyclonal vimentin (Abcam ab45939 1:200 IHC), mouse monoclonal β-actin (Sigma, St. Louis, MO A5441 1:1,000 WB), mouse β-tubulin (Santa Cruz sc55529 1:1000 WB) and citrullinated-GFAP [69] (CTGF-1221, 1:1000); Secondary antibodies were Santa Cruz goat anti-rabbit IgG HRP (sc-2301 1:1000 WB), goat anti-mouse IgG HRP (sc-2302 1:1000 WB), goat anti-mouse IgM HRP (Jackson ImmunoResearch, West Grove, PA #115-035-075 1:5,000 WB) goat anti-mouse IgM 488 (Invitrogen A21042 1:500 IHC), goat anti-rabbit IgG 488 (Invitrogen A11008 1:500 IHC), goat anti-rabbit IgG 594 (Invitrogen A11012 1:500).

Immunoprecipitation and 2-Dimensional PAGE separation

Citrullinated proteins were immunoprecipitated using the F95 antibody using protein-L agarose bead chromatography. In brief, on day 1, 500 µl protein-L agarose beads (Sigma-Aldrich) were washed 2 times for 5 minutes and once for 30 minutes in soluble buffer with phenylmethylsulfonyl fluoride (1 mM PMSF), sodium fluoride (5 mM NaF), sodium orthovanadate (1 mM Na_3VO_4), protease inhibitor cocktail and dithiothreitol (1 mM DTT). Following this wash step, the final volume of protein-L beads was brought to 500 µl with this soluble buffer. F95 antibody was added at 1:50 and incubated with washed protein-L beads overnight on a rotator at 4^{o} C. On day 2 this bead-antibody mixture was spun down at 3,000xg for 2 minutes. This mixture was then washed 2 times for 5 minutes in soluble buffer at half concentration (10 mM Tris, 100 mM NaCl, 0.5% NP-40, 0.5 mM PMSF, 2.5 mM NaF, 0.5 mM Na_3VO_4

0.5 mM DTT) and once for 30 minutes, spun down at 3000xg for 2 minutes between washes. Posterior eye-cups from 8 injured and 8 uninjured eyes were separately solubilized in 120 µl each of the original soluble buffer and treated as soluble protein. Once extracted, 100 µ1 of the soluble fraction of protein was added to bead-antibody mixture, and half concentration of soluble buffer added to 500µl final volume. This mixture was then incubated on a rotator overnight at 4^{o} C. On day 3, this bead-antibody-sample mixture was then spun down at 3,000xg for 2 minutes. Supernatant from this spin was removed. Beads were then washed with half concentration of soluble buffer 4 times for 5 minutes. After the final wash, soluble buffer was added to final volume of 500 µl. 400µl of this mixture was spun down for 3,000xg for 2 minutes, and supernatant was removed. This bead mixture was resuspended in 160µl reconstitution buffer (8 M urea, 2% CHAPS, 50 mM DTT, 0.2% Bio-Lyte 3/10 ampholytes and Bromophenol Blue, from Bio-Rad ReadyPrep 2D Starter Kit, cat #163-2105). Samples were then heated to 95-100^{o} C for 10 minutes. After boiling, the sample was spun down for 1 min at 14,000 RPM. Supernatant was considered "bound" fraction.

After immunoprecipitation, 160 µl bound fractions were added to pH 4-7 Immobilized pH Gradient (IPG) strips (Bio-Rad #163-2015) and underwent passive rehydration for 1 hour followed by active rehydration at 50 volts for 14 hours in Bio-Rad Protean IEF Cell (Bio-Rad #165-4000). After rehydration, IPG strips underwent isoelectric focusing per the manufacturer's instructions (Bio-Rad #163- 2105). IPG strips were then run on a 4-20% gradient polyacrylamide gel (Bio-Rad #567-1091). Following PAGE separation, protein was transferred to PVDF membrane, blots blocked in 5% milk in 1X TBST, and probed with primary antibodies as described. Uninjured and injured samples from the same experiment were run in parallel.

Confocal Microscopy

Immunofluorescent images were taken on a Confocal Microscope (Zeiss LSM 780, Zeiss, Oberkochen, Germany) on individual planes isolated from xyz stacks of retinal sections with 15µm thickness. Final images were 4-frame averages taken at 20X or 63X magnification that were acquired randomly from retinal sections. Laser intensity was maintained the same across all images.

Statistical Analysis

Each sample for western blot analysis contained pooled protein extracts from three separate mouse eyes, and entire injury experiments were repeated three times to obtain quantitative results. Data represented were the mean of three experiments (n=3) normalized to GAPDH or β-actin. The data was analyzed to obtain the means and ± standard deviation (SD) using t-tests, with a difference of $p < 0.05$ considered statistically significant.

2.4 Results

Citrullination is an early injury response in the retina

We modified a previously established mild alkali injury model where induction of retinal gliosis becomes prominent by day 7 post-injury, as characterized by increased detection of vimentin and GFAP in Müller glia [13]. Extending our prior findings to earlier time points (days 1, 3 and 7 post-injury), we found there was a temporal increase in GFAP immunoreactivity that was produced after injury. Notably, the soluble protein extracts reveal the increased levels of GFAP (Fig. 2-1A) and vimentin (Fig. 2-1B). We assessed injured retinal tissues to determine the time-course of gliosis-associated citrullination in the retina. We found that there was an immediate induction of citrullinated protein species that were found in the soluble fraction starting at 1 day post-injury (Fig. 2-1C). This sustained induction of citrullination lasted through 7 days. In comparison, citrullinated species in the soluble fraction of proteins were very low in the

uninjured eye (Fig. 2-1C, lane 1). By day 1 after injury, citrullinated proteins were visualized at a variety of molecular weights, with distinct bands at 50 kDa and 75 kDa and a pattern of high molecular weight bands between 150 and 250 kDa. Overall, the increased citrullination of proteins in the soluble extracts closely paralleled the increase in the major 50 kDa GFAP protein species and its several lower molecular weight cleaved forms [46] produced over this time period (Fig. 2-1A; Fig. 2-1B ~75 kDa, arrowhead; Fig. 2-1C ~50 kDa, asterisk). The distribution of citrullinated proteins within the high molecular weight range in the soluble fraction was also altered over the time course of injury, with a 250 kDa band increasing over

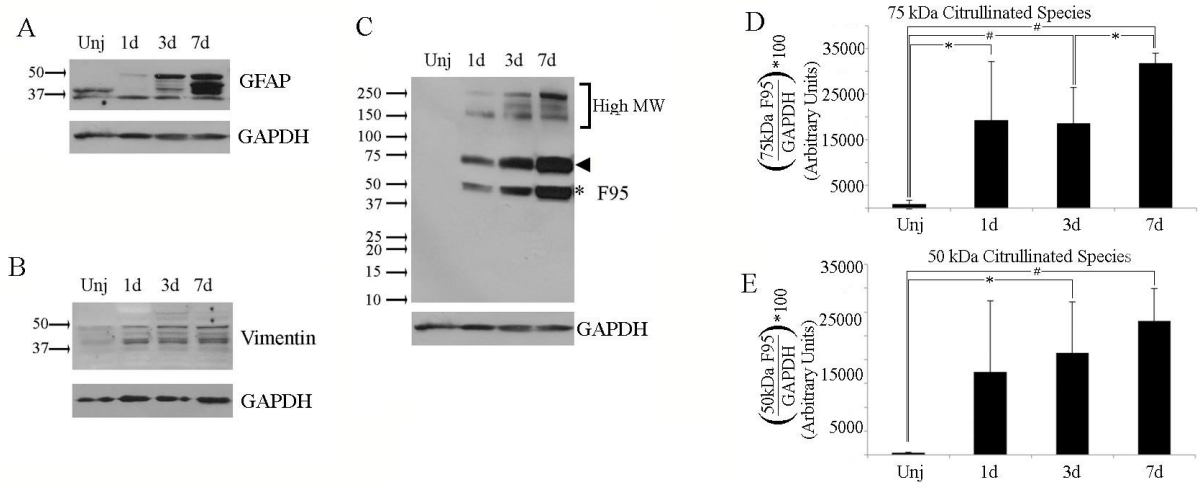

Figure 2-1. Detection of soluble citrullinated proteins after ocular alkali injury.

Western blot analysis of soluble protein extracts from retino-choroidal tissues of uninjured eyes (lane 1) and mouse eyes injured *in vivo* for 1, 3, and 7 days. Blots were probed for GFAP (A), vimentin (B) and citrullinated proteins (C), followed by GAPDH antibodies for loading control. The major 50 kDa band (C, asterisk), and 75 kDa band (C, arrowhead), along with minor high molecular weight bands over 150 kDa to 250 kDa bands (bracket) were identified at all stages post-injury when examined for citrullination. GFAP antibody reactive species were detected between 37 kDa and 50 kDa (A). Uninjured and injured eyes exhibit vimentin reactivity at isoforms ranging from 37 to 55 kDa (B). Bar graphs (D, E) represent quantification of the 75 and 50 kDa citrullinated species, respectively. Each sample contained tissue extracts pooled from 3 retinas from which soluble protein was extracted as described in Methods.

Experiments were repeated three times (n=3), *=$p<0.05$, #=$p<0.01$ by t-test

time while the 200 and 150 kDa bands leveled off between days 3 and 7, post injury.

When we assessed the insoluble fraction of retinal lysates using the F95 monoclonal antibody multiple bands reactive for citrullinated proteins were also present in the insoluble extracts of both injured and uninjured eyes (Fig. 2-2). In particular, the presence of a 75 kDa citrullinated protein was slightly increased by 3 days after injury (Fig. 2-2A; arrowhead, ~75 kDa; Fig. 2-2B). While the 50 kDa species increased early after injury and then decreased by 7 days, the changes in this species are not significant. (Fig. 2-2A, asterisk, ~50 kDa; Fig. 2-2C). On the other hand, GFAP in the insoluble fraction shows an increase through 7 days (Fig. 2-2D), while vimentin increases through 3 days and returned to uninjured levels at 7 days (Fig. 2-2E). Altogether, our findings showed that there were global changes in protein citrullination that occurred after injury and these reflect temporal progression with the early onset of retinal gliosis in this model.

Multiple isoforms of GFAP are citrullinated in the mouse retina

We next wanted to characterize the GFAP isoforms that become citrullinated after retinal injury. This proved to be a challenge for two major reasons. First, soluble tissue extracts from 7 day-injured retinas identified at least 28 distinct GFAP-antibody reactive spots by two-dimensional (2D) isoelectric focusing-polyacrylamide gel electrophoresis (IEF-PAGE) and western blot analysis (Fig. 2-S1). This suggested the likelihood of a complex citrullinated GFAP pattern. Second, a recent finding showed that with increasing levels of citrullination on GFAP its binding to the GFAP antibody is increasingly lost [19], highlighting the difficulty of identifying these modified GFAP isoforms by either F95 or GFAP immunoprecipitation. Fortunately, a novel antibody raised against citrullinated GFAP (CTGF-1221) that recognizes this PTM at positions R270 and R416 in humans (R267 and R413 in mice, respectively) was developed in that study [19]. Using immunoprecipitation, citrullinated proteins from the soluble pool of 7-day injured retinas were affinity isolated using the F95 antibody and subjected to IEF-PAGE. These protein blots were then subjected to incubation with the CTGF-1221 antibody to detect citrullinated GFAP.

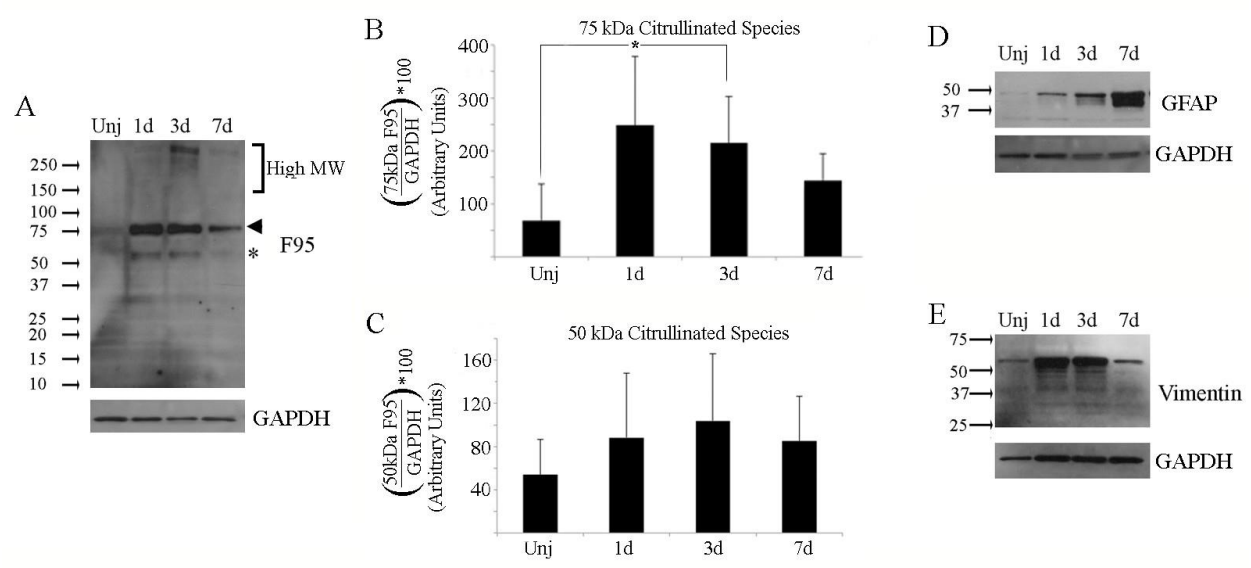

Figure 2-2. Detection of insoluble citrullinated proteins after ocular alkali injury.

Western blot analysis of insoluble proteins from retino-choroidal tissues from uninjured and injured mouse eyes as described in Figure 1. Gel blots were probed sequentially for citrullinated proteins (F95), GFAP and vimentin. Corresponding GAPDH loading controls are located beneath each blot. Citrullinated proteins were detected in all insoluble fractions (A) with major bands detected at 75 kDa (A, arrowhead) and at 50 kDa (A, asterisk), with minor bands over the high molecular weight range between 150 kDa and 250 kDa (bracket). Bar graphs (B, C) represent quantification of the 75 and 50 kDa citrullinated species, respectively. GFAP isoforms were detectable at all time points below 37 kDa and 50 kDa (D). A 55 kDa vimentin isoform was detectable at all time points (E). Each sample contained tissue extracts pooled from 3 retinas from which protein that not solubilized in low-salt buffer was extracted as described in Methods. Experiments were repeated three times (n=3), *= $p < 0.05$.

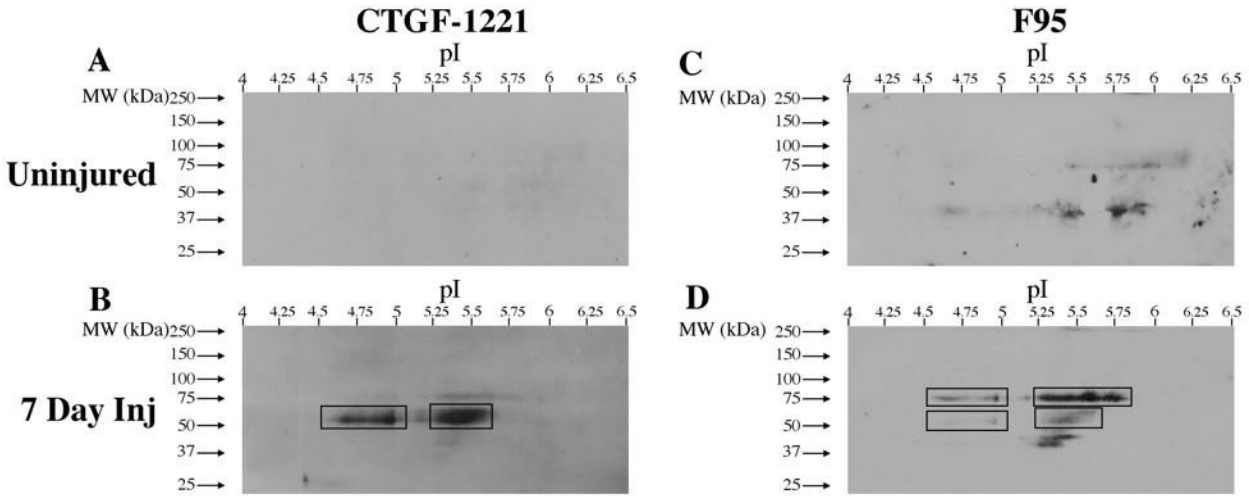

Figure 2-3. Detection of Citrullinated GFAP in uninjured and injured retinas

Two-dimensional IEF-PAGE separation of soluble proteins from uninjured and 7 day injured retinao-choroidal tissues immunoprecipitated for citrullinated proteins (F95 antibody) and western blotted first with CTGF-1221 antibody (A, B) and subsequently with the F95 antibody (C, D). Blots of the injured retinas probed with the anti-citrullinated GFAP antibody (B) showed lower relative abundance of ~50 kDa protein species compared to 75 kDa species when re-probed with F95 antibody (D).

As a comparison, soluble fractions from uninjured retinas were also analyzed by IEF-PAGE, and western blotted with the CTGF-1221 antibody. . The 2D-immunoblots from uninjured retinas probed with the CTGF-1221 antibody did not identify reactive species (Fig. 2-3A). The 2D-immunoblots from injured retinas probed with the CTGF-1221 antibody revealed intense reactivity at the anticipated 50-52 kDa size for citrullinated GFAP species (Fig. 2-3B). The major immunoreactive region showed two closely spaced 50- 52 kDa overlapping species distributed over isoelectric points of 5.25 and 5.6 (Fig. 2-3B, box). A second region between isoelectric points of 4.50 to 5.00 was detected, with additional minor species being detected between the two boxed regions (Fig. 2-3B, box). These two boxed-regions correspond to the ~50 kDa broad band that was observed by one-dimensional western blots with the F95 antibody (Fig. 2-1A). To detect all the citrullinated species the blots were re-probed with the F95 antibody. The uninjured retinas showed broad immunoreactive diffuse spots at 75 kDa and between 37 and 50 kDa with isoelectric points between 5.5 and 6.0 (75 kDa, Fig. 2-3C) and 4.5 to 5.75 (37-50 kDa, Fig. 2-3C). This detection is likely due to the immunoprecipitation with F95 antibody. Similarly, the blot from injured retinas displayed F95 immunoreactivity at a range of molecular weights and isoelectric points (Fig. 2-3D, boxed regions). Specifically, an intensely labeled broad region located around 75 kDa and less intensely labeled broad region around 50 kDa closely resembled the immunoreactive bands seen in Fig. 2-1A (arrowhead, asterisk respectively). The multiple 75 kDa species were distributed between isoelectric points from 4.50 to 5.00 and 5.25 to 5.75, whereas those at 50 kDa species of low abundance and distributed between isoelectric points from 4.50 to 5.00 and between 5.25 to 5.60 (Fig. 2-3D, boxed regions). We also identified a region between 37 kDa and 50 kDa that contained immunoreactive species between isoelectric points of 5.25 and 5.60. The protein blots of soluble extracts from 7 day injured retinas probed for native GFAP (Fig. 2-S1) when overlaid on 2D IEF western blot of extracts subjected first to F95 immunoprecipitation and then 2D separation revealed that citrullinated GFAP species (detected by CGTF-1221 antibody) migrate differently from native GFAP species (Fig. 2-S2). These data reveal that the injured retina retains considerable amount of GFAP in the soluble fraction as diverse citrullinated species.

Citrullination occurs on type III IFs within Müller glia

We next investigated the spatial and temporal patterns of citrullination upon injury during the early time points of tissue repair in relationship to vimentin and GFAP staining. The uninjured retina displayed minimal F95 reactive species in the inner retina, while the outer plexiform layer was absent of any staining (Fig. 2-4 A-C). Long filamentous structures and co-localization with F95 reactive species were observed in Müller glia as early as 1 hour after injury (Fig. 2-4 D-F, asterisk). We observed both a punctate staining starting at the ganglion cell layer (GCL) through the inner plexiform layer (IPL) and inner nuclear layer (INL) as well as filamentous structures throughout the inner retina. Immunoreactivity was also observed in the OPL (Fig. 2-4; D-F). Interestingly, filamentous structures that were interspersed with both GFAP positive and F95 positive regions were seen in Müller glia at 3 hours (Fig. 2-4G-I, brackets), but not at 1 day (Fig. 2-4H-L), and seen again by 3 days (Fig. 2-4M-O, brackets) post injury. These filaments are visually different from co-localization of GFAP and F95 immunostaining, and are referred to as "interspersed" filaments. These interspersed filaments show distinct regions of F95 immunoreactivity alternating with regions of GFAP immunoreactivity along extended filamentous structures. Filaments exhibiting co-localization of GFAP and F95 persisted through 3 hours after injury (Fig. 2-4 G, I asterisks), while long filament-like structures of citrullinated proteins (Fig. 2-4H, I, arrowheads) were observed absent of GFAP. At 1 day after injury, there was a strong detection of F95 positive species within the INL. Non-continuous filaments were observed extending below an enlarged astrocyte (Fig. 2-4L, asterisk). Strong co-localization of GFAP staining with F95 immunoreactivity was observed in the GCL and IPL at 3 days after injury (Fig. 2-4 O, asterisk). Long GFAP filaments were established by 3 days after injury, and co-localization of GFAP and F95 staining occurred near the border of the GCL and IPL. With time, nuclei in the GCL displayed F95 immunoreactivity, and GFAP positive processes extended into the vitreous, indicating a separation from the inner limiting membrane (ILM; Fig 2-S3A-B). Full-length vimentin filaments (Fig. 2-5) were observed throughout the layers of the retina in the uninjured Müller glia (Fig. 2-5 A-C), as has been previously reported [13, 17].

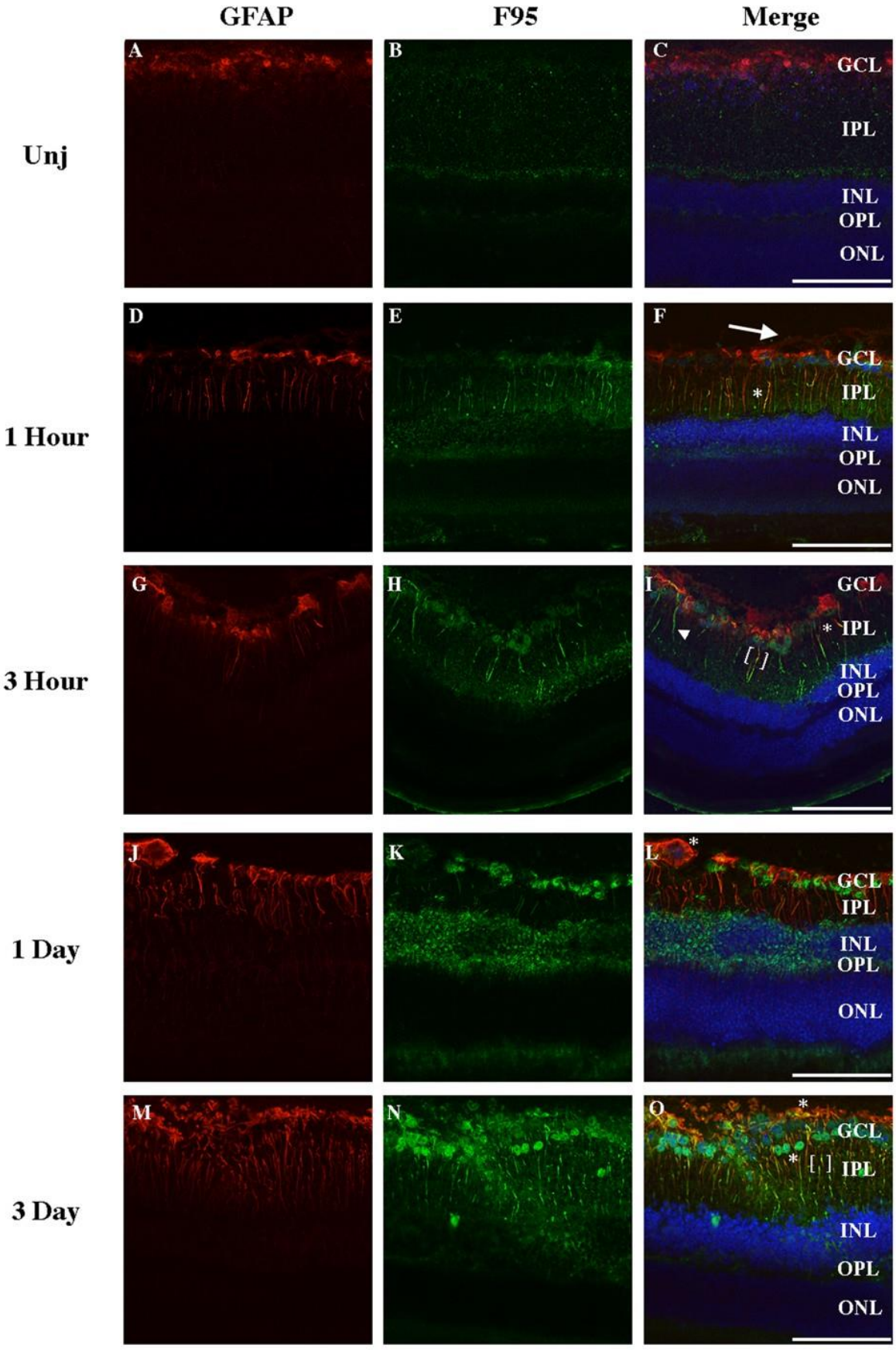
GFAP
F95
Merge
Unj
1 Hour
3 Hour
1 Day
3 Day
A
B
C
D
E
F
G
H
I
J
K
L
M
N
O
GCL
IPL
INL
OPL
ONL

Figure 2-4. Citrullination of GFAP filaments after injury.

Cryosections from uninjured and injured eyes were stained with GFAP (red) and F95 (green) and nuclei stained with DAPI (blue). Sections were examined under confocal microscope at 20X at an uninjured state (A-C), 1 hour (D-F), 3 hours (G-I), 1 day (J-L) and 3 days (M-O) post injury. Extensions of GFAP staining beyond nuclei of the GCL are marked by an arrow (F). Co-localization of GFAP and F95 antibodies are marked by asterisks (F, I, L, O). Interspersed regions of GFAP and F95 reactivity is outlined in brackets (I, O). GFAP negative, F95 positive filaments are marked by arrowhead (I). GCL, ganglion cell layer; IPL, inner plexiform layer; INL, inner nuclear layer; OPL, outer plexiform layer; ONL, outer nuclear layer. (Scale bar = 100 μm)

As early as 1 hour after injury, vimentin immunoreactivity within the outer layers of the retina was diminished, while co-localization with F95 reactive species was observed in the IPL (Fig. 2-5 D-F, asterisk). As with GFAP staining, filaments interspersed with both vimentin positive regions and F95 positive regions were seen predominantly in the IPL, extending into the GCL (2-5F, brackets). Three hours after injury, co-localization of vimentin staining and F95 immunoreactive species was observed (Fig. 2-5 G-I, asterisk), and filaments extended beyond nuclei in the GCL into intravitreal space (Fig. 2- 5I, arrows). One day after injury filamentous vimentin was observed throughout the layers of the inner retina, with nuclear F95 staining (Fig. 2-5-J-L). The extension of vimentin staining into the vitreous was also observed at 3 days post-injury (Fig. 2-5O, arrow; Fig. 2-S3C-D). Long vimentin filaments also became interspersed with F95 immunoreactive species by 1 hour (Fig. 2-5F, brackets), into 3 hours (Fig. 2-5I, brackets) and at 3 days (Fig. 2-5O, brackets) post-injury. Müller glia recovered full filament structure by 1 and 3 days after injury, but also displayed perinuclear staining of both vimentin and citrullination in the OPL (Fig 2-5O, arrowhead). Of note is the border between the OPL and the INL, which displayed a strong abundance of vimentin and F95 immunoreactivity at 1 and 3 days, respectively. The rearrangement of these filaments and their citrullination highlights the importance of examining early and immediate responses to injury.

We also examined the pattern of citrullination at higher magnification. The distinct pattern observed previously was clearly visible, as both GFAP (Fig. 2-6) and vimentin filaments (Fig. 2-7) appeared less organized at 3 hours (A-C) than at 3 days (D-F). GFAP filaments that formed at 3 hours did not strongly co-localize with F95 staining (Fig. 2-6A-D, asterisks). GFAP filaments that were extended

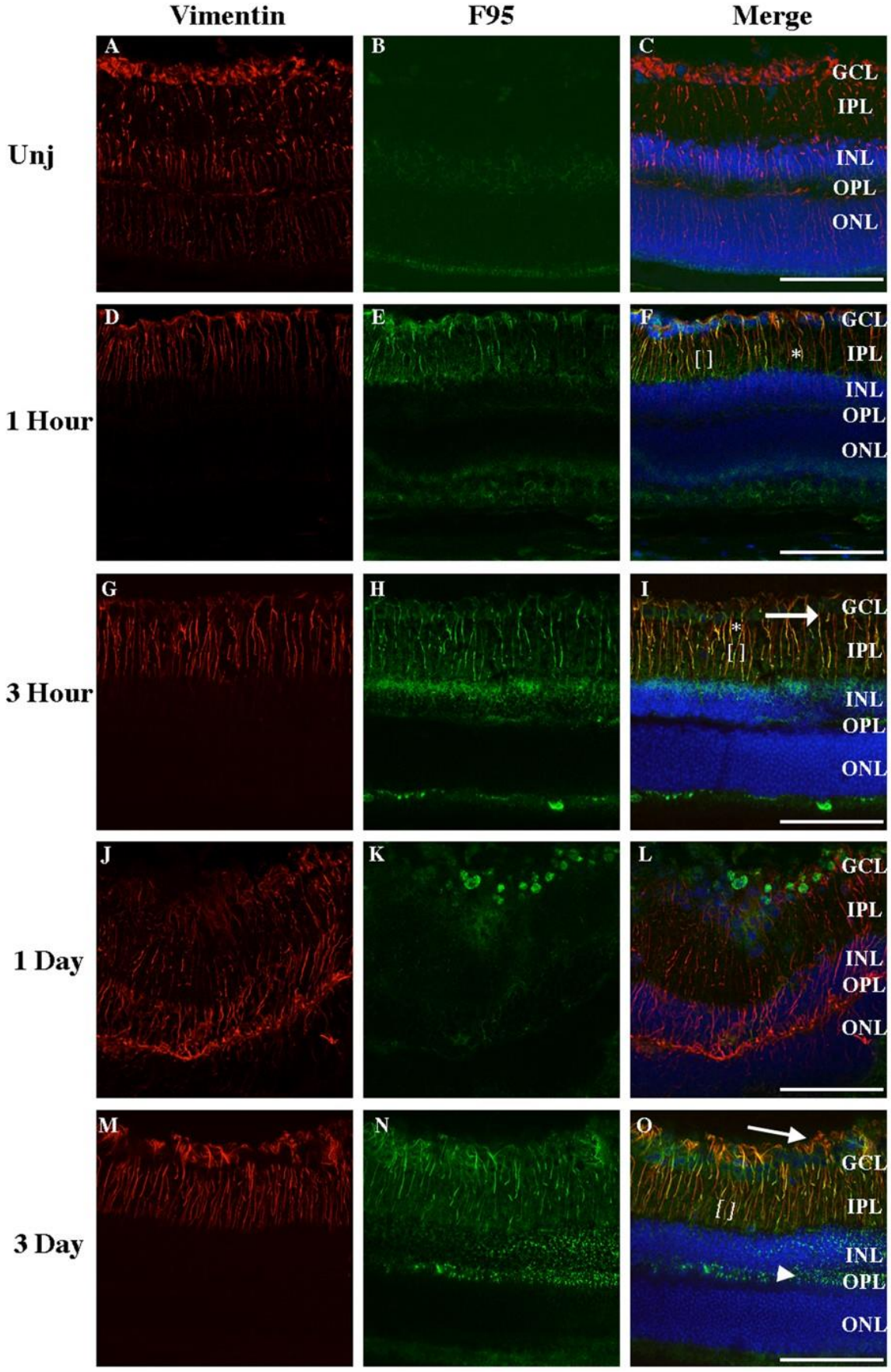
Vimentin
F95
Merge
Unj
1 Hour
3 Hour
1 Day
3 Day
A
B
C
D
E
F
G
H
I
J
K
L
M
N
O
GCL
IPL
INL
OPL
ONL
[ ]
*

Figure 2-5. Citrullination along Vimentin Filaments after Ocular Injury.

Cryosections from uninjured and injured eyes were stained using antibodies against vimentin (red) and citrullinated proteins (F95; green). Tissue sections were examined under confocal microscope at 20X maginification from uninjured eyes (A-C), and 1 hour (D-F), 3 hours (G-I), 1 day (J-L) and 3 days (M-O) post injured eyes. Extensions of vimentin staining beyond nuclei of GCL are marked by arrow (I, O). Representative regions showing the overlap of vimentin and F95 antibodies are marked by asterisks (F, I, O). Interspersed regions of vimentin and F95 reactivity is outlined in brackets (F, I, O). Diffuse staining of F95 is marked by arrowhead (O). GCL, ganglion cell layer; IPL, inner plexiform layer; INL, inner nuclear layer; OPL, outer plexiform layer; ONL, outer nuclear layer. (Scale bar = 100 μm)

by 3 days showed strong co-localization with F95 immunoreactivity (Fig. 2-6E-H, asterisks). Importantly, extension of GFAP positive processes into vitreal space occurred as early as 3 hours after injury (Fig. 2-6C, bracket). Co-staining of vimentin and citrullinated epitopes at 3 hours (Fig. 2-7 A-D, asterisks) appeared to be restricted to the layers of the inner retina (GCL, IPL), while there was a distinct and clear staining of vimentin at 3 days (Fig. 2-7 E-H) at the INL and near the border between the IPL and the INL. At this later time point F95 staining became more distinct, as glial processes stained with both vimentin and GFAP displayed an interspersed staining with citrullinated proteins (Fig. 2-6G, brackets; Fig. 2-7G, brackets), while vimentin and GFAP positive glial sprouts themselves extended through the retina (Fig. 2-S3).

Immunostaining of Müller glia does not always provide the possibility of visualizing filaments fully, due to the changing contours of the tissue. In order to more completely probe the nature of the IF relationship with F95 reactive species along the length of entire filaments through the contour of the retina, we compiled z stacks of confocal images into movies. Using tissue sections from 3 hour and 3-day post-injury time points, samples were stained with either GFAP and F95 or vimentin and F95. When we examined GFAP immunoreactivity at 63X magnification 3 hours post injury (Sup. 2-M1), filaments extending into the INL were observed. When filaments were examined throughout the z-stack, both regions of "interspersed" filamentous structures and co-localized regions could be identified (Sup. 2-M1). Several GFAP negative, F95 positive filaments were also observed. When we examined GFAP and F95 immunoreactivity at 3 days post injury (Sup. 2-M2), GFAP filaments were tracked from the GCL through the INL. At 3 days, fewer GFAP negative F95 positive filamentous structures were observed. Regions of co-localization were observed mainly in the IPL. When examined at 3 hours post injury, vimentin immunoreactivity appeared diminished in the outer retina (Sup. 2-M3). F95 positive, vimentin negative filamentous structures were not observed at 3 hours post injury. Filaments predominantly displayed both F95 and vimentin immunoreactivity, with several F95 positive regions interspersed near the boundary of the IPL and the INL. At 3 days post injury (Sup. 2-M4), vimentin positive filaments were observed extending from the ONL to the GCL. F95 immunoreactivity was also observed in the INL. Vimentin and

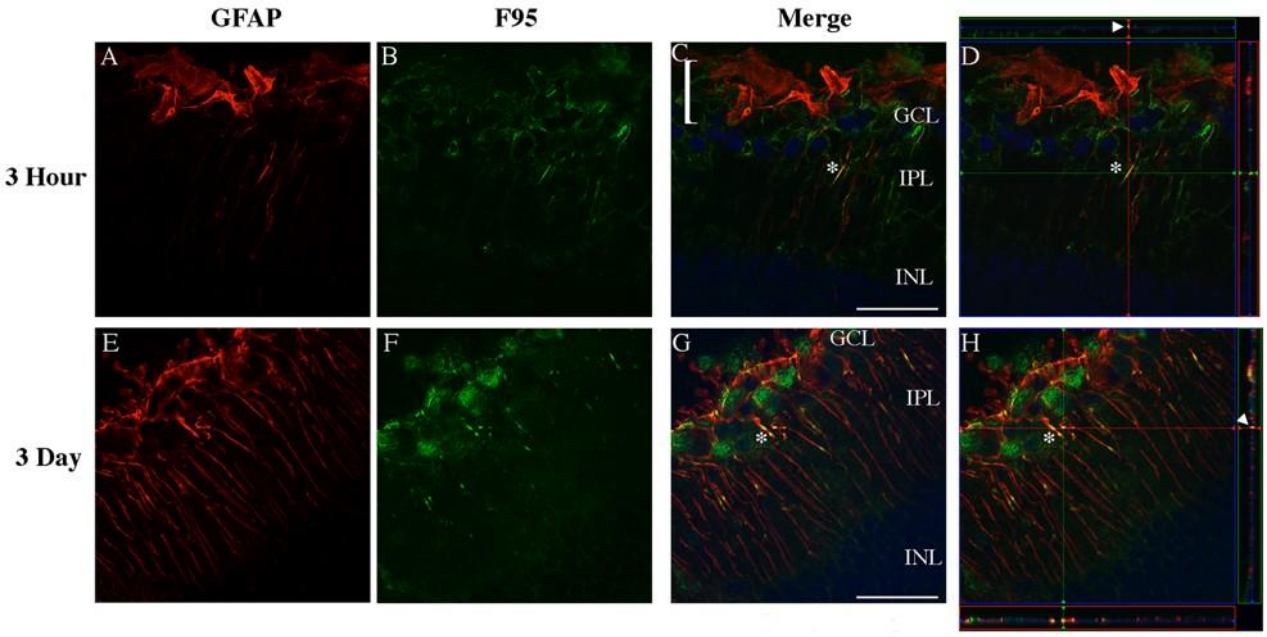

Figure 2-6. High magnification images of citrullinated GFAP filaments in the injured retina.

Tissue sections of mouse eyes injured for either 3 hours or 3 days were immunostained for GFAP (A, E, red), citrullinated proteins (B, F, F95 antibody, green) and nuclei (C, G, merged images, DAPI-blue). Sections were analyzed on a Zeiss LSM 780 confocal microscope at 63X magnification to identify GFAP filaments co-localized with citrullinated species. Co-localized filaments in 3 hour (C, D, asterisk) and 3 day samples (G, H, asterisk) were visually identifiable in the inner plexiform layer (IPL). Orthogonal planes were analyzed (D, H) to identify points of co-localization (asterisks, arrowheads). Invasion of filaments into the vitreal space past the ganglion cell layer (GCL) was identified in 3 hour injured samples (C, bracket). (Scale bar = 40 µm)

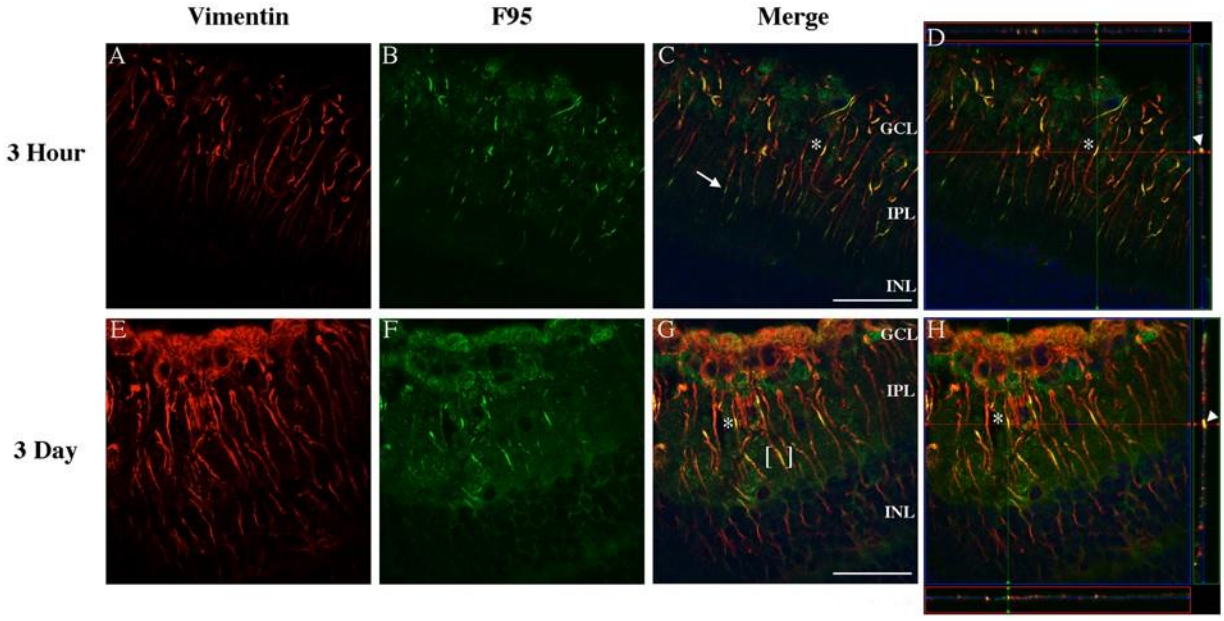

Figure 2-7. High magnification images of citrullinated vimentin filaments in retinas after ocular injury.

Eyes injured for either 3 hours or 3 days were sectioned and immunostained for vimentin (A, E, red), anti-citrullinated proteins (B, F, F95 antibody, green) along with DAPI (C, G, merged images, blue). Vimentin filaments showed staining in the GCL and IPL 3 hours post-injury (A). F95 positive filaments showed staining at 3 hours post-injury in the GCL and IPL (B). Filaments in the retina displayed co-localization of F95 and vimentin (C, asterisk; D, asterisk/arrowhead), as well as a distinct interspersed pattern with F95 reactive regions capping filaments near the boundary of the IPL and INL (C, arrow). Three days post- injury, vimentin positive filaments showed staining in the IPL and both filamentous and non-filamentous vimentin immunoreactivity was present in the GCL (E). Diffuse staining, as well as filamentous staining of F95 reactive proteins were present in the GCL and IPL 3 days post-injury (F). Vimentin and F95 displayed distinct co-localization (G, asterisk; H asterisk, arrowhead), as well as an interspersed pattern (G, bracket). Orthogonal views of xyz stacks (D, H) were obtained to identify points of co-localization (D, H, asterisk, arrowhead). (Scale bar = 40 µm)

F95 immunoreactivity along the continuous filamentous structures was predominantly co-localized. An interspersed pattern was observed with vimentin and F95 immunoreactivity immediately adjacent to this pattern (Sup. 2-M4, Fig. 2-7G, bracket). These data indicate that citrullination in the Müller glia can associate with the IF cytoskeleton and appears to be dynamically altered as the filaments form post injury.

Targeting Citrullination and the IFs in retinal gliosis reduces GFAP and Vimentin

We next hypothesized that citrullination plays a role in the injury response of the retina and could impact gliosis. To test this hypothesis we employed the PAD inhibitor Cl-amidine and exploited a retinal posterior eye-cup organ culture model as a convenient biochemical assay. The retinal posterior eye-cup model was previously employed to test inhibitors of gliosis in vitro using enucleated eyes from mice that had been subjected to alkali injury to promote gliosis [13]. This biochemical assay provides the advantage of not only relatively short time period to test drugs by bath application but also avoids issues with variability in tissue permeability and unknown pharmacodynamics faced with in vivo drug delivery to the retina. Thus, using the intact posterior eye cups dissected from 7-day post injured eyes, pilot experiments were performed to optimize the assay to ascertain dose-related effects of Cl-amidine compared to vehicle, finding a 100 μM dose of Cl-amidine effective at decreasing a broad range of citrullinated species (Fig. 2- S4). We then investigated how perturbation of soluble IFs with a low dose of WFA used alone, or in combination with Cl-amidine, affected citrullination. Interestingly, we found that injured retinas showed, in addition to the anticipated 50 kDa GFAP, also high molecular weight GFAP species (>75 kDa) in the soluble (Fig 2-8A-B) fraction, and displayed a pattern similar to that previously documented in human CNS disease [36]. Whereas Cl-amidine treatment alone reduced abundance of some of the high molecular weight (species > 75kDa) GFAP species (Fig. 2-8A-B), combined treatment of Cl-amidine and WFA significantly reduced high molecular weight GFAP (>75 kDa) in the soluble fraction of proteins (Fig. 2- 8A-B). Cl-amidine also caused levels of low molecular weight (37-50 kDa) GFAP to be increased (Fig. 2- 8A), though not to statistical significance (Fig. 2-8C). Cl-amidine treatment did, however, significantly increase the native 50 kDa GFAP species in the soluble fraction (Fig. 2-8A, asterisk). Combined

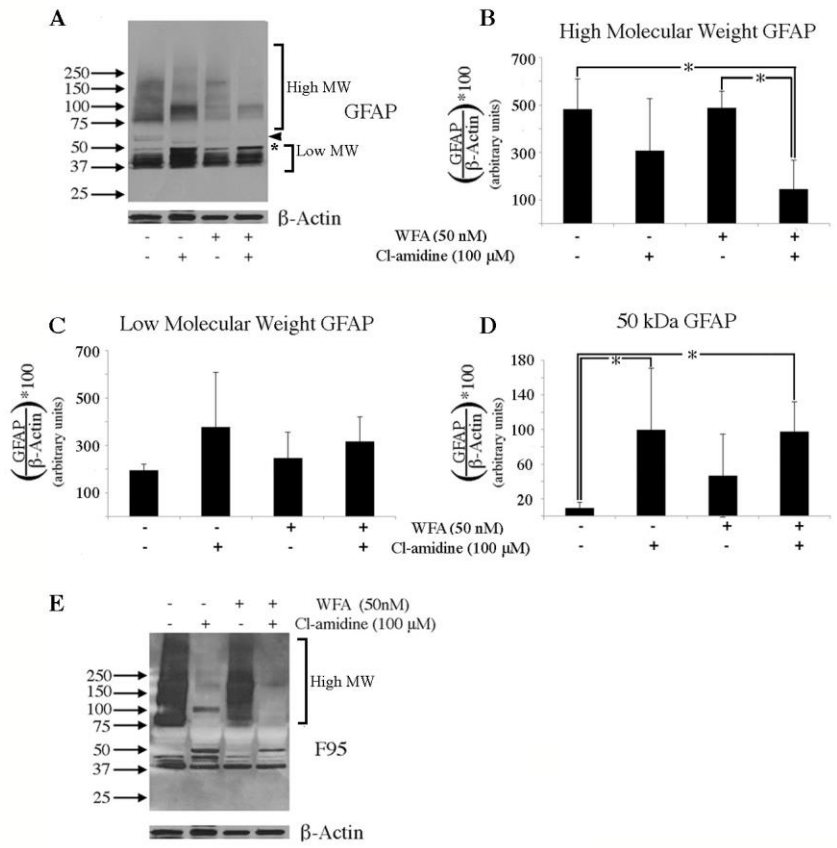

Figure 2-8. WFA and Cl-amidine have a compounding effect on soluble GFAP in the retina.

Eyes were injured and left to recover for 7 days *in vivo.* On day 7, mouse eyes were enucleated and posterior eye-cups were placed into culture with no drug added (lane 1), or containing either Cl- amidine alone (lane 2), WFA alone (lane 3), or both drugs combined (lane 4). (A) Western blot analysis of GFAP in soluble fractions of untreated, Cl-amidine treated, WFA treated, or WFA/Cl-amidine treated eye-cups. The arrowhead points to a 55 kDa band. Densitometric quantification of high molecular weight GFAP (B, >75 kDa), low molecular weight GFAP (C, 37-50 kDa), or 50 kDa GFAP (D, asterisk). (E) Western blot analysis of F95 in soluble fraction from untreated, Cl-amidine treated, WFA treated, or WFA/Cl-amidine treated eye-cups. Data are mean +/- SD, *= $p<0.05$ by t-test.

treatment with WFA and Cl-amidine increased levels of low molecular weight (37-50kDa) GFAP (Fig. 2-8A, 2-8C), though not significantly when normalized to β-Actin (Fig. 2-8C). A 55 kDa band was visibly decreased by both WFA and Cl-amidine treatment alone, and extracts from the combined treatment displayed no observable 55 kDa species (Figure 2-8A, arrowhead). Analysis of F95 antibody reactivity showed treatment with both Cl-amidine and WFA clearly diminished the levels of most of the high molecular weight citrullinated proteins in the soluble fraction (Fig. 2-8E). Analysis of the insoluble fraction of proteins showed no statistical difference in GFAP levels (Fig. 2-9A-D), but changes in the migration of these species were observed (Fig. 2-9A). Cl-amidine treatment caused a trend towards increasing abundance of the 50 kDa GFAP species as well as low molecular weight GFAP (37-50 kDa) in the insoluble fraction, but these were not significant when normalized to GAPDH (Fig. 2-9C, D). This effect was not seen with WFA treatment alone. Taken together, our data demonstrate that low dose WFA when used in conmbination with Cl-amidine enhanced the targeting of protein citrullination and restored levels of 50 kDa soluble GFAP.

In comparison, high molecular weight vimentin was not readily detected in the soluble extracts (Fig. 2-10A). Interestingly, treatment with Cl-amidine provided alone, or WFA alone, increased abundance of the 55 kDa and lower species (Fig 2-10A, arrowhead, B). Combined drug treatments significantly increased the native 55 kDa vimentin species (Fig. 2-10A, C). On the other hand, the insoluble extracts did not reveal any significant changes in vimentin levels with either drug treatments (Fig. 2-10D-F). Taken together, these biochemical experiments reveal that significant changes in the composition of the soluble pool of GFAP were affected by injury that lead to increased citrullination of this IF protein, with alterations in soluble vimentin being a minor feature of this complex reactive glial response.

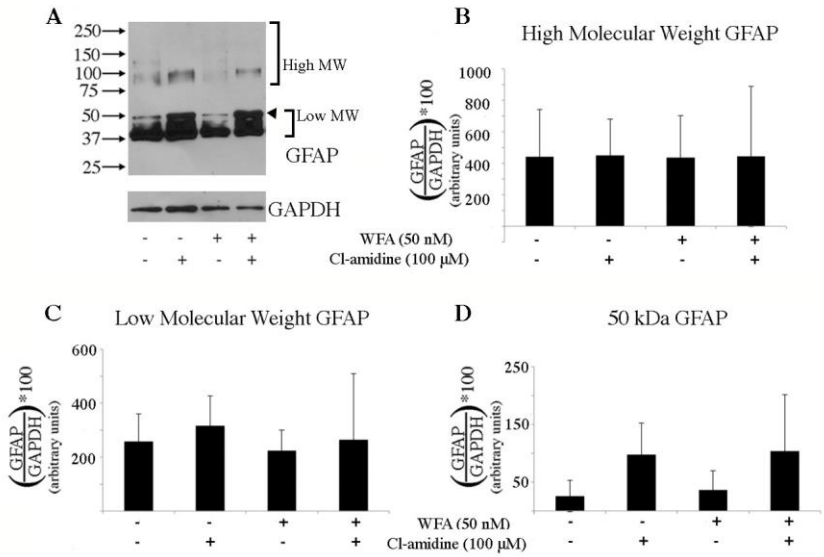

Figure 2-9. WFA and Cl-amidine have no effect on insoluble GFAP in the retina.

Eyes were injured and left to recover for 7 days in vivo. On day 7, mouse eyes were enucleated and posterior eye-cups were placed into culture with no drug added (lane 1), or containing either Cl-amidine alone (lane 2), WFA alone (lane 3), or both drugs combined (lane 4). (A) Western blot analysis of GFAP in insoluble fraction of untreated, Cl-amidine treated, WFA treated, or WFA/Cl-amidine treated eye-cups. Densitometric quantification of high molecular weight (B, >75 kDa), low molecular weight (C, 37-50 kDa), and 50 kDa species (D, arrowhead). Data are mean +/- SD, *= $p<0.05$ by t-test.

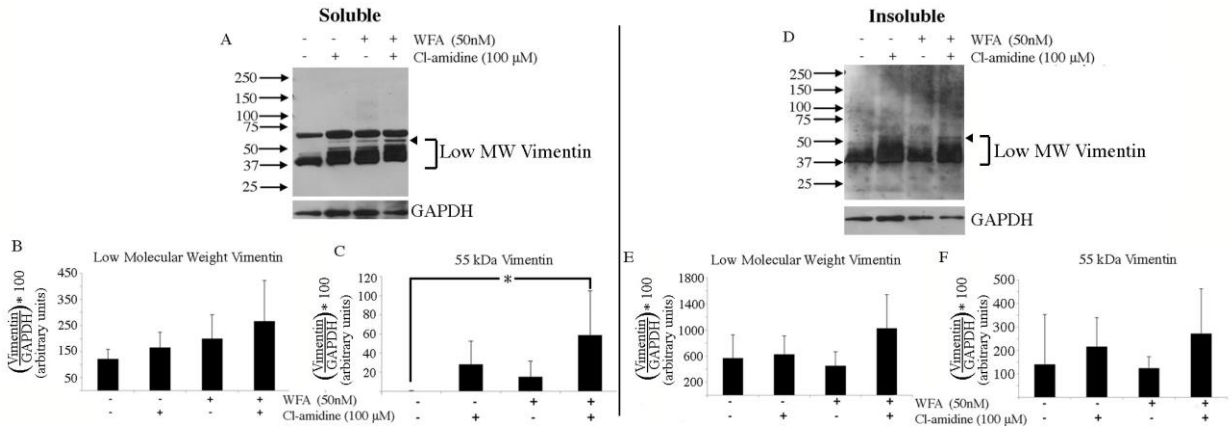

Figure 2-10. WFA and Cl-amidine alter the distribution of vimentin in the retina

Eyes were injured and left to recover for 7 days in vivo. On day 7, mouse eyes were enucleated and posterior eye-cups (neural retina, pigment epithelium, choroid) were placed into culture containing specified concentration of either Cl-amidine (lane 2), WFA (lane 3), both (lane 4) or no drug added (lane 1). (A) Western blot analysis of vimentin in soluble fractions of untreated, Cl-amidine treated, WFA treated, or WFA/Cl-amidine treated eye-cups. Densitometric quantification of low molecular weight vimentin (B, 37-55 kDa), or 55 kDa vimentin (C, arrowhead). (D) Western blot analysis of vimentin in insoluble fraction of untreated, Cl-amidine treated, WFA treated, or WFA/Cl-amidine treated eye-cups. Densitometric quantification of low molecular weight (E, 37-55 kDa), and 55 kDa species (F, arrowhead). Data are mean +/- SD, *= $p<0.05$ by t-test.

2.5 Discussion

We report for the first time that citrullination is an induced response to injury within Müller glial cells of the mouse retina. This PTM occurs on a global level in different cell layers of the retina, but a major citrullinated target, GFAP, and to a lesser extent vimentin, are two important proteins of the Müller glial response responding to injury [171, 172, 8, 55, 178, 24]. The discovery that the soluble form of GFAP becomes citrullinated after injury provided us the opportunity to demonstrate that perturbation of the IFs directly by WFA [13] when combined with the pan-PAD inhibitor Cl-amidine can interfere with citrullination. Our data is intriguing as there has been growing interest in the roles of soluble IFs, for instance, as chaperones [76] and in nuclear transport of kinases in injured neurons and corneal fibrosis [76, 77], as well as in lamellipodia formation [77, 73]. Several prior studies have focused on the Müller glial responses in different injury contexts [176, 186, 17, 13, 46, 191], but the immediate responses of IF proteins where soluble forms are regulated have not been studied. Also of note is the fact that although this study focuses on glial responses, and did not examine neuronal responses, retinal ganglion cells can become apoptotic after alkali injuries [192]. Our findings illuminate citrullination of IFs as an important early event in the injury response of the retina.

The citrullinated GFAP isoforms that result from this severe alkali injury showed a wide distribution of both basic and acidic species that contain the antigenic R267 or R413 citrullination sites. These data do not rule out that other arginines in GFAP could be citrullinated, as their mobilities in the 2D western blot analysis were clustered together. The presence of acidic citrullinated GFAP species, however, indicate that phosphorylation may also be contributing to the solubility of these GFAP filaments, as increased phosphorylation is known to depolymerize cytoskeletal forms of IF proteins [180, 193].

Interestingly, we found that the retinal explant culturing process enhanced the extent of citrullination causing hypercitrullination, making this explant biochemical assay not only reliable, but also suitable for drug testing under controlled conditions. The hypercitrullination pattern observed in cultured retinal explants appeared similar to that reported for human astrocytes cultured under hypoxia where the early detection of PAD enzyme and that of a ~65 kDa GFAP citrullinated isoform was also reported [156]. The robust hypercitrullination being observed largely in the soluble fraction, in stark contrast to the minor changes in citrullination in the insoluble fraction, indicated that the majority of citrullinated proteins in this system represent proteins that were solubilized at low salt conditions. These data, in conjunction with the diffuse citrullinated GFAP spots seen by 2D western blots and the interrupted staining pattern of F95 in GFAP-containing filaments, suggested that dynamic exchange of citrullinated and phosphorylated soluble GFAP with filamentous structures may be occurring during gliosis. It is possible that citrullination of vimentin may also alter antigenic reactivity, as it does with GFAP [193]. It will be important in the future to examine citrullination patterns of both GFAP and vimentin in less severe retinal injuries that recover structural integrity to ascertain how the phenotype-biomarker relationship in retinas changes in models of reversible gliosis that promote healing over fibrosis.

Since WFA and Cl-amidine both have established targets with pathological roles that can be inhibited at non-toxic drug doses [116, 13, 46, 151, 153, 67, 162], our interest in knowing whether these drug targets interacted to affect global citrullination revealed an interesting result. Binding of WFA to soluble IFs [13], which likely causes increased IF phosphorylation [153, 77], was found to increase the effectiveness of PAD inhibition for inhibiting global citrullination. One explanation for the synergistic drug effect is that WFA-bound soluble GFAP may complex with active PADs, and thereby, sensitize PADs to Cl- amidine. Soluble phosphorylated vimentin bound by WFA has been shown to complex with phosphorylated ERK1/2 and filamin A in myofibroblasts and co-exist in multimeric protein complexes that blocked nuclear translocation of pERK1/2 by WFA treatment [77]. Similarly, complexes between

soluble GFAP and PADs might be induced by WFA activity that could effectively alter PAD intracellular localization or its activity through mechanisms as yet unknown.

The presence of IFs that display a colocalization with citrullinated epitopes at the early stages after injury and temporal changes observed along both established and developing filaments, implicate this PTM as a likely dynamic regulator of cytoskeletal alterations in Müller glia. The confocal microscopic orthogonal views highlight this importance by noting that not only were citrullinated epitopes directly co-localized with IFs from the earliest stages, but these modifications also occurred interspersed along the length of filaments. Immunohistochemical analysis of injured retinas also showed a protrusion into the vitreal space that is reminiscent of the "glial sprouts" (Fig. 2-S3), which show some similarity to idiopathic human retinas from AMD patients [40]. These extensions into the vitreal space indicate a breakdown in inner limiting membrane (ILM) integrity, which is made largely from Müller glial end feet. To this end, it will be important in the future to examine how such changes to the IFs impacts the architecture of the Müller cell.

The initial activation in injury indicates that the Müller cells, with their position near the vitreous space and presence of stretch receptors [194], are the major glial sensors in the retina and organizers of retinal injury response. Our findings parallel those found using the laser injury model that showed early reactivity of Müller glia that precede choroidal neovascularization, suggesting gliosis sensitizes the entire retina to retinal pigment epithelial injury [195, 196]. Recent research has found that both citrullination and PAD levels were increased after exposure to increased ocular pressure (IOP) [38, 39, 183, 197]. The mouse alkali injury models clinical alkali injuries associated with glaucomatous pathology and increased IOP [61]. Müller glial cells responding to such increased IOP may be responsible for the increase in citrullination we observed after injury and in glaucoma. While the *in vivo* injury maintains pressure throughout the vitreous, the explant system devoid of this increased IOP could trigger the response of

Müller glia, possibly accounting for the differences seen between the *in vivo* injury and the explant culture system.

Gliosis has remained an untreatable condition, despite numerous attempts to unravel the intricate responses involved in the mammalian system. Here, we have identified that the PTM of citrullination is an important mechanism in reactive gliosis that could provide a druggable target for retinal disorders as it has in other clinical conditions [198].

Acknowledgements

This work was supported in part by funding from the National Eye Institute/NIH grant R01EY016782 and from the John A. and Florence Mattern Solomon Endowed Chair in Vision Biology and Eye Diseases.

Supplemental Information

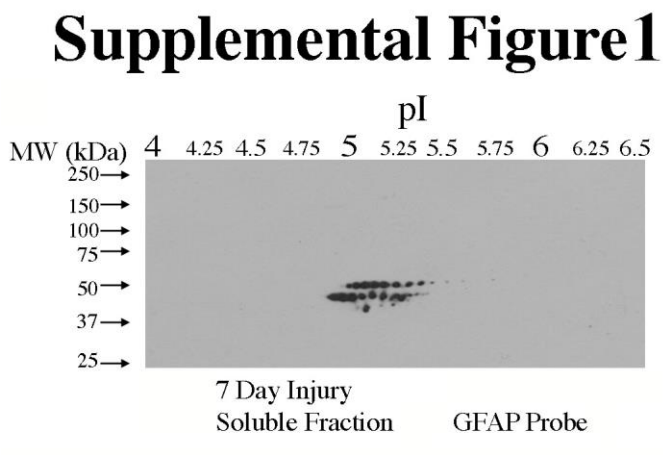

Fig. 2-S1. Two Dimensional IEF analysis of GFAP from injured retinas.

Eyes from 7 day injured mouse retinas were collected and retino-choroidal tissues from the posterior eye-cups were extracted into the soluble lysate. This soluble fraction was directly separated by 2-dimensional gel electrophoresis and protein blot was probed with the rabbit anti-GFAP antibody that recognizes native unmodified species.

Supplemental Figure 2

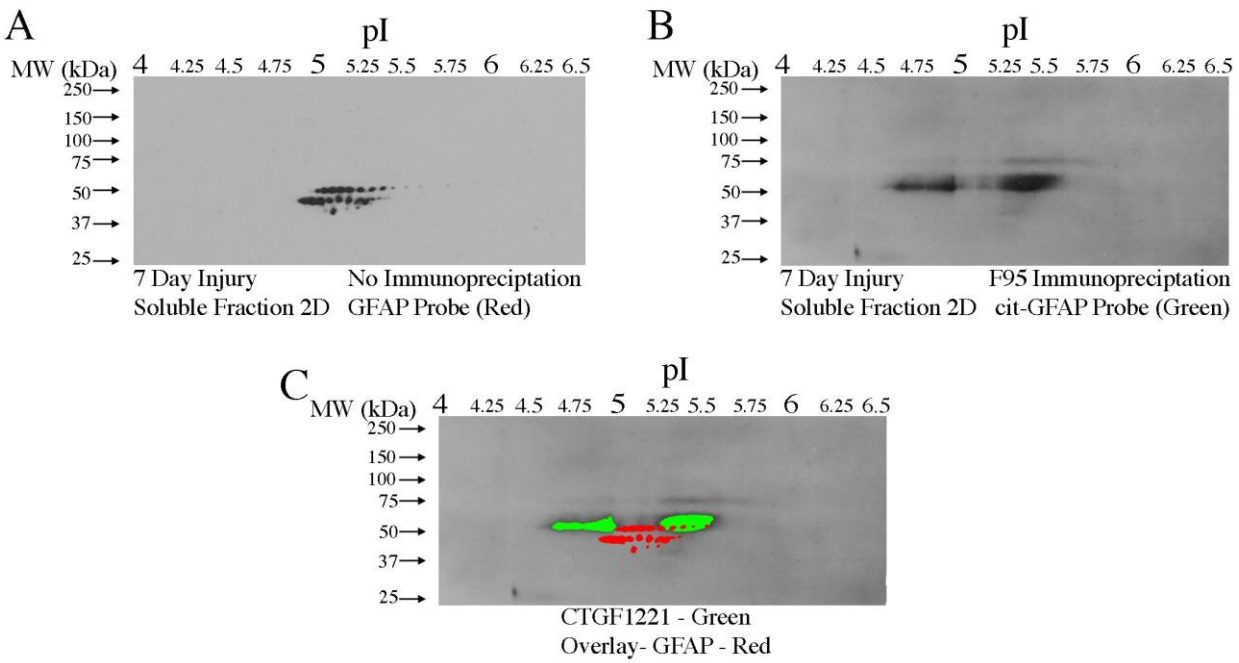

Fig. 2-S2. Overlaid images of GFAP and citrullinated GFAP.

Mouse eyes were injured and left to recover for 7 days in vivo. On day 7, retino-choroidal tissues from the posterior eye-cups were extracted into soluble fractions. The soluble fractions were then either (A) directly separated by 2-dimensional gel electrophoresis or (B) immunoprecipitated for F95 reactive species and then separated by 2-dimensional gel electrophoresis. The protein blots from these analysis were then probed for (A) total GFAP or (B) citrullinated GFAP (CGTF-1221 antibody). The digital images were then overlaid (C) to compare different GFAP species (red) with those that contained citrullinated species (green).

Supplemental Figure 3

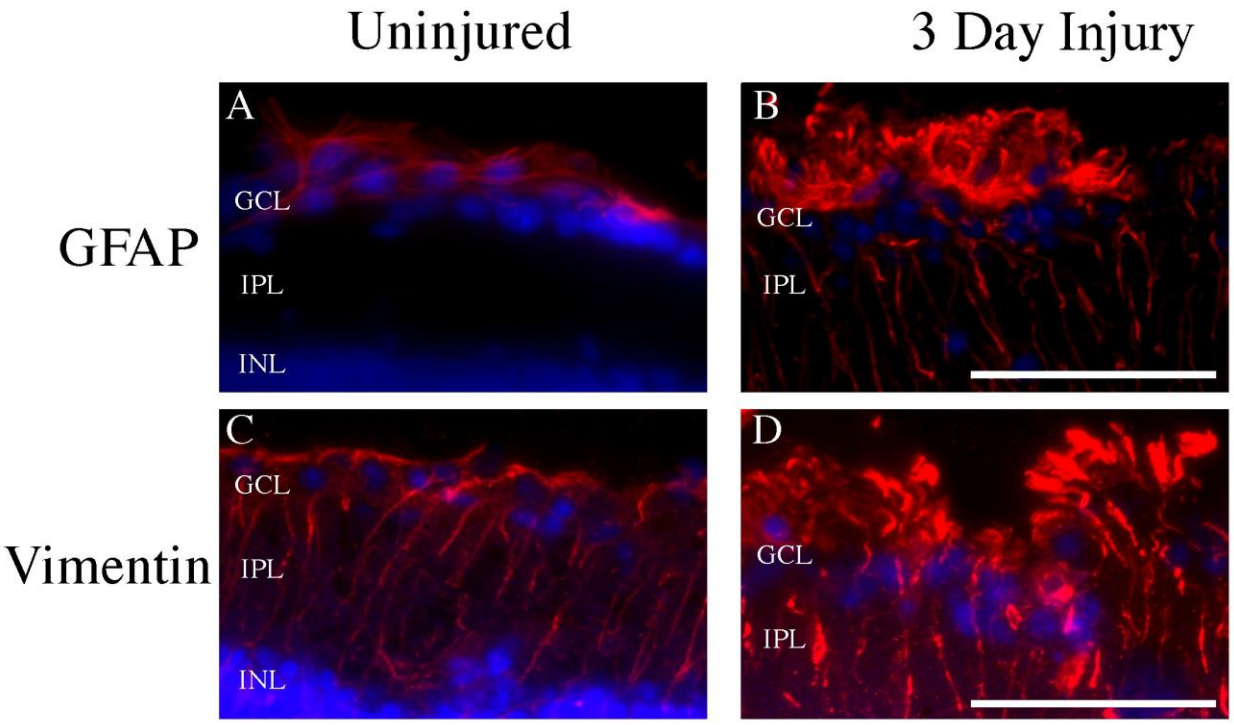

Figure 2-S3. Glial Sprouts as a Result of Alkali Injury

Mouse eyes were either left uninjured or injured and left to recover for 3 days. Eyes were then examined by immunohistochemistry at uninjured or 3 days for GFAP (A-B) or vimentin (C-D) and treated with DAPI to stain nuclei. (Scale bar =70 µm)

Supplemental Figure 4

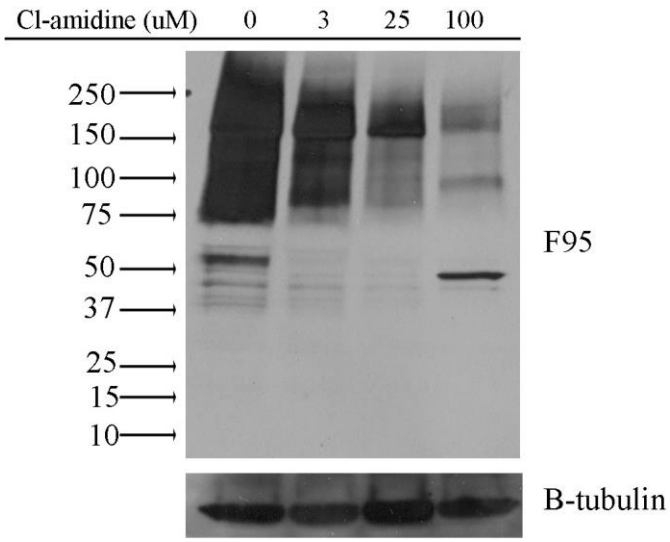

Fig. 2-S4. Response of citrullinated proteins to Cl-amidine dosage in posterior eye-cup explant culture.

Mouse eyes were injured and left to recover for 7 days *in vivo*. On day 7, eyes were enucleated and intact posterior eye-cups were placed into culture with vehicle DMSO (lane 1) or different concentrations of Cl-amidine (lanes 2-4) for 3 days. Retino-choroidal tissues from the posterior eye-cups were extracted and soluble fractions analyzed by western blotting for citrullinated proteins (F95 antibody), and subsequently, for β-tubulin on the same membrane for loading control.

Fig. 2-M1: Co-localization of Citrullination on GFAP Filaments at 3 hours

Plane-by-Plane Confocal Imaging of 3 Hour Injured eyes Immunostained for F95 (green), GFAP (red), DAPI (blue). Confocal z-stacks were obtained on a Zeiss 780 Confocal microscope at 63X. Individual planes were then increased in brightness to the same level in Lightroom. Images were re-assembled as a .mov at 0.5 seconds per focal plane. Images encompass planes containing GFAP filaments to highlight co-localization with citrullinated species over the length of individual filaments.

Fig. 2-M2: Co-localization of Citrullination on GFAP Filaments at 3 days

Plane-by-Plane Confocal Imaging of 3 Day Injured eyes Immunostained for F95 (green), GFAP (red), DAPI (blue). Confocal z-stacks were obtained on a Zeiss 780 Confocal microscope at 63X. Individual planes were then increased in brightness to the same level in Lightroom. Images were re-assembled as a .mov at 0.5 seconds per focal plane. Images encompass planes containing GFAP filaments to highlight co-localization with citrullinated species over the length of filaments.

Fig. 2-M3: Co-localization of Citrullination on Vimentin Filaments at 3 hours

Plane-by-Plane Confocal Imaging of 3 Hour Injured eyes Immunostained for F95 (green), vimentin (red), DAPI (blue). Confocal z-stacks were obtained on a Zeiss 780 Confocal microscope at 63X. Individual planes were then increased in brightness to the same level in Lightroom. Images were re-assembled as a .mov at 0.5 seconds per focal plane. Images encompass planes containing vimentin filaments to highlight co-localization with citrullinated species over the length of individual filaments.

Fig. 2-M4: Co-localization of Citrullination on Vimentin Filaments at 3 days

Plane-by-Plane Confocal Imaging of 3 Day Injured eyes Immunostained for F95 (green), vimentin (red), DAPI (blue). Confocal z-stacks were obtained on a Zeiss 780 Confocal microscope at 63X. Individual planes were then increased in brightness to the same level in Lightroom. Images were re-assembled as a .mov at 0.5 seconds per focal plane. Images encompass planes containing vimentin filaments to highlight co-localization with citrullinated species over the length of individual filaments.

Chapter 3

Expression and Contribution of Peptidylarginine Deiminase (PAD) 4 Enzyme to Retinal Gliosis

John W. Wizeman and Royce Mohan

Author Contributions:

John Wizeman: Conception and design of experiments, collection, analysis and interpretation of results, manuscript writing

Royce Mohan: Conception and design of experiments, interpretation of results, financial support, manuscript writing

This chapter prepared to be submitted in a peer-reviewed journal.

3.1 Introduction

Retinal gliosis is a reactive process that underlies most retinal pathologies [8, 22]. Astrogliosis in all areas of the central nervous system (CNS) has many similar characteristics [199, 200]. In the retina it is undertaken by Müller glial cells and the ganglion cell layer astrocytes [22, 40]. These cells provide trophic and structural support to the neuronal cells of the retina [8, 22]. The reactivity seen in both injury [13, 46, 17, 192] and disease [201] is often characterized by the increased expression of the type III intermediate filament (IF) proteins vimentin and glial fibrillary acidic protein (GFAP) [13, 46]. While GFAP and vimentin are the cytoskeletal proteins in the uninjured astrocyte and Müller cell, respectively, these proteins are upregulated in pathological conditions, to both the benefit and the detriment of the retina [22, 202]. A better understanding of the IFs, from both a physiological and pharmacological [14, 13] standpoint remains an important goal to be achieved.

One of the ways in which the IFs are controlled *in vivo* is by post-translation modification [77]. Among these is the relatively understudied modification known as citrullination [33]. Citrullination, or deimination, is a calcium dependent post-translational modification to arginine that removes a positive charge [34]. This process is carried out by the peptidylarginine deiminase (PADs, EC 3.5.3.15) family of enzymes. In mammals there are five PAD enzymes, often found to have differing tissue expression [34]. Interestingly, PAD4 is abundant at the synovial joint in rheumatoid arthritis [37], where there is a coincident increase of citrullinated vimentin in human patients [221]. This citrullinated vimentin is a biomarker of disease in RA [37]

In the mammalian retina, citrullination levels are increased in patients with Age-Related Macular Degeneration (AMD) compared to controls [38]. In cultured astrocytes, PAD enzyme and citrullination levels are increased when subjected to increases in mechanical pressure [183]. Increased levels of citrullination and PADs have been identified in a number of different CNS disorders, including Alzheimers Disease [19, 134], Glaucoma [39], Parkinsons Disease [134], Scrapie [144], Creutzfeldt- Jakob Disease [145], and Multiple Sclerosis (MS) [35]. In MS, the PAD4 enzyme is overexpressed and can translocate to the nucleus to citrullinate histone H3 [203]. The direct contribution of PAD4 and the effect of deimination on different targets remain unknown in many of these diseases.

Previously, we have shown that GFAP and vimentin levels are increased [13] and filaments become deiminated after injury. This change happens quickly after injury (1 hour), and can be targeted by a synthetic PAD inhibitor in an *ex vivo* retinal explant system that induces hypercitrullination. Here, we set out to determine the expression and location of the PAD4 enzyme, associated with CNS disorders, in the injured retina. We found that several PAD genes are transcribed in the uninjured and injured retina, and that the different isozymes have different cellular sources, although both PAD2 and PAD4 are expressed in glial cells. Further, these enzymes can be targeted by intravitreal injection in the retina after injury. Surprisingly, by targeting PAD4 with streptonigrin [168], a potent PAD4 specific inhibitor, we were able to show a decrease in detectable levels of GFAP. This new information indicates that the PAD

enzymes are present in the retina, meaning that they could react quickly to changes after injury or slowly during disease, and that this modification may play an important role in the initiation of gliosis.

3.2 Materials and Methods

Mice

All animal experiments were conducted in accordance with procedures approved by IACUC committee of the University of Connecticut Health Center. Mice were housed in specific pathogen free cages in designated laboratory animal housing facilities.

Alkali Injury

Corneal alkali injuries were performed in 129S6/SvEVTac (Taconic, Hudson, NY) mice as previously described [13, 46] between 2 and 3 months with a minor modification. Mice were given an intraperitoneal (i.p.) injection of Ketamine/Xylazine, and corneas were anesthetized with proparacaine eye drops. A 1 µl drop of 1N sodium hydroxide was then applied directly to the central cornea for 45 seconds. Following injury, the eye was immediately flushed extensively with sterile phosphate buffered saline (PBS) solution. The corneal epithelium was gently removed using a Tooke knife, and eyes were then treated topically with atropine, followed by tobramycin and erythromycin. For time course studies, injured mice were treated daily with topical applications of tobramycin and erythromycin for 3 days post-injury and humanely sacrificed by CO_2 inhalation at different times.

RNA extraction, RT-PCR and qPCR

RNA was extracted from the indicated tissues using a Qiagen RNeasy Mini Kit (Cat #74104, Qiagen) according to manufacturers instructions. RNA was treated with DNAse (Ambion AM1907) to remove contaminating genomic DNA. RNA was then reverse transcribed into corresponding cDNA using SuperScript III Reverse Transcriptase and diluted to 75 ng/ul. Tissue was screened for each of the

following primer pairs: GAPDH (For 5' – ATG ACA TCA AGA AGG TGG TG; Rev 5' CAT ACC AGG AAA TGA GCT TG); PAD2 (For 5' – GTT ATG TTC AAG GGC CTG GGA GGC ATG; Rev 5' – TAG CAC GAT CAT GTT CAC CAT GTT AGG); PAD3 (For 5' – TTC TCC GAG ACC CCC ATC TT; Rev 5' – TTA TTC CTC ACC CGG CAC AC); PAD4 (For 5' – CGA TTG GCT CTT TGT GGG TC; Rev 5' – CCG AAA ACC CTG CTT GTC C; or For 5' – TCT TTG TGG GTC ACG TGG ATG AGT; Rev 5' AGC TCC TGG AAC AGC TGA TAG CAA) and under the following cycling conditions: GAPDH – RT-PCR 1: 94C for 3 minutes; 2: 94C for 30s; 3: 45C for 30s; 4: 72C for 1 minute; repeat 2-4 for 35X; 72C for 5 minutes; qPCR – 1: 95C for 1 minute, 2: 95C for 15s, 3: 60C for 30s, repeat 2-3 for 40X; PAD2 – RT-PCR 1: 94C for 3 minutes, 2: 94C for 40s, 3: 57C for 30s, 4: 72C for 40s, repeat 2-4 for 35X, 5: 72C for 7 minutes; qPCR – 1: 95C for 3 minutes, 2: 95C for 30s, 3: 55C for 30s, repeat 2-3 for 39X; PAD3 – RT-PCR 1: 94C for 3 minutes, 2: 94C for 1 minute, 3: 58 C for 1 minute, 4: 72C for 3 minutes, repeat 2-4 for 40X, 5: 72C for 10 minutes; PAD4 – RT-PCR 1:94C for 3 minutes, 2: 94C for 30s, 3: 52C for 30s, 4: 72C for 45s, repeat 2-4 for 34X, 5:72C for 5 minutes; qPCR – 1: 95C for 3 minutes, 2: 95C for 15s, 3: 51.5C for 45s, repeat 2-3 for 40X. Triplicates were analyzed by qPCR for GAPDH, PAD2 and PAD4 on a Bio-Rad CFX96 Touch real time PCR detection system. Fold change (normalized to GAPDH levels) was compared to uninjured and is expressed as fold change +/- standard deviation. Statistical differences were identified by two-tailedt-test.

Antibodies

The antibodies used were GFAP (IHC: EMD Millipore AB5541 1:500; WB: AB7260 1:4,000), PAD2 (Abcam ab50257 1:50), PAD4 (IHC: Abcam ab50247 1:100; WB: Bioloegend #684202 1:1,000), β-III Tubulin (Abcam ab18207 1:100), F95 antibody for citrullinated proteins (EMD Millipore MABN328 1:50), GAPDH (Santa Cruz sc-25778 1:1,000), goat anti-mouse IgM 488 (Alexa 1:500), goat anti-rabbit 488 (Alexa 1:500), goat anti-chicken 594 (Alexa 1:500), goat anti-rabbit 594 (Alexa 1:500), goat anti- rabbit HRP (Santa Cruz 1:1,000), goat anti-mouse IgM HRP (Jackson Immunoresearch 1:5,000).

Protein Extraction and Western Blotting

Three mouse eye-cups were placed in ice-cold soluble buffer (20 mM Tris buffer, 200 mM NaCl, 1% NP-40) supplemented with a proteinase inhibitor cocktail (Roche, Indianapolis, IN) and tissue was minced into pieces on ice. Samples were left on ice for 45 minutes and then spun at 14,000 RPM for 5 minutes at 4 ^{o}C. The supernatant was removed and labeled as the "soluble" fraction (containing soluble forms of IF proteins). Lysates were then passed repeatedly through a 26-gauge needle 10 times to shear DNA. After, Bicinchoninic Acid Assay (Pierce, Waltham, MA) was used for quantification of protein. Protein samples were boiled 95-100 ^{o}C for 5 to 10 minutes in Laemmli buffer and then loaded on 4-20% Tris-HCl SDS-polyacrylamide gels (Bio-Rad). Proteins were transferred onto a 0.2 µm PVDF membrane (Bio-Rad, Hercules, CA). Membranes were blocked in 5% milk in 1X Tris Buffered Saline + Tween (TBST) for 1 hour at room temperature, then incubated with primary antibody for 1 hour at room temperature or overnight at 4^{o} C. Membranes were washed 3 times for 15 minutes, then incubated with secondary antibody for 45-60 minutes at room temperature. Membranes were washed 4 times for 15 minutes and developed with Enhanced Chemiluminescence (ECL; Bio-Rad) solution. To normalize for protein loading, membranes were stripped in 10X Tris-Glycine-SDS buffer for 30 minutes at RT, then probed as above with glyceraldehyde 3-phosphate dehydrogenase (GAPDH). All figures are shown with corresponding GAPDH control beneath. Western blots were then quantified using ImageJ to generate densitometric graphs. Experiments were repeated three times, and are presented as mean +/- standard deviation (SD). Significance was determined by t-test ($p \leq 0.05$).

Intravitreal injections

1ul of 125nM streptonigrin (Sigma) was injected intravitreally, assuming a final volume of ~5ul by Hamilton Syringe, to achieve ~25nM final concentration. Mice were injured in vivo and humanely sacrificed by CO2 inhalataion. After sacrifice, eyes were enucleated and kept in 1X Phosphate Buffered

Saline (PBS) +Antibiotic/Antimycotic (GE Life Sciences), at RT until injection. First, an initial puncture of the outer layers of the globe was made using a Becton Dickinson 30G x ½ in needle, keeping intact the globe structure (BD #305106). Next, we injected 1 ul of streptonigrin dissolved in DMSO/PBS directly into the vitreal space. After injection, eyes were incubated for 5 hours at 37C and 5% CO2. After 5 hours, posterior eye-cups were separated from the anterior eye and subjected to protein extraction as described.

3.3 Results

PAD2 and PAD4 mRNA transcripts are detectable in the retina

We employed an ocular injury model that induces retinal gliosis [13, 46] to identify changes in the expression of PAD enzymes within the central nervous system. Previously, we have shown that there are increases in citrullinated proteins as early as 1 hour after injury (Chapter 2). These citrullinated epitopes are found along GFAP and vimentin filaments within Müller glial cells of the retina, and GFAP specifically has been shown to be citrullinated. It has been previously reported that PAD2 is present in the retina and optic nerve of patients with glaucoma [197] and AMD [38]. Additionally, PAD3 is expressed in human neural stem cells [123], and PAD4 is found in the brain of Alzheimer's [143] and Multiple Sclerosis [203] patients. We set out initially to determine the expression of the known neural PAD enzymes in the uninjured and injured retina. PAD2 transcript was found in the uninjured and injured retina (Fig 3-1A), although present at modestly higher levels in the uninjured retina than 7 days after injury (Fig. 3-1A, B). PAD3 transcript was absent in the retina at all stages (Fig. 3-1A). PAD4 transcript was found in both the injured and uninjured retina (Fig. 3-1A,C) though increased in the retina greater than 4 fold early after injury and greater than 24 fold by 7 days (Fig. 3-1D). Due to the reported expression patterns we did not screen for PAD1 [106] or PAD6 [133] transcripts in the injured or uninjured retina.

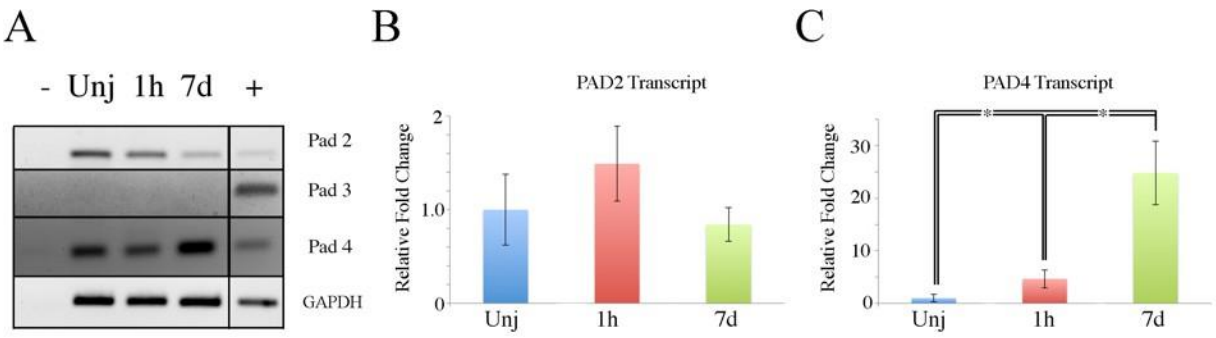

Figure 3-1. PAD2 and PAD4 transcripts are expressed in the retina

PCR analysis of PADs 2-4 in the uninjured posterior eye-cup (unj) and eye-cups at 1 hour (1h) and 7 days (7d) post injury. (A) RT-PCR products from different timepoints run on a 1.2% agarose gel. Positive controls contained cDNA from brain, spleen, skin and hair. H2O was run as negative control. (B) Quantitation of fold change (normalized to GAPDH levels) identified by qPCR of PAD2 transcripts at different timepoints compared to uninjured qPCR. (C) Quantitation of fold change (normalized to GAPDH levels) identified by qPCR of PAD4 transcripts at different timepoints compared to uninjured qPCR results (* = $p \leq 0.05$, t-test).

PAD4 protein is increased in the injured retina

The identification of increased levels of PAD4 transcript suggested that the PAD4 protein may be responsible for deimination in the posterior eye-cup. We therefore set out to determine whether PAD4 protein levels were also altered by injury. When we examined levels of PAD4 in the uninjured and injured retina, we observed that a ~65-67 kDa species was significantly increased in the injured retina over uninjured controls (Fig. 3-2A,B, Unj =1.91±.0.38; 7d=3.59±0.42). PAD4 immunoreactivity was also observed in the uninjured posterior-eye cup. Interestingly, we also observed a PAD4 immunoreactive cleavage product at 50 kDa in the injured eye (Fig. 3-2A).

PAD2 is expressed in Astrocytes in the Uninjured Retina

Having identified the PAD enzymes present in the injured and uninjured retina, we next wanted to localize PAD expression in the retina after injury. We have previously identified that citrullinated proteins are expressed along GFAP and vimentin filaments. This indicated that the location of modified species in the retina was likely in Müller glial cells or astrocytes. To test this hypothesis, we examined expression of PAD2 in uninjured and injured eyes along with GFAP expression. In the uninjured eye, PAD2 expression can be seen in the inner layers of the retina (Fig 3-3A, C), including GFAP positive cells in the ganglion cell layer and inner plexiform layer. 7 days after injury, we observed minimal PAD2 expression (Fig. 3-3D-F). GFAP increased expression throughout the layers of the inner retina after injury, as previously observed (Chapter 2). Disorganization seen in the ganglion cell layer mimics previous findings (Chapter 2).

PAD4 expression in the Uninjured and Injured Retina

We next examined PAD4 expression in the same timeframe of injury. Again, GFAP expression was restricted to the ganglion cell layer astrocytes (Fig. 3-4A) in the uninjured eye. Surprisingly, in the uninjured eye, there was no distinct PAD4 protein expression pattern (Fig. 3-4B) identifiable by immunohistochemistry, despite the presence of an immunoreactive species by western blot. 7 days after

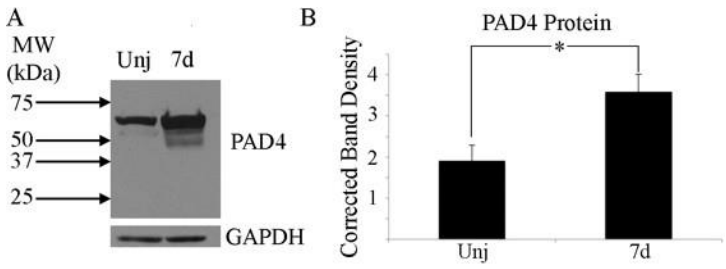

Figure 3-2. PAD4 Protein Expression is increased in the Injured Retina

Western blot analysis of PAD4 protein in posterior eye-cups from uninjured mice (Unj, A lane 1) and eye-cups from mice 7 days post injury (7d, A lane 2). Species immunoreactive against PAD4 antibody were identified in uninjured and injured eye-cups at ~65-70 kDa. Immunoreactivity against a ~50 kDa species is identifiable in the injured eye (lane 2). (B) Densitometric quantitation of immunoreactive bands with ImageJ (* = $p < 0.05$, t-test).

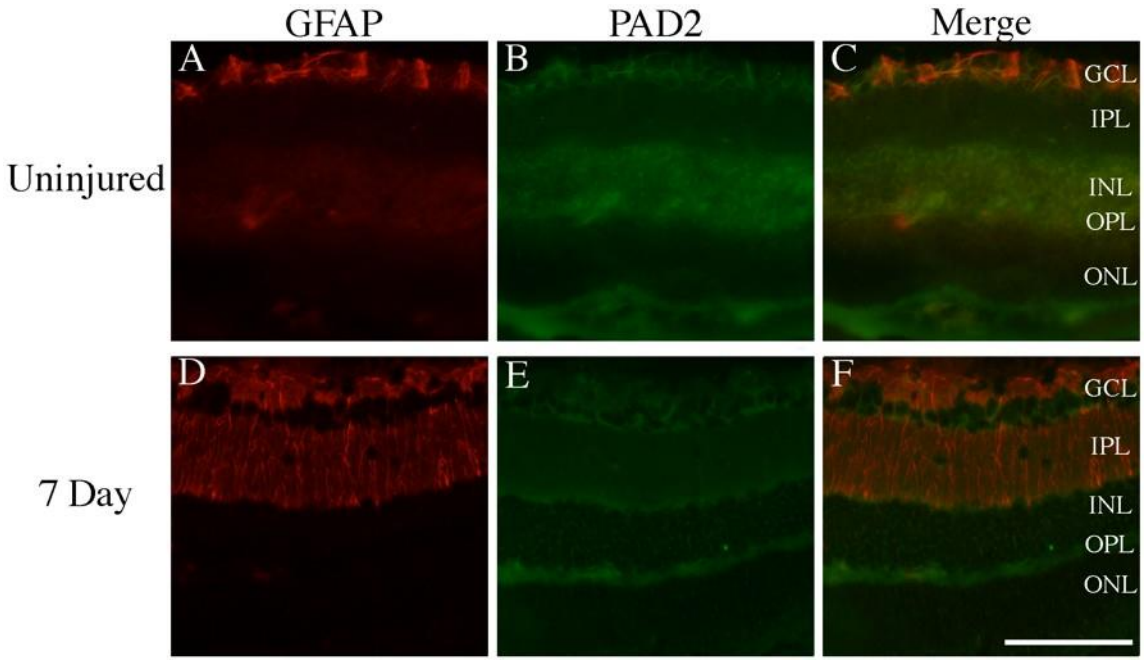

Figure 3-3. PAD2 localization in the Uninjured and Injured Retina

Cryosections from uninjured and injured eyes were stained using antibodies against GFAP (red) and PAD2 (green). Tissue sections were examined under fluorescent microscope at 20X maginification from uninjured eyes (A-C), and 7 day (D-F) post injury eyes. (A) GFAP and (B) PAD2 expression was restricted to the Ganglion Cell Layer astrocytes (C) in the uninjured retina. Scale bar = 100 µm

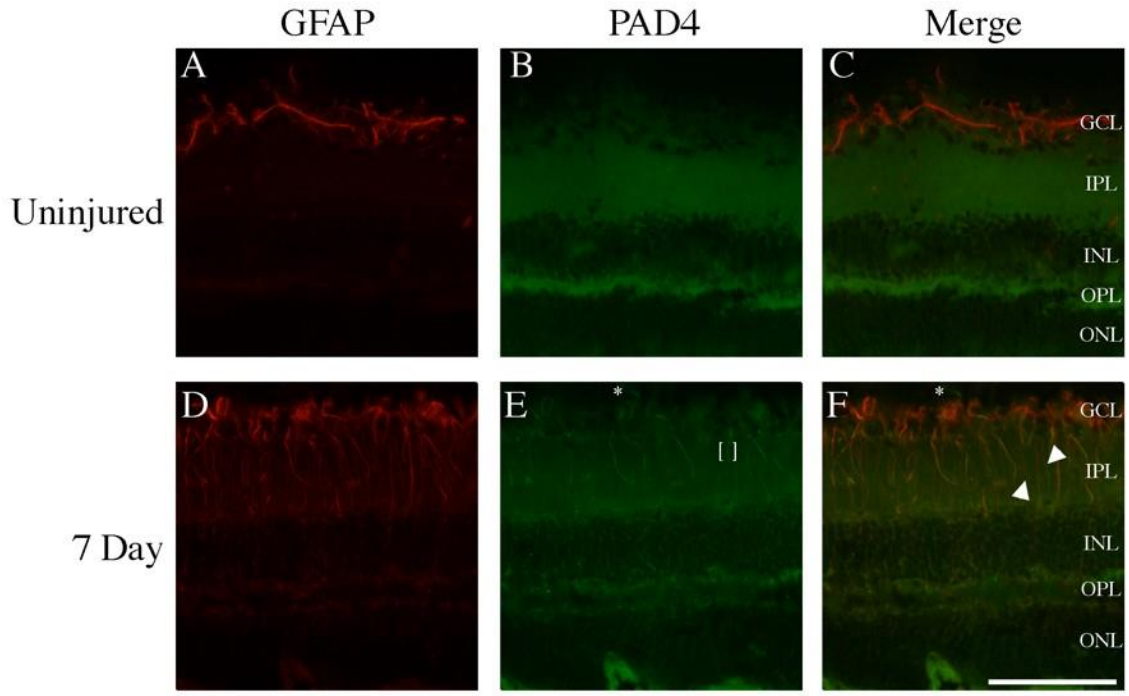

Figure 3-4. Localization of PAD4 protein in the Uninjured and Injured Retina

Cryosections from uninjured and injured eyes were stained using antibodies against GFAP (red) and PAD4 (green). Tissue sections were examined under fluorescent microscope at 20X magnification from uninjured eyes (A-C), and 7 day (D-F) post injury eyes. (E, bracket) Filamentous PAD4 expression in the inner retina. GFAP filaments without PAD4 immunoreactivity (F, arrowheads). Protrusion of PAD4 positive cell into vitreal space (E, F, asterisk). Scale bar = 100 µm

injury, PAD4 expression was observed through the layers of the inner retina (Fig. 3-4F). This PAD4 expression aligns with GFAP expression in Müller glial cells after injury. Interestingly, the expression of PAD4 did not coincide at a 1:1 ratio with GFAP filaments (Fig. 3-4E, F, arrowheads). PAD4 immunoreactivity exhibited a filament like expression pattern (Fig 3-4E bracket), with PAD4 positive processes extending toward the vitreous (Fig. 3-4E, asterisk).

Intravitreal Inhibition of PAD4 prevents GFAP expression

Identifying PAD4 as a potential source of citrullination in Müller glial cells allowed us to more thoroughly investigate its role in retinal healing. Streptonigrin [168, 169] is a potent and irreversible PAD inhibitor selective for PAD4. We modified a previous explant system [Chapter 2, 17] to allow for short- term assessment of reactivity after injury. We tested the effect of streptonigrin compared to a vehicle after intravitreal injection and 5 hour incubation. We found that streptonigrin reliably inhibited the citrullination response after injury, as observed by levels of the F95 antibody by western blotting (Fig. 3- 5A). Interestingly, streptonigrin was potent at reducing GFAP expression at a 25nM intravitreal dose (Fig. 3-5B, C; Veh=2.78±0.57; 25nM=1.56±0.12 $p<0.05$).

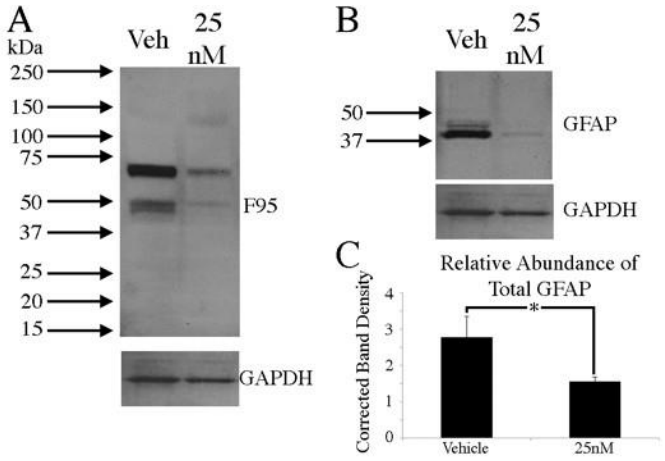

Figure 3-5. Intravitreal Injection of Streptonigrin downregulates GFAP expression in Injury

Western blot analysis of citrullinated proteins (A), and GFAP (B, C) with and without intravitreal injection of streptonigrin. Mice were injured and sacrificed 10 minutes after injury. Eyes were enucleated and kept in PBS +A/A for 5 hours. Eyes were injected with either DMSO (veh) or with streptonigrin (25nM). After 5 hours, posterior eye-cups were dissected and soluble lysate extracted. Lysate was run on SDS-PAGE gel and examined for immunoreactivity to F95 antibody (A, citrullinated proteins) or GFAP (B). Quantitation of GFAP bands by ImageJ (C) after streptonigrin treatment (*= $p<.05$, t-test)

3.4 Discussion

The control of retinal gliosis, specifically as it relates to the intermediate filaments, remains a goal within ocular research. Herein we have analyzed the levels of PAD4 transcript, PAD4 protein expression, and location of PAD4 after injury in the mouse retina. We have also identified citrullination as an important factor regulating the GFAP protein expression throughout the retina. As GFAP is a reliable marker for retinal stress [8], specifically in Müller glia, we were able to use the alkali injury model to show that inhibiting PAD4 was able to alter the gliosis process by leading to a decrease in detectable levels of GFAP. This finding indicates that citrullination in the retina is mediated by two specific PAD enzymes, and that they play an important role in the initiation of gliosis.

PAD4 is a known deimination target of itself [204]. Deimination of PAD4 decreases enzymatic activity, and can alter antigenic reactivity, as it does with GFAP. The identification of PAD4 in the uninjured retina, as well as the identification by immunoreactivity on western blot, suggests that the protein is expressed at some level within the uninjured posterior eye-cup. As this self-regulation of PAD4 may alter antigenic availability, the use of multiple PAD4 antibodies to fully examine PAD4 in the retina was required. The lack of immunogenic availability in the uninjured eye suggests that the pool of PAD4 protein in this condition may be a high turnover species.

The finding that the PADs are present in the uninjured retina suggests that they are expressed as a way to respond immediately to a change in calcium [205, 206], which has been experimentally shown to increase in Müller glial cells after cell stretching [207]. PAD2, present in the uninjured retina, is known to citrullinate vimentin, another type III IF [113]. PADs 1-4 are many orders of magnitude more enzymatically active in the presence of calcium, creating an ideal system to respond to changes induced by increased mechanosensitivity from Müller glia after increases in intraocular pressure [194, 205], or as a mechanism to respond to changes from excess calcium release from dying neurons. The propagation of calcium waves between Müller glia and astrocytes also provides a mechanism to synchronize the retinal response across the entire retina [208, 209, 210].

The development of more specific PAD inhibitors [211] has been beneficial not only in targeting the different PAD isozymes, but also in the identification of the targets and effects of specific PADs. Here, the use of streptonigrin as a PAD4-specific inhibitor [169] allowed us to identify this as the isozyme responsible for the initiation of gliosis. The effects of citrullination on the intermediate filaments are still widely unknown. We have previously identified citrullinated species along GFAP and vimentin filaments as early as 1 hour after injury, as well as the presence of two different citrullinated GFAP isoforms. The presence of these isoforms in the soluble fraction indicates that they are harnessed by Müller cells for a non-cytoskeletal function, such as chaperones and for transport [76, 77] seen in other systems. The finding that inhibiting PAD4 causes a downregulation of GFAP levels, indicative of overall gliotic response, suggests it has an effect on Müller glia at the transcriptional level. Considering that PAD4 contains a nuclear localization sequence and can be found in the nucleus [212], one possible mechanism involves the activation of PADs in the Müller endfeet and astrocytes of the ganglion cell layer by the increase in calcium, which leads to their transport toward the Müller nuclei along GFAP and vimentin filaments to trigger a cell-wide transcriptional response. This is supported when realizing that the deimination that occurs quickly after injury (1 hour) and precedes a number of other factors, including immune reactivity, which are increased [192] later in the alkali injury model, or that accumulate at a number of different times in other injury and disease models [201, 17].

The control of GFAP and vimentin as a means of controlling gliosis in the retina is a goal that remains incomplete. Here, we have established a method by which the control of IFs by PTMs and their expression can be controlled within the retina. This opens the possibility of examining the use of specific PAD4 inhibitors in controlling filament expression and the initiation of gliosis in more clinical settings.

Chapter 4

Clinical implications of Ocular Citrullination

John W. Wizeman and Royce Mohan

Author Contributions:

John Wizeman: Conception and design of experiments, collection, analysis and interpretation of results, manuscript writing

Royce Mohan: Conception and design of experiments, interpretation of results, manuscript revision, financial support

4.1 Introduction

Alkali Injury to the eye, as a robust clinical model, has given many insights into the processes of gliosis and fibrosis [13, 77, 46]. It also mimics several retinal disorders that have a higher prevalence and incidence. For instance, alkali injury leads to an increase in intraocular pressure, such as that seen in glaucoma [61, 213]. More severe alkali injuries correspond to higher intraocular pressure [61]. It also leads to the upregulation of the type III Intermediate filaments in the cornea (vimentin) and in the retina (GFAP and vimentin). In the cornea, this injury induces massive neovascularization and angiogenesis as a consequence of fibrosis, which can be targeted with small molecules [13]. In the retina this leads to gliosis, an underlying condition in a number of retinal diseases, such as age-related macular degeneration (AMD) and glaucoma [46, 77]. This gliosis has been seen in a glaucoma mouse model (DBA/2J mouse line), associated with an increase in intraocular pressure [58, 59, 60].

We have previously used this alkali injury model to identify citrullination as a major initiator of gliosis in the retina. Importantly, we have shown that there is an increase in citrullination in the retina after injury and that the major enzyme responsible for this modification, peptidylarginine deiminase (PAD) 4, is increased after injury. Importantly, this model is the first to identify that direct injury to the cornea causes retinal pathology, highlighting important secondary effects that are not often considered in

a clinical setting [13, 46, 192]. Damage to the cornea increased levels of GFAP, vimentin, PAD4 and citrullination, all of which can be targeted in the research setting through the use of small molecules [13, 77, 46, 169]. The importance of identifying gliosis in ocular disorders that are not primarily targeting the retina remains an important but understudied aspect of ocular research.

Also important is the ability to identify markers of ocular disease and injury severity. While a number of different surgical options are available for conditions of the cornea and the lens, clinical interventions for the retina are limited. Even though increases in levels of GFAP are an excellent indicator of retinal health, the identification of a marker of total ocular health remains an important goal.

Acknowledging the importance of studies of the intermediate filaments to gliosis and fibrosis in ocular diseases, and having identified their upregulation [13, 77, 46], modification by the PAD enzymes, and ability to be targeted, we wanted to examine the role of citrullination and the filaments in other models of disease, as well as in non-retinal tissues. We set out to test the hypothesis that in glaucoma and alkali injury models citrullination of intermediate filaments was increased in ocular tissues, and that injury mimics a number of disease pathologies.

4.2 Materials and Methods

Mice

Eyes from 8 month old male and female DBA/2J (Jax) and C57BL6 (Jax) were enucleated after sacrifice and stored at -80C or immediately frozen in OCT (Tissue-Tek) for immunohistochemistry. WT129SvEV mice (Taconic) were used in alkali injuries.

Alkali Injury

Corneal alkali injuries were performed in 129S6/SvEVTac (Taconic, Hudson, NY) mice as previously described [13, 46] with a minor modification. Mice were given an intraperitoneal (i.p.) injection of Ketamine/Xylazine, and corneas were anesthetized with proparacaine eye drops. A 1 µl drop of 1.0N

sodium hydroxide was then applied directly to the central cornea for 45 seconds (1.0N). Following injury, the eye was immediately flushed extensively with sterile phosphate buffered saline (PBS) solution. The corneal epithelium was gently removed using a Tooke knife, and eyes were then treated topically with atropine, followed by tobramycin and erythromycin. For time course studies, injured mice were treated daily with topical applications of tobramycin and erythromycin for 3 days post-injury and humanely sacrificed by CO2 inhalation at different times.

Protein extraction

Three mouse eye-cups or three mouse corneas were placed in ice-cold soluble buffer (20 mM Tris buffer, 200 mM NaCl, 1% NP-40) supplemented with a proteinase inhibitor cocktail (Roche, Indianapolis, IN) and tissue was minced into pieces on ice. Samples were left on ice for 45 minutes and then spun at 14,000 RPM for 5 minutes at 4 ^{o}C. The supernatant was removed and labeled as the "soluble" fraction (containing soluble forms of IF proteins), while the pellet was placed into 1:3 diluted β-mercaptoethanol:Laemmli buffer to extract cytoskeletal forms of IFs and spun down at 14,000 RPM for 5 minutes at 4 ^{o}C. This protein extract was labeled as the "insoluble" cytoskeletal fraction. Both soluble and insoluble fractions were then passed repeatedly through a 26-gauge needle 10 times to shear DNA.

Western Blots

Bicinchoninic Acid Assay (Pierce, Waltham, MA) was used for quantification of protein. Protein samples were boiled 95-100 ^{o}C for 5 to 10 minutes in Laemmli buffer and then loaded on 4-20% Tris-HCl SDS-polyacrylamide gels (Bio-Rad). Proteins were transferred onto a 0.2 µm PVDF membrane (Bio-Rad, Hercules, CA). Membranes were blocked in 5% milk in 1X Tris Buffered Saline + Tween (TBST) for 1 hour at room temperature, then incubated with primary antibody for 1 hour at room temperature or overnight at 4^{o} C. Membranes were washed 3 times for 15 minutes, then incubated with secondary antibody for 45-60 minutes at room temperature. Membranes were washed 4 times for 15 minutes and

developed with Enhanced Chemiluminescence (ECL; Bio-Rad) solution. To normalize for protein loading, membranes were stripped in 10X Tris-Glycine-SDS buffer for 30 minutes at RT, then probed as above with glyceraldehyde 3-phosphate dehydrogenase (GAPDH).

Immunohistochemistry

Unfixed eyes were first frozen in OCT (Tissue-Tek, Radnor, PA) at -80 ^{o}C, before being cut on a cryostat at -24 ^{o}C. Sections were cut at 10 or 15 µm thickness, attached to Superfrost slides and stored at -80 ^{o}C until used. Slides were air dried for 30 minutes and then fixed in ice-cold methanol/acetone (5 min/1 min). Fixed slides were washed in PBS 3 times for 5 minutes, and then primary antibody was added in Dako background reducing solution (Dako, Glostrup, Denmark) at the specified concentration. Slides were incubated with primary antibody at 4 ^{o}C overnight and then washed 5 times for 10 minutes afterwards. Slides were then incubated with secondary antibodies at specified concentrations at room temperature in the dark for 1 hour, and subsequently washed 5 times for 10 minutes prior to imaging.

Antibodies

Primary antibodies used in the experiments included: rabbit polyclonal anti-GFAP (Abcam, Cambridge UK, 7779 1:4,000 WB, 1:500 IHC; Abcam 7260 1:20,000 WB, 1:500 IHC), mouse-IgM monoclonal F95 (anti-peptidyl-citrulline antibody, Millipore MABN328, 1:500 WB 1:200 IHC), rabbit polyclonal GAPDH (Santa Cruz, Dallas TX sc25778 1:500 WB), TGF- β2 (Santa Cruz sc-90 1:250 WB), rabbit polyclonal vimentin (Abcam ab45939 1:200 IHC); Secondary antibodies were Santa Cruz goat anti-rabbit IgG HRP (sc-2301 1:1000 WB), goat anti-mouse IgG HRP (sc-2302 1:1000 WB), goat anti-mouse IgM HRP (Jackson ImmunoResearch, West Grove, PA #115-035-075 1:5,000 WB) goat anti-mouse IgM 488 (Invitrogen A21042 1:500 IHC), goat anti-rabbit IgG 594 (Invitrogen A11012 1:500).

4.3 Results

Citrullination is elevated in the glaucomatous retina at symptom onset

In the DBA/2J model of glaucoma, symptoms that mimic the glaucoma pathology, such as increased intraocular pressure, are seen as early as 8 months [58, 59]. We compared DBA/2J retinas at 8 months of age to those of age matched C57BL6 mice. There was a marked increase in F95 reactive species (citrullinated proteins) at 8 months of age in both soluble and insoluble fractions of proteins in the DBA2J mice (Fig. 4-1A, B respectively). This increase in citrullination precedes any noticeable difference in levels of GFAP at the predicted molecular weight between the two mouse strains (Fig. 4-2A), indicating that gliotic activity in the glaucomatous retina is at a basal level. Interestingly, we were able to identify the aberrant high molecular weight GFAP in both mouse strains by 8 months of age, although only in the soluble fraction (Fig. 4-2A) of proteins, suggesting strain differences in the expression of GFAP.

Citrullination occurs along intermediate filaments in the glaucomatous retina

We next wanted to identify the potential targets of citrullination in the retinas of DBA/2J mice. We employed immunohistochemical staining of 8 month old C57BL6 and DBA2J eyes for GFAP, vimentin and F95 to examine the localization of citrullination along the intermediate filaments, as previously seen (Chapter 2). We found that at 8 months, both C57 and DBA2J mice showed immunoreactivity for GFAP expression through the layers of the retina, indicating at least a mild ongoing gliosis (Fig 4-3A,D). GFAP filaments showed a co-reactivity with citrullinated species in both mouse strains (F95; Fig 4-3 B,E). When examining vimentin, both DBA and C57 mice have vimentin filaments throughout the width of the retina, extending into the layers of the outer retina (Fig.4-3 G,J). Citrullinated species were also found along vimentin filaments, at a greater frequency than along GFAP filaments (Fig. 4-3 I, L). The ganglion cell layer in the DBA mice is also disorganized when compared to age matched controls, with GFAP expression extending beyond the ganglion cell nuclei (Fig. 4-3C, F, I, L).

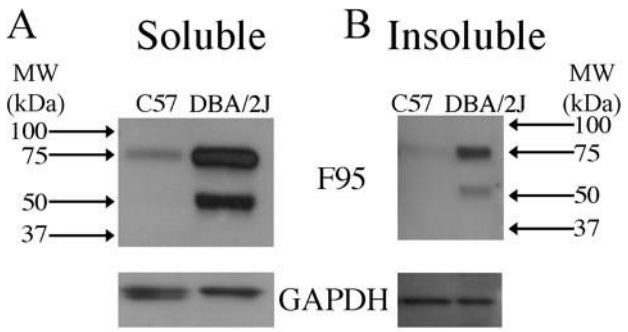

Figure 4-1. Citrullination in the glaucomatous retina

Western blot analysis of citrullinated proteins (F95) in posterior eye-cups from uninjured C57BL/6 (C57, lane 1) and DBA/2J (lane 2) mice at 8 months of age. Protein was extracted from either the soluble (A) or insoluble (B) fraction of proteins and run on SDS-PAGE gel.

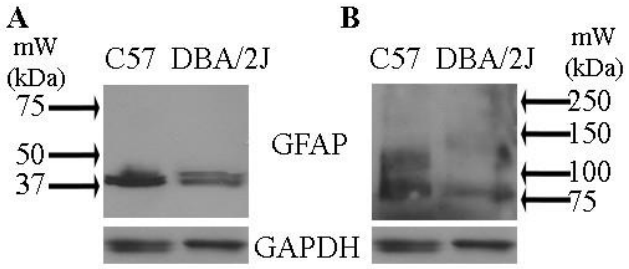

Figure 4-2. High molecular weight GFAP in the Retina

Western blot analysis of GFAP in posterior eye-cups from uninjured C57BL/6 (C57, lane 1) and DBA/2J (lane 2) mice at 8 months of age. Protein was extracted from either the soluble fraction of proteins and run on SDS-PAGE gel. (A) Predicted GFAP species in the retina. (B) High Molecular Weight GFAP identified in C57BL/6 and DBA/2J mice at 8 months on long exposure. GAPDH loading control from the same membrane is found underneath the corresponding lanes.

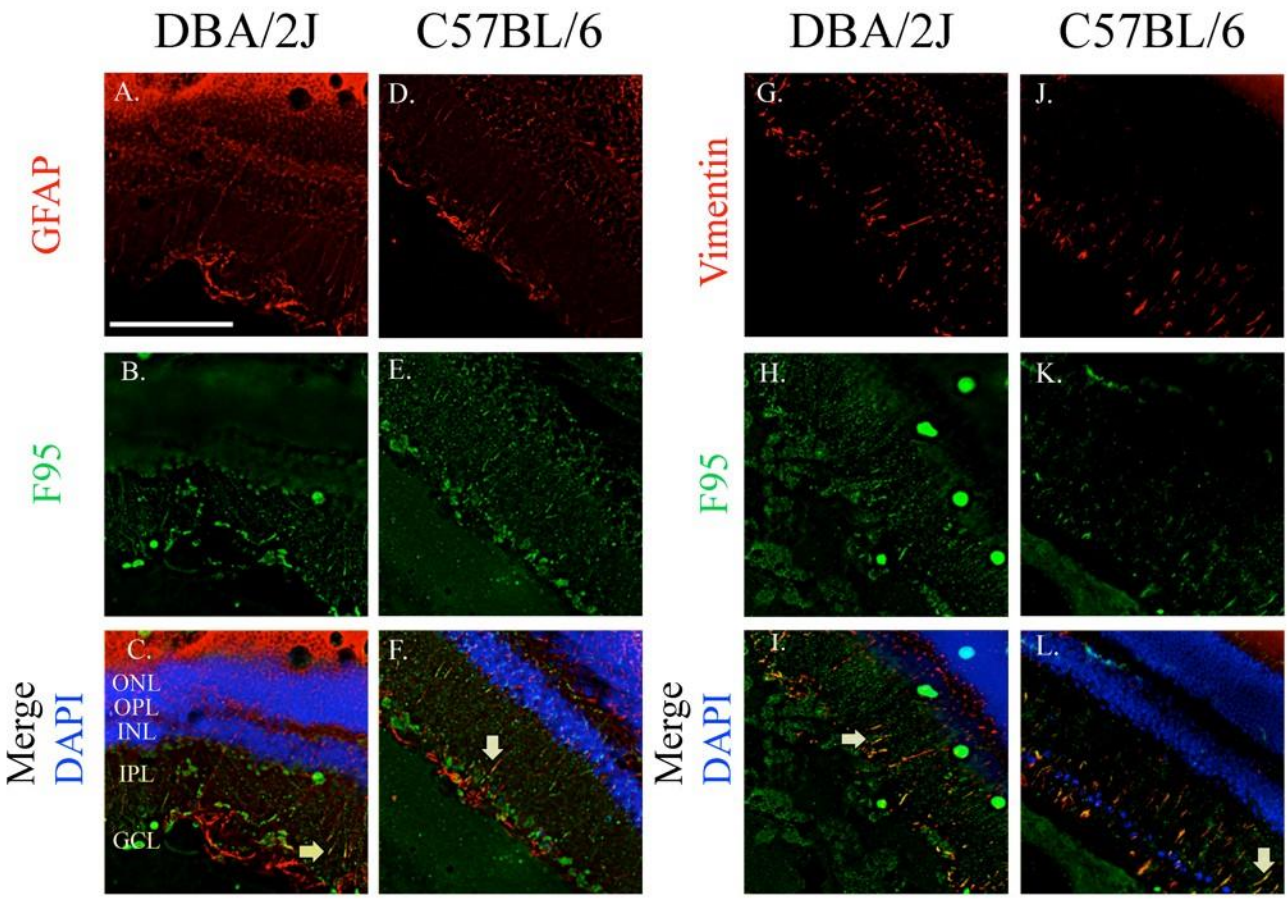

Figure 4-3. Citrullination along Müller Glial filaments in Control and Glaucomatous Retinas

Immunohistochemical examination of citrullinated proteins (F95), GFAP and vimentin of retinas from uninjured mice of either a DBA/2J or C57BL/6 strain at 8 months of age. Glaucomatous retinas (A-C, G-I) and control eyes (D-F, J-L) were examined for GFAP (A,D), and F95 (B, E) and merged images (C,F), as well as vimentin (G, J) and F95 (H, K) and merged images (I,L). Co-reactive filaments are marked by arrows (C, F, I, L). Scale bar = 70 µm

Citrullination is increased in the injured cornea

Lastly, as a means of examining total ocular health, we examined the cornea for the PTM citrullination. Interestingly, we found a significant increase in immunodetection at ~55kDa and a band at 75 kDa (Fig. 4-4). This corresponds to a similar increase seen in the retina as early as 1 day after injury (Chapter 2). Unlike the retina, there was no band at 50 kDa, but closer to the expected size of vimentin (~55kDa).

4.4 Discussion

Here, we have identified an increase in the levels of citrullinated proteins at an early stage of a glaucoma mouse model, and the presence of these citrullinated species along filaments of GFAP and vimentin in Müller glial cells, before a relevant increase in levels of GFAP protein. The alkali injury we have used also surprisingly exhibits glial sprouts, a sign of aging and AMD that may lead to retinal detachments. Finally, these citrullinated proteins also accumulate in the injured cornea, although different species appear to be citrullinated. Taken in context, this data indicates that citrullination is an important marker of the general state of the retina. It also indicates that alkali injury is an important and useful model of different pathologies seen in a number of ocular disorders.

Glaucoma, from a clinical standpoint, is mainly treated as a disease of the anterior segment of the eye [214]. Similar to clinical injuries to the cornea, the retina is often an afterthought. The initial expression of citrullinated proteins, before a noticeable increase in GFAP in the retina, in the DBA/2J mouse model indicates that the retina is responding at the same time as the recorded onset of increased intraocular pressure, the most well characterized clinical symptom of glaucoma. Combined with the increase in IOP that is seen in alkali injuries, and the increase in citrullinated proteins in both the cornea and retina, glaucoma appears to have an increase in citrullinated proteins that either precedes or corresponds to the major symptomatic presentation of the disease.

The formation of glial sprouts is common in AMD [40]. Importantly, these sprouts are also thought to influence the interaction between the retina and the vitreous [40], and are likely to be precursors to epiretinal membranes that can create retinal detachments [40]. The finding that these glial

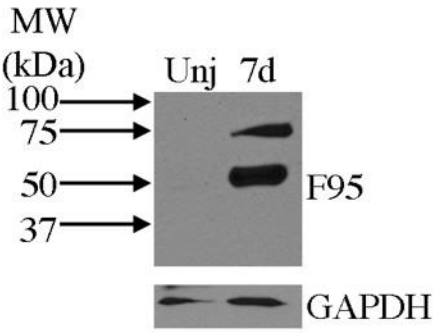

Figure 4-4. Citrullination is increased in the injured cornea

Western blot analysis of soluble fractions of uninjured corneal tissue or corneas left to recover for 7 days after injury. Injured corneas (7d) display immunoreactivity for citrullinated species (F95) at ~75 kDa and ~55kDa when compared to uninjured control tissue.

sprouts are present in alkali injury allows for investigation into their pathology that is less time-sensitive than genetic mouse models.

The identification of alkali injury as a model that mimics a number of different systems has provided us excellent insight into the response of the retina in a pathological state. It has also allowed for the identification of citrullination as a factor in a number of different diseases and tissues. The *in vivo* control of citrullination remains an important milestone for ocular research.

Chapter 5

Discussion, Significance, Working Model, Challenges and Future Directions

5.1 Discussion

The novel inhibitor withaferin A (WFA), which targets soluble forms of the type III intermediate filaments (IFs) vimentin and the glial fibrillary acidic protein (GFAP) [14], has proven to be a useful pharmacological tool in the study of retinal gliosis [13, 46]. Previous work in the Mohan lab identified this molecule as able to alter clinically relevant outcomes in corneal and glaucoma models of fibrosis [67] as well as retinal gliosis [13] by specifically altering the regulation of soluble GFAP and vimentin. In my thesis work I have examined another regulator of these IFs, the post-translational modification known as citrullination. Work shown in the previous chapters identifies a significant increase in levels of citrullinated proteins in retinal gliosis, and identified GFAP as a major target of citrullination in the retina. The use of PAD inhibitors, supplemented by the use of WFA, was able to downregulate these species in an injury explant system, highlighting the importance of being able to target these IFs. Building on previous work, which discovered that targeting soluble vimentin in a glaucoma model led to clinically relevant improvements [67], I observed citrullination of GFAP and vimentin filaments in the retina in a mouse model of glaucoma. Evidence of changes in citrullinated proteins preceded differences in GFAP protein levels. This suggests that citrullination is an initiating factor in GFAP expression, a major marker of gliosis. This citrullination occurs along GFAP filaments, as does the expression of PAD4 after injury. PAD4 protein is also significantly increased after injury. Meanwhile, PAD2 is expressed in astrocytes of the uninjured eye, but decreased after injury. Highlighting the importance of PAD4 in the pathological state, the use of the PAD4 specific inhibitor streptonigrin was able to decrease accumulation of GFAP when delivered via intravitreal injection. These findings of citrullination in the injured retina are mirrored in glaucomatous retina as well as injured corneas. It was also discovered that perturbation of vimentin effectively blocked the translocation of ERK to the nucleus, identifying a mechanism by which WFA effectively alters the soluble function of vimentin [77]. Important to the development of a similar working

model in the retina, we found that levels of TGF-β2 protein in retinal tissue were increased early after injury and decreased coincident with increased levels of citrullinated proteins (Fig. 5-1).

Taken together, my findings highlight the expression levels, modifications, and changes to these IFs in response to a number of inhibitors after injury and brings to the forefront the necessity of targeting and controlling the non-filamentous forms of the type III IF proteins. The sensitivity of phosphorylated forms of the IFs to inhibition, and the ability of citrullination to prevent phosphorylation [77] of the IFs, provides a foundation on which studies of citrullination in the eye can advance.

5.2 Significance

Gliosis is associated with most retinal pathologies. The role of the intermediate filaments in gliosis, especially in the retina, is complex. The regulation of these filaments, harnessing both endogenous mechanisms such as citrullination and perturbation by small molecules, is an important goal towards mitigating any damage from the gliosis process in the retina. To that end, the identification and prevention of citrullination in ocular disorders remains an important issue in the development of potential therapeutics for eye disorders.

Fibrosis is also a normal healing process in a number of different tissues throughout the body [215, 216, 15, 217]. It involves the differentiation of fibroblasts into myofibroblasts as a form of wound healing and scarring. This process interferes with the basic function of the cornea, which is to allow light to pass through mostly unobstructed. While we have shown that inhibition of the IFs, as well as changes to their post-translational modifications, can dramatically improve outcomes in this condition, there is still important insight to be gained by unraveling the role of citrullination in this process.

One of the most significant results of my thesis work is the finding that an intravitreal injection of a PAD inhibitor had a direct impact on gliosis. As intravitreal injections are a common procedure in ophthalmic delivery of drugs to the retina, this route of drug delivery can now be exploited for *in vivo* applications in live animals. A second important finding of my thesis work is that the PADs expressed by glial cells are responsive to drug effects at both early [Chapter 3] and late [Chapter 2] stages of the injury

response. During the courses of diseases in which the pathological condition slowly builds, such as retinitis pigmentosa or Age-related macular degeneration (AMD) this is exceptionally important. Symptoms in retinitis pigmentosa often begin with the deterioration of dark vision in children, and may not be considered a clinical issue until there is significant damage to the retina. Alternatively, the fact that AMD is often confused with regular aging can lead to similar pathological conditions without treatment. Citrullination has already been identified in humans with AMD, and the ability to target late stage injury may open a therapeutic window for this disease.

My work is the first to show that WFA may have some ability to alter the citrullination process, and therefore inclusion of this inhibitor along with PAD-targeting inhibitors could potentially enhance the efficacy of PAD inhibition. The complex alteration of high molecular weight species that was observed when treated in an explant system [Chapter 2, Fig. 2-8 and 2-9] suggests there is a synergistic effect of the two inhibitors, targeting the IFs as an important pathological axis. This synergistic effect of WFA and PAD inhibitors on the IFs is a valuable avenue for future research.

While this work has focused on changes in retinal gliosis and corneal fibrosis, many of the mechanistic insights into the control of vimentin and GFAP are likely to be important to other disorders, including the epithelial-to-mesenchymal transition in cancer (vimentin) and the increased invasiveness of astrocytomas that correlates with the delta isoform of GFAP [218]. The interaction of vimentin and GFAP with PAD4, known to be found in a number of different tumors, will likely have to be probed further to understand if the interaction between these two players has any role in tumor progression. Additionally, the anti-angiogenic activity of WFA, which targets these filaments, highlights the importance of determining if citrullination is a major factor in the development of these tumors.

5.3 Working Model

Interestingly, in addition to the changes in deimination and the intermediate filaments we have seen mentioned above, we have also seen that TGF-β2 is significantly increased early after injury, and subsequently decreases with time (Fig. 5-1). It is known that TGF-β2 increases in Müller cells with time after retinal detachment, although no information is available for deimination in the same model [219]. It has also been theorized that TGF-β2 is an important regulator of retinal progenitor and Müller glial proliferation [220] and is released by retinal neurons [220]. This allows for the development of a working model of ocular injury that incorporates the responses of the intermediate filaments and of the PADs (Fig. 5-1). After alkali injury, the change in intraocular pressure likely triggers an influx in calcium into the inner retina, initiated by stretched Müller glia and quickly spreading to astrocytes [194, 208, 209, 210]. This increase in calcium triggers the activation of the PADs. The PADs then citrullinate a number of proteins, including GFAP and vimentin. The citrullination of vimentin likely causes the breakdown of the filamentous structure, allowing for the reorganization of vimentin [Chapter 2; 50]. Citrullination of GFAP appears to play a role in the breakdown of filaments to reorganize the inner limiting membrane, allowing for the glial sprouts seen at 3 days. This also indicates the vimentin breakdown occurs with citrullination, and may act as a method to increase incorporation of GFAP along vimentin filaments. Citrullination of GFAP may also allow for the interaction with PAD4, which is seen along GFAP filaments. This interaction likely plays a role in the movement of PAD4 toward Müller cell nuclei, where it can subsequently alter gene expression to trigger Müller glial reactivity in the retina. This may cause the downregulation of TGF-β2 activity, in turn minimizing Müller glial proliferation and differentiation early after injury.

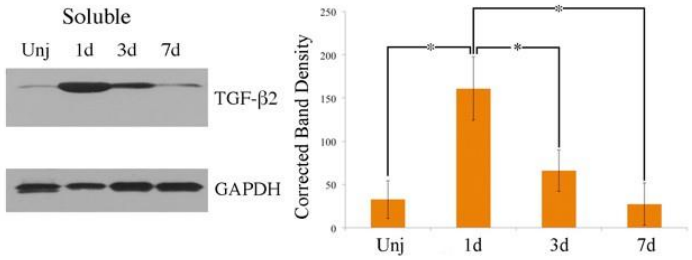

Figure 5-1. TGF-β2 is increased early after injury

(A) Western blot analysis of TGF-β2 in the posterior eye cup of uninjured (unj) mice or mice subject to alkali injury and left to recover for 1 day (1d), 3 days (3d), or 7 days (7d) after injury. (B) Densitometric quantitation of TGF-β2 immunoreactive bands using ImageJ (*=p<.05, students t-test).

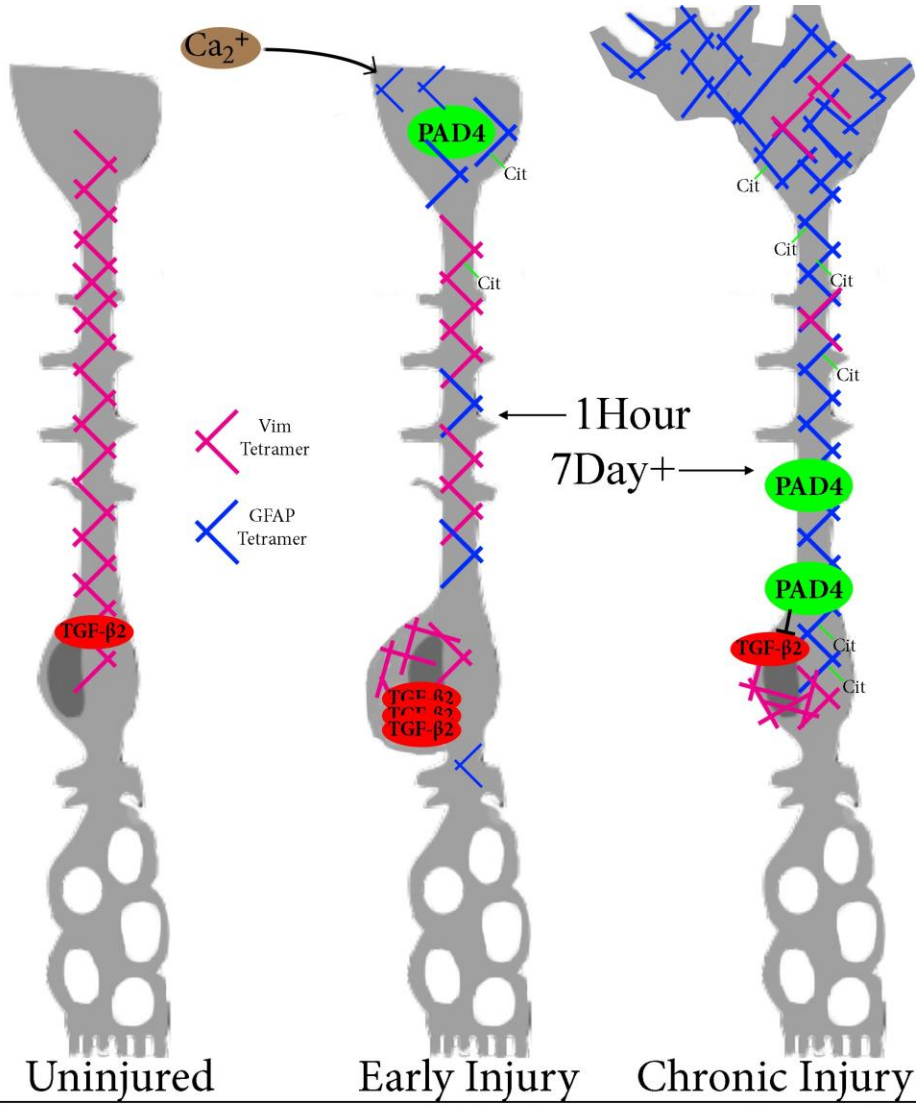

GFAP	Low	Increased Soluble and Insoluble	High Soluble and Insoluble
Vim	High Insoluble	Increased Soluble, Insoluble Breakdown	High Insoluble
PAD	PAD2-Astrocytic	PAD4 Muller Glia	PAD4 Muller Glia
Citrullination	Low	Increased	High
Proliferation	Absent	Increased	Absent
TGF-β2	Low	High	Low
IOP	Regulated	Increased	High

Figure 5-2. Working Model of Muller glial reactivity after injury

Muller glial cells in an uninjured state contain full length vimentin filaments, with minimal GFAP expression, PAD expression or Citrullination. After injury, these are all increased immediately. TGF-β2 may act upon Muller glial cells, either from Muller glia or from retinal neurons, to immediately enhance proliferation. PAD4 is increased in a chronic injury, shutting down TGF-β2 related proliferation. Modified from [22].

5.4 Challenges

One of the major challenges when examining citrullination in the retina is the lack of functional knowledge outside of the context of rheumatoid arthritis (RA). While vimentin in RA becomes an auto-antigen [221], the same has yet to be observed in the retina with regards to GFAP. It is necessary to note, however, that this may be a consequence of few clinical studies into the field, as the field is still in infancy regarding the role of citrullination in retinal disorders. Citrullination of GFAP, vimentin, and desmin has been studied *in vitro*, however [33]. Initial findings strongly suggest that citrullination of the type III IFs inhibits phosphorylation, necessary for the reorganization of insoluble forms of the IFs as well as the control of the soluble forms. This study also found that filament formation of GFAP and vimentin was prevented after IF proteins were incubated with PADs.

The challenges present in the study of intermediate filaments stem from their dynamic nature and the traditional methods for examining their expression. As is becoming clearer, static images, while useful, are more difficult to interpret for a cytoskeletal structure that is capable of exchanging subunits along its entire length. This exchange allows for interactions with different proteins to be transported or modified along the length of the filament. While live imaging may capture this, it is difficult to identify small but important events through static imaging. The use of live cell imaging will likely become increasingly important in the study of both the soluble and insoluble fraction of filaments. Additionally, the overwhelming abundance of cytoskeletal intermediate filaments makes interpretation of immunohistochemistry that identifies the less abundant soluble form difficult. For this reason, assembly dynamics will likely need to be studied in depth in cell cultures, with insights gained from these studies tested *in vivo* later.

In conjunction with this, another major challenge is the fact that the biochemical identity of the high molecular weight GFAP species that can be observed by western blotting is still unknown. While several articles have observed a species above the predicted value, few made any mention into its relevance. Others show the expected bands only, which prevented any insight into our interpretations of this aberrant expression of GFAP. Ultimately, we were able to attribute some portion of this aberrant

species to the hypercitrullination profile we observed. These species likely represent aggregates of protein, such as those found in Alexander Disease, although this still needs to proven experimentally.

Another major challenge is the overwhelming number of arginines found in both GFAP [93] and vimentin [96]. It appears that citrullination occurs on many of these sites, as indicated by our results from a 2-dimensional separation of protein lysates from injured retina when probed with a citrullinated GFAP antibody. As GFAP becomes citrullinated, the epitopes appear to become less reactive to GFAP antibodies, as has been noted [19]. This biochemical phenomenon, in conjunction with the abundance of a number of both modified and non-modified forms in the injured lysate, made direct identification of the citrullinated sites of GFAP difficult, although two citrullinated sites (R267 and R413 in mice) were identified in injured retinas.

5.5 Future Directions

Pressure and Glial Reactivity

One of the most important aspects of study that remains from this work is the understanding of the interplay between intraocular pressure (IOP) and the increase of levels of citrullinated proteins. In the intact *in vivo* alkali injury experiments presented here, there is a set of distinct citrullinated bands that are present in the injured eye. In the eye-cup explant system used, however, there is a robust hypercitrullination, leading to a number of unexpected species of filaments. When the eye was enucleated and incubated as an intact globe for 5 hours, as in the streptonigrin experiments described in chapter 4, the pattern of citrullination returned to that seen *in vivo*. A quick assessment of this pattern can be accomplished through a stepwise increase in the size and severity of cut in the eye. With a small incision, little structure is lost within the globe. With incisions increasing to one quarter, one half, or total removal of the eye-cup, the citrullination profile after 5 hours can be assessed as a means of identifying globe integrity, as a proxy of intraocular pressure regulation, as necessary to prevent a hypercitrullination profile.

With insights into IOP that we gain from the glaucoma system, the regulation of pressure appears to be important as either a sensor for the rest of the retina or a trigger to initiate gliosis. Indeed, astrocytes exposed to an experimental stretch showed an increase in deimination [183]. This can most effectively be addressed *in vivo* in two different models. First, the genetic DBA/2J mouse model can be treated long term, starting at 5 months, with a PAD inhibitor to determine if glaucomatous outcomes can be changed. Second, an experimental model of glaucoma in rabbits treated with intravitreal injections of pan-PAD inhibitors such as Cl-amidine or PAD4 specific inhibitors such as streptonigrin will allow us to determine if the increase in IOP after experimental glaucoma directly alters outcomes for glial and neuronal cells, and if the process can be mitigated by the PAD inhibitors.

We would also hypothesize that WFA can directly alter the citrullination profile of glial cells in response to pressure and stretch. Examination of primary glial cultures in a standardized pressure system [223], which can apply pressure in a gradient from a focal point, either pre-treated or treatment following pressure with varying doses of WFA could provide insight into the ability of WFA to target citrullinated IFs. It is likely that the expression of citrullinated proteins, as they interact with phosphorylated proteins, will decrease, as WFA can target GFAP. This system could also be used with a biotin tagged WFA to determine the capability of WFA to target citrullinated forms of GFAP, as has previously been used to determine both vimentin [14] and GFAP [13] binding.

Identification of Citrullination sites on GFAP and Vimentin

Identification of specific citrullination sites on GFAP and vimentin will allow for better studies into specific changes that occur on the filaments, and how each affects the biophysical properties of the protein. Gleaning insight from the changes that are known to occur to vimentin with phosphorylation [77], and the interaction of citrullination with phosphorylation on the filaments, it will be very important to identify the sites citrullinated as well as the domain each belongs to. As a practical approach, it will be necessary to mutate the sites in each domain in a GFAP-GFP construct. Ideally, all arginine sites within

the head domain, the rod domain, or the tail domain will be mutated and transfected into GFAP-negative primary astrocytes. The induction of citrullination after stretch [223] or in response to nanoparticles [224] can then be examined under electron microscope to identify effects of domain-specific citrullination on polymerization of GFAP and, in similar experiments, vimentin.

To that end, studies harnessing WFA to examine the impact it has on the citrullination of its targets is likely to be an important, although extremely complex, future avenue for studies. The finding that hyperphosphorylation of vimentin makes myofibroblasts sensitive to WFA perturbation in the soluble form suggests that citrullination, thought to break down filaments, would be involved in the switch in a phosphorylation-dependent role. If citrullination is involved in the breakdown of filaments, and the soluble form of vimentin more sensitive to perturbation, we would hypothesize that mutations to arginine that prevent citrullination would alter the course of fibrotic initiation.

Functional Effects of Citrullination on the IFs GFAP and vimentin

Functional assessment of the effect of citrullination on GFAP and vimentin has not been studied thoroughly. Studies into the assembly and disassembly mechanics will require a movement from the *in vivo* system into a cell culture system, in which GFAP-GFP or Vim-GFP astrocytes can be visualized in live cells in real time to determine how changes in citrullination, induced either by the pressure system described [223] or in response to nanoparticles [224] in a culture dish alters the assembly dynamics. This will also involve the use of calcium chelators, such as EGTA, to act as a control and limit PAD activity.

The interaction of GFAP with the ubiquitin proteasome pathway is an interesting avenue that needs more attention, as this interaction is dramatically altered in Alexander disease [79]. It is of great interest that not only does mutated GFAP alter this interaction, but overexpression of wild-type GFAP significantly alters proteasomal activity [225]. Using the explant system we have described to cause hypercitrullination and aberrant GFAP expression, we can use the proteasome inhibitor epoxomicin to examine increases of these aberrant species, as we would hypothesize. We can also examine the different components of the proteasomal process in the presence and absence of the IF modifier WFA. It will also

be important to identify changes in this interaction after use with the PAD inhibitors to examine any effects of citrullination.

Interestingly, the zebrafish retina is capable of regenerating retinal neurons, and only has one PAD enzyme, closely resembling PAD2 [104]. The chicken retina is partially capable of neuroregeneration, and has 3 PAD enzymes. The mouse, rat, and human retina are incapable of endogenous neuroregenration, and have 5 PAD enzymes. It will be interesting to determine *in vivo* if the effects of PAD inhibition, both from a genetic and a pharmacological deficiency, an approach we have employed in the past [153, 67, 15, 13, 14], has an effect on the proliferation and dedifferentiation of Müller glial cells. In this approach, the PAD2 knockout [112] and PAD4 knockout [125] mice should be crossed to form genetic knockouts of the two PADs present in the retina, and the alkali injury model used in this system to initiate gliosis. Examination of glial markers in this system, including GFAP, but also proliferation markers (Ki67) [226] and dedifferentiation markers (Ascl1a) [227], will give clear insight into the role of citrullination and the filaments in Müller glial response. The intravitreal injection of PAD inhibitors, both with and without WFA as a co-injected molecule, in the alkali injury model, as well as in laser injuries, will open up a therapeutic avenue into treatments for human retinal disorders.

Citrullination in other CNS disorders and disease models

Glaucoma is also known to involve changes in citrullination. Specifically in humans, citrullinated proteins and PAD2 levels are increased in the optic nerve, which can be severely damaged in glaucoma [228]. Continued experiments with the DBA/2J mice that are a good genetic model of glaucoma will give excellent insight into the role that citrullination plays in the glaucoma process. While characterization of the glaucoma timeline as it pertains to citrullination needs to be established, the tools to examine disease onset and severity also exist in the form of the PAD and IF inhibitors. Studies measuring intraocular pressure, glial reactivity and ganglion cell death [229] after weekly treatments with WFA or Cl-amidine will allow for the role of citrullination in glaucoma to be more firmly identified. Ultimately, glaucoma represents the most relevant clinical paradigm in which to examine the therapeutic effect of PAD inhibition in the eye.

Corneal fibrosis involves the reactivity of stromal keratinocytes and their ultimate differentiation into myofibroblasts [77]. Our discovery that citrullination is occurring in a fibrotic cornea, in a pattern reminiscent of vimentin expression, is an indicator that not only is phosphorylation of the filaments an important switch to initiate fibrosis, but that citrullination is a response in this same pathway. Studies determining the targets, effects, and inhibition of citrullination in the cornea, similar to those described in the retina, will help establish the role of citrullination in fibrosis in a global sense.

Age-Related Macular Degeneration (AMD) involves the degradation of the macula in the aging population. There is an increase of PAD2 levels and deimination in the AMD population [38]. Insight into the relevance of citrullination in AMD in humans is limited, however, to these levels of expression. It will be interesting to examine post-mortem tissue of AMD patients for citrullinated GFAP and vimentin. Alternatively, it will become important to identify changes in deimination in human tissue with aging, as both AMD and age-matched control eyes expressed deimination markers [38]. More important is the relation of citrullination to gliosis, a factor within AMD. Many of the insights into gliosis will be beneficial to the treatment of AMD as a long-term clinical goal. Supplementary clinical treatment with PAD inhibitors as a therapeutic to attempt to downregulate glial reactivity in AMD will be an intriguing topic.

5.6 Conclusions

The presence of citrullination in our alkali injury model was a novel finding that we were able to relate to a number of other diseases and experimental models. Importantly, it appears to play a major role in the initiation of gliosis, a factor in a number of different retinal, brain and spinal cord pathologies. The work reported in this thesis represents a substantial contribution to the fields of citrullination, retinal gliosis, and the type III intermediate filaments, and will hopefully help to provide insights for researchers in a number of different systems.

References

[1] - Quigley HA. *Glaucoma*. Lancet. 2011; 377 (9774):1367-77. doi: 10.1016/S0140-6736(10)61423-7. PubMed PMID: 21453963

[2] - Lim LS, Mitchell P, Seddon JM, Holz FG, Wong TY. *Age-related macular degeneration*. Lancet. 2012; 379 (9827):1728-38. doi:10.1016/S0140-6736(12)60282-7. PubMed PMID: 22559899

[3] - Georgoulas S, Dahlmann-Noor A, Brocchini S, Khaw PT. *Modulation of wound healing during and after glaucoma surgery*. Prog Brain Res. 2008; 173:237-54. doi: 10.1016/S0079-6123(08)01117-5. Review. PubMed PMID: 18929113

[4] - Daniel E, Toth CA, Grunwald JE, Jaffe GJ, Martin DF, Fine SL, Huang J, Ying GS, Hagstrom SA, Winter K, Maguire MG; *Comparison of Age-related Macular Degeneration Treatments Trials Research Group. Risk of scar in the comparison of age-related macular degeneration treatments trials*. Ophthalmology. 2014; 121(3):656-66. doi: 10.1016/j.ophtha.2013.10.019. PubMed PMID: 24314839.

[5] - Leavitt T, Hu MS, Marshall CD, Barnes LA, Lorenz HP, Longaker MT. *Scarless wound healing: finding the right cells and signals*. Cell Tissue Res. 2016 PubMed PMID: 27256396

[6] - Garg P, Krishna PV, Stratis AK, Gopinathan U. *The value of corneal transplantation in reducing blindness*. Eye (Lond). 2005; 19(10):1106-14. PubMed PMID: 16304591.

[7] - Garweg JG, Tappeiner C, Halberstadt M. *Pathophysiology of proliferative vitreoretinopathy in retinal detachment*. Surv Ophthalmol. 2013; 58(4):321-9. doi: 10.1016/j.survophthal.2012.12.004. PubMed PMID: 23642514.

[8] - Bringmann A, Wiedemann P. *Müller glial cells in retinal disease*. Ophthalmologica. 2012;227(1):1-19. doi: 10.1159/000328979. Epub 2011 Sep 15. Review. PubMed PMID: 21921569

[9] - Thomas JL, Ranski AH, Morgan GW, Thummel R. *Reactive gliosis in the adult zebrafish retina*. Exp Eye Res. 2016; 143:98-109. doi:10.1016/j.exer.2015.09.017. PubMed PMID: 26492821

[10] - Eastlake K, Banerjee PJ, Angbohang A, Charteris DG, Khaw PT, Limb GA. *Müller glia as an important source of cytokines and inflammatory factors present in the gliotic retina during proliferative vitreoretinopathy*. Glia. 2016; 64(4):495-506. doi: 10.1002/glia.22942. PubMed PMID:26556395

[11] - Brenner M. *Role of GFAP in CNS injuries*. Neurosci Lett. 2014; 565:7-13. doi: 10.1016/j.neulet.2014.01.055. Epub 2014 Feb 6. Review. PubMed PMID:24508671;

[12] - Ekmark-Lewén S, Lewén A, Israelsson C, Li GL, Farooque M, Olsson Y, Ebendal T, Hillered L. *Vimentin and GFAP responses in astrocytes after contusion trauma to the murine brain*. Restor Neurol Neurosci. 2010; 28(3):311-21. doi:10.3233/RNN-2010-0529. PubMed PMID:20479526.

[13] - Bargagna-Mohan P, Paranthan RR, Hamza A, Dimova N, Trucchi B, Srinivasan C, Elliott GI, Zhan CG, Lau DL, Zhu H, Kasahara K, Inagaki M, Cambi F, Mohan R. *Withaferin A targets intermediate*

filaments glial fibrillary acidic protein and vimentin in a model of retinal gliosis. J Biol Chem. 2010; 285(10):7657-69. doi: 10.1074/jbc.M109.093765. Epub 2010 Jan 4. PubMed PMID: 20048155

[14] - Bargagna-Mohan P, Hamza A, Kim YE, Khuan Abby Ho Y, Mor-Vaknin N, Wendschlag N, Liu J, Evans RM, Markovitz DM, Zhan CG, Kim KB, Mohan R. *The tumor inhibitor and antiangiogenic agent withaferin A targets the intermediate filament protein vimentin*. Chem Biol. 2007; 14(6):623-34. PubMed PMID: 17584610

[15] - Bargagna-Mohan P, Paranthan RR, Hamza A, Zhan CG, Lee DM, Kim KB, Lau DL, Srinivasan C, Nakayama K, Nakayama KI, Herrmann H, Mohan R. *Corneal antifibrotic switch identified in genetic and pharmacological deficiency of vimentin*. J Biol Chem. 2012; 287(2):989-1006. doi: 10.1074/jbc.M111.297150. Epub 2011 Nov 22. PubMed PMID: 22117063

[16] - Raposo C, Schwartz M. *Glial scar and immune cell involvement in tissue remodeling and repair following acute CNS injuries*. Glia. 2014; 62(11):1895-904. doi: 10.1002/glia.22676. PubMed PMID: 24756949.

[17] - Lewis GP, Chapin EA, Luna G, Linberg KA, Fisher SK. *The fate of Müller's glia following experimental retinal detachment: nuclear migration, cell division, and subretinal glial scar formation*. Mol Vis. 2010; 16:1361-72. PubMed PMID: 20664798.

[18] - Martin P, Nunan R. *Cellular and molecular mechanisms of repair in acute and chronic wound healing*. Br J Dermatol. 2015; 173(2):370-8. doi:10.1111/bjd.13954. PubMed PMID: 26175283;

[19] - Ishigami A, Masutomi H, Handa S, Nakamura M, Nakaya S, Uchida Y, Saito Y, Murayama S, Jang B, Jeon YC, Choi EK, Kim YS, Kasahara Y, Maruyama N, Toda T. *Mass spectrometric identification of citrullination sites and immunohistochemical detection of citrullinated glial fibrillary acidic protein in Alzheimer's disease brains.* J Neurosci Res. 2015; 93(11):1664-74. doi: 10.1002/jnr.23620. Epub 2015 Jul 18. PubMed PMID: 26190193.

[20] -Phillips BN, Chun DW, Colyer M. *Closed globe macular injuries after blasts in combat*. Retina. 2013; 33(2):371-9. doi: 10.1097/IAE.0b013e318261a726. PubMed PMID: 23023525.

[21] - Reichenbach A, Bringmann A. *New functions of Müller cells*. Glia. 2013; 61(5):651-78. doi: 10.1002/glia.22477. PubMed PMID:23440929.

[22] - Bringmann A, Pannicke T, Grosche J, Francke M, Wiedemann P, Skatchkov SN, Osborne NN, Reichenbach A. *Müller cells in the healthy and diseased retina.* Prog Retin Eye Res. 2006; 25(4):397-424. Epub 2006 Jul 12. Review. PubMed PMID: 16839797.

[23] - Verardo MR, Lewis GP, Takeda M, Linberg KA, Byun J, Luna G, Wilhelmsson U, Pekny M, Chen DF, Fisher SK. *Abnormal reactivity of muller cells after retinal detachment in mice deficient in GFAP and vimentin*. Invest Ophthalmol Vis Sci. 2008; 49(8):3659-65. doi: 10.1167/iovs.07-1474. PubMed PMID:18469190

[24] - Lundkvist A, Reichenbach A, Betsholtz C, Carmeliet P, Wolburg H, Pekny M. *Under stress, the absence of intermediate filaments from Müller cells in the retina has structural and functional consequences.* J Cell Sci. 2004; 117(Pt 16):3481-8. Epub 2004 Jun 29. PubMed PMID: 15226376

[25] - Pekny M, Levéen P, Pekna M, Eliasson C, Berthold CH, Westermark B, Betsholtz C. *Mice lacking glial fibrillary acidic protein display astrocytes devoid of intermediate filaments but develop and reproduce normally*. EMBO J. 1995; 14(8):1590-8. PubMed PMID: 7737111

[26] - Kinouchi R, Takeda M, Yang L, Wilhelmsson U, Lundkvist A, Pekny M, Chen DF. *Robust neural integration from retinal transplants in mice deficient in GFAP and vimentin*. Nat Neurosci. 2003; 6(8):863-8. PubMed PMID: 12845328

[27] - Wilhelmsson U, Li L, Pekna M, Berthold CH, Blom S, Eliasson C, Renner O, Bushong E, Ellisman M, Morgan TE, Pekny M. *Absence of glial fibrillary acidic protein and vimentin prevents hypertrophy of astrocytic processes and improves post-traumatic regeneration*. J Neurosci. 2004; 24(21):5016-21. PubMed PMID: 15163694.

[28] - Messing A, Head MW, Galles K, Galbreath EJ, Goldman JE, Brenner M. *Fatal encephalopathy with astrocyte inclusions in GFAP transgenic mice*. Am J Pathol. 1998; 152(2):391-8. PubMed PMID: 9466565

[29] - Sihag RK, Inagaki M, Yamaguchi T, Shea TB, Pant HC. *Role of phosphorylation on the structural dynamics and function of types III and IV intermediate filaments*. Exp Cell Res. 2007; 313(10):2098-109. Epub 2007 Apr 12. Review. PubMed PMID: 17498690

[30] - Inagaki M, Nakamura Y, Takeda M, Nishimura T, Inagaki N. *Glial fibrillary acidic protein: dynamic property and regulation by phosphorylation*. Brain Pathol. 1994; 4(3):239-43. PubMed PMID: 7952265.

[31] - Snider NT, Omary MB. *Post-translational modifications of intermediate filament proteins: mechanisms and functions*. Nat Rev Mol Cell Biol. 2014; 15(3):163-77. doi: 10.1038/nrm3753. Review. PubMed PMID: 24556839

[32] - Eriksson JE, He T, Trejo-Skalli AV, Härmälä-Braskén AS, Hellman J, Chou YH, Goldman RD. *Specific in vivo phosphorylation sites determine the assembly dynamics of vimentin intermediate filaments*. J Cell Sci. 2004; 117(Pt 6):919-32. PubMed PMID: 14762106.

[33] - Inagaki M, Takahara H, Nishi Y, Sugawara K, Sato C. *Ca2+-dependent deimination-induced disassembly of intermediate filaments involves specific modification of the amino-terminal head domain*. J Biol Chem. 1989; 264(30):18119-27. PubMed PMID: 2808368.

[34] - Wang S, Wang Y. *Peptidylarginine deiminases in citrullination, gene regulation, health and pathogenesis.* Biochim Biophys Acta. 2013; 1829(10):1126-35. doi: 10.1016/j.bbagrm.2013.07.003. Epub 2013 Jul 13. Review. PubMed PMID: 23860259

[35] 24907905 - Bradford CM, Ramos I, Cross AK, Haddock G, McQuaid S, Nicholas AP, Woodroofe MN. *Localisation of citrullinated proteins in normal appearing white matter and lesions in the central nervous system in multiple sclerosis*. J Neuroimmunol. 2014; 273(1-2):85-95. doi: 10.1016/j.jneuroim.2014.05.007. Epub 2014 May 27. PubMed PMID: 24907905.

[36] - Nicholas AP, Sambandam T, Echols JD, Tourtellotte WW. *Increased citrullinated glial fibrillary acidic protein in secondary progressive multiple sclerosis.* J Comp Neurol. 2004; 473(1):128-36. PubMed PMID: 15067723.

[37] - Lundberg K, Nijenhuis S, Vossenaar ER, Palmblad K, van Venrooij WJ, Klareskog L, Zendman AJ, Harris HE. *Citrullinated proteins have increased immunogenicity and arthritogenicity and their presence in arthritic joints correlates with disease severity*. Arthritis Res Ther. 2005; 7(3):R458-67. Epub 2005 Feb 21. PubMed PMID: 15899032

[38] - Bonilha VL, Shadrach KG, Rayborn ME, Li Y, Pauer GJ, Hagstrom SA, Bhattacharya SK, Hollyfield JG. *Retinal deimination and PAD2 levels in retinas from donors with age-related macular degeneration (AMD)*. Exp Eye Res. 2013; 111:71-8. doi: 10.1016/j.exer.2013.03.017. Epub 2013 Apr 3. PubMed PMID: 23562679

[39] - Bhattacharya SK, Crabb JS, Bonilha VL, Gu X, Takahara H, Crabb JW. *Proteomics implicates peptidyl arginine deiminase 2 and optic nerve citrullination in glaucoma pathogenesis*. Invest Ophthalmol Vis Sci. 2006; 47(6):2508-14. PubMed PMID: 16723463.

[40] - Edwards MM, McLeod DS, Bhutto IA, Villalonga MB, Seddon JM, Lutty GA. *Idiopathic preretinal glia in aging and age-related macular degeneration*. Exp Eye Res. 2015. pii: S0014- 4835(15)00242-0. doi: 10.1016/j.exer.2015.07.016. [Epub ahead of print] PubMed PMID: 26220834

[41] - Langelaan M, de Boer MR, van Nispen RM, Wouters B, Moll AC, van Rens GH. *Impact of visual impairment on quality of life: a comparison with quality of life in the general population and with other chronic conditions*. Ophthalmic Epidemiol. 2007; 14(3):119-26. PubMed PMID: 17613846.

[42] - Köberlein J, Beifus K, Schaffert C, Finger RP. The economic burden of visual impairment and blindness: a systematic review. BMJ Open. 2013 Nov 7;3(11):e003471. doi: 10.1136/bmjopen-2013-003471. PubMed PMID: 24202057; PubMed Central PMCID: PMC3822298.

[43] - van Lookeren Campagne M, LeCouter J, Yaspan BL, Ye W. *Mechanisms of age-related macular degeneration and therapeutic opportunities*. J Pathol. 2014; 232(2):151-64. doi: 10.1002/path.4266. Review. PubMed PMID: 24105633.

[44] - Weinreb RN, Aung T, Medeiros FA. *The pathophysiology and treatment of glaucoma: a review*. JAMA. 2014; 311(18):1901-11. doi:10.1001/jama.2014.3192. Review. PubMed PMID: 24825645

[45] - Smith RE, Conway B. *Alkali retinopathy*. Arch Ophthalmol. 1976; 94(1):81-4. PubMed PMID: 1247413.

[46] - Paranthan RR, Bargagna-Mohan P, Lau DL, Mohan R. *A robust model for simultaneously inducing corneal neovascularization and retinal gliosis in the mouse eye.* Mol Vis. 2011;17:1901-8. Epub 2011 Jul 14. PubMed PMID: 21850164

[47] - Campbell TG, Razavi H, Turner AW. *Bomb blast maculopathy*. BMJ Case Rep. 2014; 2014. pii: bcr2014204305. doi: 10.1136/bcr-2014-204305. PubMed PMID: 25406211.

[48] - Kolb, Helga "*Gross Anatomy of the Eye*". Webvision. Moran Eye Center, January 25, 2012. Web. (August 15, 2016). http://webvision.med.utah.edu/book/part-i-foundations/gross-anatomy-of-the-ey/

[49] - Wynn TA. *Common and unique mechanisms regulate fibrosis in various fibroproliferative diseases*. J Clin Invest. 2007; 117(3):524-9. Review. PubMed PMID: 17332879

[50] - Torricelli AA, Santhanam A, Wu J, Singh V, Wilson SE. *The corneal fibrosis response to epithelial-stromal injury*. Exp Eye Res. 2016; 142:110-8. doi: 10.1016/j.exer.2014.09.012. PubMed PMID: 26675407

[51] - Kwon OW, Song JH, Roh MI. *Retinal Detachment and Proliferative Vitreoretinopathy*. Dev Ophthalmol. 2016; 55:154-62. doi: 10.1159/000438972. 2015. Review. PubMed PMID: 26501375.

[52] - Bringmann A, Wiedemann P. *Involvement of Müller glial cells in epiretinal membrane formation*. Graefes Arch Clin Exp Ophthalmol. 2009; 247(7):865-83. doi: 10.1007/s00417-009-1082-x. PubMed PMID: 19415318.

[53] - Franze K, Grosche J, Skatchkov SN, Schinkinger S, Foja C, Schild D, Uckermann O, Travis K, Reichenbach A, Guck J. *Muller cells are living optical fibers in the vertebrate retina*. Proc Natl Acad Sci U S A. 2007; 104(20):8287-92. PubMed PMID: 17485670

[54] - Lu YB, Franze K, Seifert G, Steinhäuser C, Kirchhoff F, Wolburg H, Guck J, Janmey P, Wei EQ, Käs J, Reichenbach A. *Viscoelastic properties of individual glial cells and neurons in the CNS*. Proc Natl Acad Sci U S A. 2006; 103(47):17759-64. PubMed PMID: 17093050

[55] - Pekny M, Wilhelmsson U, Pekna M. *The dual role of astrocyte activation and reactive gliosis*. Neurosci Lett. 2014; 565:30-8. doi: 10.1016/j.neulet.2013.12.071. PubMed PMID: 24406153.

[56] - Betts-Obregon BS, Gonzalez-Fernandez F, Tsin AT. *Interphotoreceptor retinoid-binding protein (IRBP) promotes retinol uptake and release by rat Müller cells (rMC-1) in vitro: implications for the cone visual cycle*. Invest Ophthalmol Vis Sci. 2014; 55(10):6265-71. doi: 10.1167/iovs.14-14721. PubMed PMID: 25183762

[57] - Dubois-Dauphin M, Poitry-Yamate C, de Bilbao F, Julliard AK, Jourdan F, Donati G. *Early postnatal Müller cell death leads to retinal but not optic nerve degeneration in NSE-Hu-Bcl-2 transgenic mice*. Neuroscience. 2000; 95(1):9-21. PubMed PMID: 10619458.

[58] - Sawada K, Hiraoka M, Ohguro H. *Effect of Antiglaucoma Medicine on Intraocular Pressure in DBA/2J Mice*. Ophthalmic Res. 2016; 55(4):205-11. doi: 10.1159/000444057. Epub 2016 Mar 5. PubMed PMID: 26942413.

[59] 16332275 - Libby RT, Anderson MG, Pang IH, Robinson ZH, Savinova OV, Cosma IM, Snow A, Wilson LA, Smith RS, Clark AF, John SW. *Inherited glaucoma in DBA/2J mice: pertinent disease features for studying the neurodegeneration*. Vis Neurosci. 2005; 22(5):637-48. PubMed PMID: 16332275.

[60] - Huang W, Xing W, Ryskamp DA, Punzo C, Križaj D. *Localization and phenotype-specific expression of ryanodine calcium release channels in C57BL6 and DBA/2J mouse strains*. Exp Eye Res. 2011; 93(5):700-9. doi:10.1016/j.exer.2011.09.001. PubMed PMID: 21933672

[61] - Lin MP, Ekşioğlu Ü, Mudumbai RC, Slabaugh MA, Chen PP. *Glaucoma in patients with ocular chemical burns*. Am J Ophthalmol. 2012; 154(3):481-485.e1. doi:10.1016/j.ajo.2012.03.026. PubMed PMID: 22633350.

[62] - Dyer MA, Cepko CL. *Control of Müller glial cell proliferation and activation following retinal injury*. Nat Neurosci. 2000; 3(9):873-80. PubMed PMID: 10966617.

[63] - Omary MB, Coulombe PA, McLean WH. *Intermediate filament proteins and their associated diseases*. N Engl J Med. 2004; 351(20):2087-100. PubMed PMID: 15537907.

[64] - Eriksson JE, Dechat T, Grin B, Helfand B, Mendez M, Pallari HM, Goldman RD. *Introducing intermediate filaments: from discovery to disease*. J Clin Invest. 2009; 119(7):1763-71. doi: 10.1172/JCI38339. Epub 2009 Jul 1. Review. PubMed PMID: 19587451

[65] - Eckes B, Dogic D, Colucci-Guyon E, Wang N, Maniotis A, Ingber D, Merckling A, Langa F, Aumailley M, Delouvée A, Koteliansky V, Babinet C, Krieg T. *Impaired mechanical stability, migration and contractile capacity in vimentin-deficient fibroblasts*. J Cell Sci. 1998; 111 (Pt 13):1897-907. PubMed PMID: 9625752.

[66] - Eckes B, Colucci-Guyon E, Smola H, Nodder S, Babinet C, Krieg T, Martin P. *Impaired wound healing in embryonic and adult mice lacking vimentin*. J Cell Sci. 2000; 113 (Pt 13):2455-62. PubMed PMID: 10852824

[67] - Bargagna-Mohan P, Deokule SP, Thompson K, Wizeman J, Srinivasan C, Vooturi S, Kompella UB, Mohan R. *Withaferin A effectively targets soluble vimentin in the glaucoma filtration surgical model of fibrosis*. PLoS One. 2013; 8(5):e63881. doi: 10.1371/journal.pone.0063881. Print 2013. PubMed PMID: 23667686

[68] - Kreplak L, Aebi U, Herrmann H. *Molecular mechanisms underlying the assembly of intermediate filaments*. Exp Cell Res. 2004; 301(1):77-83. Review. PubMed PMID: 15501448.

[69] - Herrmann H, Häner M, Brettel M, Müller SA, Goldie KN, Fedtke B, Lustig A, Franke WW, Aebi U. *Structure and assembly properties of the intermediate filament protein vimentin: the role of its head, rod and tail domains*. J Mol Biol. 1996; 264(5):933-53. PubMed PMID: 9000622.

[70] - Herrmann H, Aebi U. *Intermediate filament assembly: fibrillogenesis is driven by decisive dimer-dimer interactions.* Curr Opin Struct Biol. 1998; 8(2):177-85. Review. PubMed PMID: 9631290.

[71] - Hess JF, Budamagunta MS, Voss JC, FitzGerald PG. *Structural characterization of human vimentin rod 1 and the sequencing of assembly steps in intermediate filament formation in vitro using site-directed spin labeling and electron paramagnetic resonance*. J Biol Chem. 2004; 279(43):44841-6. Epub 2004 Jul 1. PubMed PMID: 15231822

[72] - Soellner P, Quinlan RA, Franke WW. *Identification of a distinct soluble subunit of an intermediate filament protein: tetrameric vimentin from living cells*. Proc Natl Acad Sci U S A. 1985; 82(23):7929-33. PubMed PMID: 3865206

[73] - Helfand BT, Mendez MG, Murthy SN, Shumaker DK, Grin B, Mahammad S, Aebi U, Wedig T, Wu YI, Hahn KM, Inagaki M, Herrmann H, Goldman RD. *Vimentin organization modulates the formation of lamellipodia*. Mol Biol Cell. 2011; 22(8):1274-89. doi: 10.1091/mbc.E10-08-0699. Epub 2011 Feb 23. PubMed PMID: 21346197

[74] - Mahammad S, Murthy SN, Didonna A, Grin B, Israeli E, Perrot R, Bomont P, Julien JP, Kuczmarski E, Opal P, Goldman RD. *Giant axonal neuropathy-associated gigaxonin mutations impair*

intermediate filament protein degradation. J Clin Invest. 2013; 123(5):1964-75. doi: 10.1172/JCI66387. Epub 2013 Apr 15. PubMed PMID: 23585478

[75] - Strelkov SV, Herrmann H, Geisler N, Wedig T, Zimbelmann R, Aebi U, Burkhard P. *Conserved segments 1A and 2B of the intermediate filament dimer: their atomic structures and role in filament assembly*. EMBO J. 2002; 21(6):1255-66. PubMed PMID: 11889032;

[76] - Perlson E, Hanz S, Ben-Yaakov K, Segal-Ruder Y, Seger R, Fainzilber M. *Vimentin-dependent spatial translocation of an activated MAP kinase in injured nerve*. Neuron. 2005; 45(5):715-26. PubMed PMID: 15748847.

[77] - Bargagna-Mohan P, Lei L, Thompson A, Shaw C, Kasahara K, Inagaki M, Mohan R. *Vimentin Phosphorylation Underlies Myofibroblast Sensitivity to Withaferin A In Vitro and during Corneal Fibrosis.* PLoS One. 2015; 10(7):e0133399. doi: 10.1371/journal.pone.0133399. eCollection 2015. PubMed PMID: 26186445

[78] - Kumar N, Robidoux J, Daniel KW, Guzman G, Floering LM, Collins S. *Requirement of vimentin filament assembly for beta3-adrenergic receptor activation of ERK MAP kinase and lipolysis*. J Biol Chem. 2007; 282(12):9244-50. Epub 2007 Jan 24. PubMed PMID: 17251187.

[79] - Tang G, Perng MD, Wilk S, Quinlan R, Goldman JE. *Oligomers of mutant glial fibrillary acidic protein (GFAP) Inhibit the proteasome system in alexander disease astrocytes, and the small heat shock protein alphaB-crystallin reverses the inhibition*. J Biol Chem. 2010; 285(14):10527-37. doi: 10.1074/jbc.M109.067975. Epub 2010 Jan 28. PubMed PMID: 20110364

[80] - Bär H, Strelkov SV, Sjöberg G, Aebi U, Herrmann H. *The biology of desmin filaments: how do mutations affect their structure, assembly, and organisation?* J Struct Biol. 2004; 148(2):137-52. Review. PubMed PMID: 15477095.

[81] - Chernyatina AA, Guzenko D, Strelkov SV. *Intermediate filament structure: the bottom-up approach.* Curr Opin Cell Biol. 2015; 32:65-72. Epub 2015 Jan 14. Review. PubMed PMID: 25596497.

[82] - Köster S, Weitz DA, Goldman RD, Aebi U, Herrmann H. *Intermediate filament mechanics in vitro and in the cell: from coiled coils to filaments, fibers and networks*. Curr Opin Cell Biol. 2015; 32:82-91. doi: 10.1016/j.ceb.2015.01.001. Epub 2015 Jan 23. Review. PubMed PMID: 25621895

[83] - Pérez-Sala D, Oeste CL, Martínez AE, Carrasco MJ, Garzón B, Cañada FJ. *Vimentin filament organization and stress sensing depend on its single cysteine residue and zinc binding*. Nat Commun. 2015; 6:7287. doi: 10.1038/ncomms8287. PubMed PMID: 26031447

[84] - Strelkov SV, Herrmann H, Aebi U. *Molecular architecture of intermediate filaments*. Bioessays. 2003; 25(3):243-51. Review. PubMed PMID: 12596228.

[85] - Li H, Guo Y, Teng J, Ding M, Yu AC, Chen J. *14-3-3gamma affects dynamics and integrity of glial filaments by binding to phosphorylated GFAP*. J Cell Sci. 2006; 119(Pt 21):4452-61. Epub 2006 Oct 10. PubMed PMID: 17032734.

[86] - Helfand BT, Chang L, Goldman RD. *Intermediate filaments are dynamic and motile elements of cellular architecture*. J Cell Sci. 2004; 117(Pt 2):133-41. Review. PubMed PMID: 14676269.

[87] - Middeldorp J, Hol EM. *GFAP in health and disease*. Prog Neurobiol. 2011; 93(3):421-43. doi: 10.1016/j.pneurobio.2011.01.005. Epub 2011 Jan 8. Review. PubMed PMID: 21219963.

[88] - Perreau J, Lilienbaum A, Vasseur M, Paulin D. *Nucleotide sequence of the human vimentin gene and regulation of its transcription in tissues and cultured cells*. Gene. 1988; 62(1):7-16. PubMed PMID: 3371665.

[89] - Medrano S, Steward O. *Differential mRNA localization in astroglial cells in culture*. J Comp Neurol. 2001; 430(1):56-71. PubMed PMID: 11135245.

[90] - Thomsen R, Daugaard TF, Holm IE, Nielsen AL. *Alternative mRNA splicing from the glial fibrillary acidic protein (GFAP) gene generates isoforms with distinct subcellular mRNA localization patterns in astrocytes*. PLoS One. 2013; 8(8):e72110. doi: 10.1371/journal.pone.0072110. eCollection 2013. PubMed PMID: 23991052

[91] - Hol EM, Pekny M. *Glial fibrillary acidic protein (GFAP) and the astrocyte intermediate filament system in diseases of the central nervous system*. Curr Opin Cell Biol. 2015; 32:121-30. doi: 10.1016/j.ceb.2015.02.004. PubMed PMID: 25726916.

[92] - Fujita K, Yamauchi M, Matsui T, Titani K, Takahashi H, Kato T, Isomura G, Ando M, Nagata Y. *Increase of glial fibrillary acidic protein fragments in the spinal cord of motor neuron degeneration mutant mouse*. Brain Res. 1998; 785(1):31-40. PubMed PMID: 9526038.

[93] - Chen MH, Hagemann TL, Quinlan RA, Messing A, Perng MD. *Caspase cleavage of GFAP produces an assembly-compromised proteolytic fragment that promotes filament aggregation*. ASN Neuro. 2013; 5(5):e00125. doi: 10.1042/AN20130032. PubMed PMID: 24102621

[94] - Bomont P. *Degradation of the Intermediate Filament Family by Gigaxonin.* Methods Enzymol. 2016;569:215-31. doi: 10.1016/bs.mie.2015.07.009. Epub 2015 Aug 24. PubMed PMID: 26778561.

[95] - Kitada T, Asakawa S, Hattori N, Matsumine H, Yamamura Y, Minoshima S, Yokochi M, Mizuno Y, Shimizu N. *Mutations in the parkin gene cause autosomal recessive juvenile parkinsonism*. Nature. 1998; 392(6676):605-8. PubMed PMID: 9560156.

[96] - Omary MB, Ku NO, Tao GZ, Toivola DM, Liao J. *"Heads and tails" of intermediate filament phosphorylation: multiple sites and functional insights.* Trends Biochem Sci. 2006; 31(7):383-94. Epub 2006 Jun 19. Review. PubMed PMID: 16782342.

[97] - Takemura M, Gomi H, Colucci-Guyon E, Itohara S. *Protective role of phosphorylation in turnover of glial fibrillary acidic protein in mice*. J Neurosci. 2002; 22(16):6972-9. PubMed PMID: 12177195.

[98] - Ando S, Tokui T, Yano T, Inagaki M. *Keratin 8 phosphorylation in vitro by cAMP-dependent protein kinase occurs within the amino- and carboxyl-terminal end domains*. Biochem Biophys Res Commun. 1996; 221(1):67-71. PubMed PMID: 8660345.

[99] - Geisler N, Hatzfeld M, Weber K. *Phosphorylation in vitro of vimentin by protein kinases A and C is restricted to the head domain. Identification of the phosphoserine sites and their influence on filament formation*. Eur J Biochem. 1989; 183(2):441-7. PubMed PMID: 2503376.

[100] - Ando S, Tokui T, Yamauchi T, Sugiura H, Tanabe K, Inagaki M. *Evidence that Ser-82 is a unique phosphorylation site on vimentin for Ca2(+)-calmodulin-dependent protein kinase II*. Biochem Biophys Res Commun. 1991; 175(3):955-62. PubMed PMID: 1850997.

[101] - Matsuyama M, Tanaka H, Inoko A, Goto H, Yonemura S, Kobori K, Hayashi Y, Kondo E, Itohara S, Izawa I, Inagaki M. *Defect of mitotic vimentin phosphorylation causes microophthalmia and cataract via aneuploidy and senescence in lens epithelial cells*. J Biol Chem. 2013; 288(50):35626-35. doi: 10.1074/jbc.M113.514737. Epub 2013 Oct 18. PubMed PMID: 24142690

[102] - AC Kurtz, *A Simple Synthesis of dl-Citrulline.* JBC 1938, 122:477-484

[103] - Vossenaar ER, Zendman AJ, van Venrooij WJ, Pruijn GJ. *PAD, a growing family of citrullinating enzymes: genes, features and involvement in disease*. Bioessays. 2003; 25(11):1106-18. Review. PubMed PMID: 14579251.

[104] - Bhattacharya SK, Nicholas AP. 2014. *Protein Deimination in Human Health and Disease*. Springer: New York, New York. DOI 10.1007/978-1-4614-8317-5

[105] - Chavanas S, Méchin MC, Takahara H, Kawada A, Nachat R, Serre G, Simon M. *Comparative analysis of the mouse and human peptidylarginine deiminase gene clusters reveals highly conserved non-coding segments and a new human gene, PADI6*. Gene. 2004; 330:19-27. PubMed PMID: 15087120.

[106] - Nachat R, Méchin MC, Takahara H, Chavanas S, Charveron M, Serre G, Simon M. *Peptidylarginine deiminase isoforms 1-3 are expressed in the epidermis and involved in the deimination of K1 and filaggrin*. J Invest Dermatol. 2005; 124(2):384-93. PubMed PMID: 15675958.

[107] - Terakawa H, Takahara H, Sugawara K. *Three types of mouse peptidylarginine deiminase: characterization and tissue distribution*. J Biochem. 1991; 110(4):661-6. PubMed PMID: 1778991.

[108] - Ishida-Yamamoto A, Senshu T, Takahashi H, Akiyama K, Nomura K, Iizuka H. *Decreased deiminated keratin K1 in psoriatic hyperproliferative epidermis*. J Invest Dermatol. 2000; 114(4):701-5. PubMed PMID: 10733676.

[109] - Jang B, Shin HY, Choi JK, Nguyen du PT, Jeong BH, Ishigami A, Maruyama N, Carp RI, Kim YS, Choi EK. *Subcellular localization of peptidylarginine deiminase 2 and citrullinated proteins in brains of scrapie-infected mice: nuclear localization of PAD2 and membrane fraction-enriched citrullinated proteins*. J Neuropathol Exp Neurol. 2011; 70(2):116-24. doi: 10.1097/NEN.0b013e318207559e. PubMed PMID: 21343880.

[110] - Shimada N, Handa S, Uchida Y, Fukuda M, Maruyama N, Asaga H, Choi EK, Lee J, Ishigami A. *Developmental and age-related changes of peptidylarginine deiminase 2 in the mouse brain*. J Neurosci Res. 2010; 88(4):798-806. doi: 10.1002/jnr.22255. PubMed PMID: 19830834.

[111] - Ishigami A, Ohsawa T, Hiratsuka M, Taguchi H, Kobayashi S, Saito Y, Murayama S, Asaga H, Toda T, Kimura N, Maruyama N. *Abnormal accumulation of citrullinated proteins catalyzed by peptidylarginine deiminase in hippocampal extracts from patients with Alzheimer's disease*. J Neurosci Res. 2005; 80(1):120-8. PubMed PMID: 15704193.

[112] - van Beers JJ, Zendman AJ, Raijmakers R, Stammen-Vogelzangs J, Pruijn GJ. *Peptidylarginine deiminase expression and activity in PAD2 knock-out and PAD4-low mice*. Biochimie. 2013; 95(2):299-308. doi: 10.1016/j.biochi.2012.09.029. Epub 2012 Sep 28. PubMed PMID: 23026755.

[113] - Hojo-Nakashima I, Sato R, Nakashima K, Hagiwara T, Yamada M. *Dynamic expression of peptidylarginine deiminase 2 in human monocytic leukaemia THP-1 cells during macrophage differentiation.* J Biochem. 2009; 146(4):471-9. doi: 10.1093/jb/mvp097. Epub 2009 Jun 29. PubMed PMID: 19564157.

[114] - Wood DD, Ackerley CA, Brand Bv, Zhang L, Raijmakers R, Mastronardi FG, Moscarello MA. *Myelin localization of peptidylarginine deiminases 2 and 4: comparison of PAD2 and PAD4 activities*. Lab Invest. 2008; 88(4):354-64. doi: 10.1038/labinvest.3700748. Epub 2008 Jan 28. PubMed PMID: 18227806.

[115] - Raijmakers R, Vogelzangs J, Raats J, Panzenbeck M, Corby M, Jiang H, Thibodeau M, Haynes N, van Venrooij WJ, Pruijn GJ, Werneburg B. *Experimental autoimmune encephalomyelitis induction in peptidylarginine deiminase 2 knockout mice.* J Comp Neurol. 2006; 498(2):217-26. PubMed PMID: 16856138.

[116] - Moscarello MA, Lei H, Mastronardi FG, Winer S, Tsui H, Li Z, Ackerley C, Zhang L, Raijmakers R, Wood DD. *Inhibition of peptidyl-arginine deiminases reverses protein-hypercitrullination and disease in mouse models of multiple sclerosis*. Dis Model Mech. 2013; 6(2):467-78. doi: 10.1242/dmm.010520. Epub 2012 Nov 1. PubMed PMID: 23118341

[117] - McElwee JL, Mohanan S, Horibata S, Sams KL, Anguish LJ, McLean D, Cvitaš I, Wakshlag JJ, Coonrod SA. *PAD2 overexpression in transgenic mice promotes spontaneous skin neoplasia*. Cancer Res. 2014; 74(21):6306-17. doi: 10.1158/0008-5472.CAN-14-0749. Epub 2014 Sep 11. PubMed PMID: 25213324

[118] - Cherrington BD, Zhang X, McElwee JL, Morency E, Anguish LJ, Coonrod SA. *Potential role for PAD2 in gene regulation in breast cancer cells*. PLoS One. 2012;7(7):e41242. doi: 10.1371/journal.pone.0041242. Epub 2012 Jul 24. PubMed PMID: 22911765

[119] - Nachat R, Méchin MC, Charveron M, Serre G, Constans J, Simon M. *Peptidylarginine deiminase isoforms are differentially expressed in the anagen hair follicles and other human skin appendages*. J Invest Dermatol. 2005; 125(1):34-41. PubMed PMID: 15982300

[120] - Li G, Hayward IN, Jenkins BR, Rothfuss HM, Young CH, Nevalainen MT, Muth A, Thompson PR, Navratil AM, Cherrington BD. *Peptidylarginine Deiminase 3 (PAD3) Is Upregulated by Prolactin Stimulation of CID-9 Cells and Expressed in the Lactating Mouse Mammary Gland*. PLoS One. 2016; 11(1):e0147503. doi: 10.1371/journal.pone.0147503. eCollection 2016. PubMed PMID: 26799659

[121] - Keilhoff G, Prell T, Langnaese K, Mawrin C, Simon M, Fansa H, Nicholas AP. *Expression pattern of peptidylarginine deiminase in rat and human Schwann cells.* Dev Neurobiol. 2008; 68(1):101-14. PubMed PMID: 17948239

[122] - Senshu T, Akiyama K, Kan S, Asaga H, Ishigami A, Manabe M. *Detection of deiminated proteins in rat skin: probing with a monospecific antibody after modification of citrulline residues*. J Invest Dermatol. 1995; 105(2):163-9. PubMed PMID: 7543546

[123] - U KP, Subramanian V, Nicholas AP, Thompson PR, Ferretti P. *Modulation of calcium-induced cell death in human neural stem cells by the novel peptidylarginine deiminase-AIF pathway*. Biochim Biophys Acta. 2014; 1843(6):1162-71. doi: 10.1016/j.bbamcr.2014.02.018. Epub 2014 Mar 5. PubMed PMID: 24607566

[124] - Stephan A, Fabri M. *The NET, the trap and the pathogen: neutrophil extracellular traps in cutaneous immunity*. Exp Dermatol. 2015; 24(3):161-6. doi: 10.1111/exd.12599. PubMed PMID: 25421224.

[125] - Li P, Li M, Lindberg MR, Kennett MJ, Xiong N, Wang Y. *PAD4 is essential for antibacterial innate immunity mediated by neutrophil extracellular traps.* J Exp Med. 2010; 207(9):1853-62. doi: 10.1084/jem.20100239. Epub 2010 Aug 23. PubMed PMID: 20733033

[126] - Hemmers S, Teijaro JR, Arandjelovic S, Mowen KA. *PAD4-mediated neutrophil extracellular trap formation is not required for immunity against influenza infection*. PLoS One. 2011; 6(7):e22043. doi: 10.1371/journal.pone.0022043. Epub 2011 Jul 11. PubMed PMID: 21779371

[127] - Nakashima K, Arai S, Suzuki A, Nariai Y, Urano T, Nakayama M, Ohara O, Yamamura K, Yamamoto K, Miyazaki T. *PAD4 regulates proliferation of multipotent haematopoietic cells by controlling c-myc expression.* Nat Commun. 2013; 4:1836. doi: 10.1038/ncomms2862. PubMed PMID: 23673621

[128] - Baka Z, Barta P, Losonczy G, Krenács T, Pápay J, Szarka E, Sármay G, Babos F, Magyar A, Géher P, Buzás EI, Nagy G. *Specific expression of PAD4 and citrullinated proteins in lung cancer is not associated with anti-CCP antibody production*. Int Immunol. 2011; 23(6):405-14. doi: 10.1093/intimm/dxr026. Epub 2011 May 19. PubMed PMID: 21602177

[129] - Chang X, Han J. *Expression of peptidylarginine deiminase type 4 (PAD4) in various tumors*. Mol Carcinog. 2006; 45(3):183-96. PubMed PMID: 16355400

[130] - Li P, Yao H, Zhang Z, Li M, Luo Y, Thompson PR, Gilmour DS, Wang Y. *Regulation of p53 target gene expression by peptidylarginine deiminase 4.* Mol Cell Biol. 2008; 28(15):4745-58. doi: 10.1128/MCB.01747-07. Epub 2008 May 27. PubMed PMID: 18505818

[131] - Zhang J, Dai J, Zhao E, Lin Y, Zeng L, Chen J, Zheng H, Wang Y, Li X, Ying K, Xie Y, Mao Y. *cDNA cloning, gene organization and expression analysis of human peptidylarginine deiminase type VI.* Acta Biochim Pol. 2004; 51(4):1051-8. PubMed PMID: 15625577

[132] - Esposito G, Vitale AM, Leijten FP, Strik AM, Koonen-Reemst AM, Yurttas P, Robben TJ, Coonrod S, Gossen JA. *Peptidylarginine deiminase (PAD) 6 is essential for oocyte cytoskeletal sheet formation and female fertility*. Mol Cell Endocrinol. 2007; 273(1-2):25-31. Epub 2007 May 17. PubMed PMID: 17587491

[133] - Wright PW, Bolling LC, Calvert ME, Sarmento OF, Berkeley EV, Shea MC, Hao Z, Jayes FC, Bush LA, Shetty J, Shore AN, Reddi PP, Tung KS, Samy E, Allietta MM, Sherman NE, Herr JC, Coonrod SA. *ePAD, an oocyte and early embryo-abundant peptidylarginine deiminase-like protein that localizes to egg cytoplasmic sheets.* Dev Biol. 2003; 256(1):73-88. PubMed PMID: 12654293

[134] - Nicholas AP. *Dual immunofluorescence study of citrullinated proteins in Parkinson diseased substantia nigra*. Neurosci Lett. 2013; 545:107-111. doi: 10.1016/j.neulet.2013.04.028. PubMed PMID: 134

[135] - Jin Z, Fu Z, Yang J, Troncosco J, Everett AD, Van Eyk JE. *Identification and characterization of citrulline-modified brain proteins by combining HCD and CID fragmentation*. Proteomics. 2013; 13(17):2682-91. doi: 10.1002/pmic.201300064. Epub 2013 Aug 7. PubMed PMID: 23828821

[136] - Kuna AT. *Mutated citrullinated vimentin antibodies in rheumatoid arthritis*. Clin Chim Acta. 2012; 413(1-2):66-73. doi: 10.1016/j.cca.2011.10.020. Epub 2011 Oct 19. Review. PubMed PMID: 22037509

[137] - Senshu T, Kan S, Ogawa H, Manabe M, Asaga H. *Preferential deimination of keratin K1 and filaggrin during the terminal differentiation of human epidermis*. Biochem Biophys Res Commun. 1996; 225(3):712-9. PubMed PMID: 8780679

[138] - Wood DD, Moscarello MA. *The isolation, characterization, and lipid-aggregating properties of a citrulline containing myelin basic protein*. J Biol Chem. 1989; 264(9):5121-7. PubMed PMID: 2466844

[139] - Zhao X, Okeke NL, Sharpe O, Batliwalla FM, Lee AT, Ho PP, Tomooka BH, Gregersen PK, Robinson WH. *Circulating immune complexes contain citrullinated fibrinogen in rheumatoid arthritis*. Arthritis Res Ther. 2008; 10(4):R94. doi: 10.1186/ar2478. Epub 2008 Aug 18. PubMed PMID: 18710572

[140] - Loos T, Mortier A, Gouwy M, Ronsse I, Put W, Lenaerts JP, Van Damme J, Proost P. *Citrullination of CXCL10 and CXCL11 by peptidylarginine deiminase: a naturally occurring posttranslational modification of chemokines and new dimension of immunoregulation*. Blood. 2008; 112(7):2648-56. doi: 10.1182/blood-2008-04-149039. Epub 2008 Jul 21. PubMed PMID: 18645041

[141] - Proost P, Loos T, Mortier A, Schutyser E, Gouwy M, Noppen S, Dillen C, Ronsse I, Conings R, Struyf S, Opdenakker G, Maudgal PC, Van Damme J. *Citrullination of CXCL8 by peptidylarginine deiminase alters receptor usage, prevents proteolysis, and dampens tissue inflammation*. J Exp Med. 2008; 205(9):2085-97. doi: 10.1084/jem.20080305. Epub 2008 Aug 18. PubMed PMID: 18710930

[142] – Lee YH, Coonrod SA, Kraus WL, Jelinek MA, Stallcup MR. *Regulation of coactivator complex assembly and function by protein arginine methylation and demethylimination.* Proc Natl Acad Sci U S A. 2005; 102(10):3611-6. Epub 2005 Feb 24. PubMed PMID: 15731352

[143] - Acharya NK, Nagele EP, Han M, Coretti NJ, DeMarshall C, Kosciuk MC, Boulos PA, Nagele RG. *Neuronal PAD4 expression and protein citrullination: possible role in production of autoantibodies associated with neurodegenerative disease.* J Autoimmun. 2012; 38(4):369-80. doi: 10.1016/j.jaut.2012.03.004. Epub 2012 May 2. PubMed PMID: 22560840

[144] - Jang B, Kim E, Choi JK, Jin JK, Kim JI, Ishigami A, Maruyama N, Carp RI, Kim YS, Choi EK. *Accumulation of citrullinated proteins by up-regulated peptidylarginine deiminase 2 in brains of scrapie-infected mice: a possible role in pathogenesis*. Am J Pathol. 2008; 173(4):1129-42. doi: 10.2353/ajpath.2008.080388. Epub 2008 Sep 11. PubMed PMID: 18787103

[145] - Jang B, Jin JK, Jeon YC, Cho HJ, Ishigami A, Choi KC, Carp RI, Maruyama N, Kim YS, Choi EK. *Involvement of peptidylarginine deiminase-mediated post-translational citrullination in pathogenesis of sporadic Creutzfeldt-Jakob disease*. Acta Neuropathol. 2010; 119(2):199-210. doi: 10.1007/s00401- 009-0625-x. Epub 2009 Dec 16. PubMed PMID: 20013286

[146] - Moscarello MA, Mastronardi FG, Wood DD. *The role of citrullinated proteins suggests a novel mechanism in the pathogenesis of multiple sclerosis*. Neurochem Res. 2007; 32(2):251-6. Epub 2006 Sep 22. Review. PubMed PMID: 17031564

[147] - Grin B, Mahammad S, Wedig T, Cleland MM, Tsai L, Herrmann H, Goldman RD.

Withaferin a alters intermediate filament organization, cell shape and behavior. PLoS One. 2012; 7(6):e39065. doi: 10.1371/journal.pone.0039065. PubMed PMID: 22720028

[148] - Parry DA, Strelkov SV, Burkhard P, Aebi U, Herrmann H. *Towards a molecular description of intermediate filament structure and assembly*. Exp Cell Res. 2007; 313(10):2204-16. Epub 2007 Apr 12. Review. PubMed PMID: 17521629.

[149] - Jayaprakasam B, Zhang Y, Seeram NP, Nair MG. *Growth inhibition of human tumor cell lines by withanolides from Withania somnifera leaves*. Life Sci. 2003; 74(1):125-32. PubMed PMID: 14575818.

[150] - Sharada AC, Solomon FE, Devi PU, Udupa N, Srinivasan KK. *Antitumor and radiosensitizing effects of withaferin A on mouse Ehrlich ascites carcinoma in vivo*. Acta Oncol. 1996; 35(1):95-100. PubMed PMID: 8619948.

[151] - Mohan R, Hammers HJ, Bargagna-Mohan P, Zhan XH, Herbstritt CJ, Ruiz A, Zhang L, Hanson AD, Conner BP, Rougas J, Pribluda VS. *Withaferin A is a potent inhibitor of angiogenesis*. Angiogenesis. 2004; 7(2):115-22. PubMed PMID: 15516832

[152] - Agapova OA, Kaufman PL, Hernandez MR. *Androgen receptor and NFkB expression in human normal and glaucomatous optic nerve head astrocytes in vitro and in experimental glaucoma*. Exp Eye Res. 2006; 82(6):1053-9. PubMed PMID: 16310187.

[153] - Mohan R, Bargagna-Mohan P. *The Use of Withaferin A to Study Intermediate Filaments*. Methods Enzymol. 2016; 568:187-218. doi: 10.1016/bs.mie.2015.09.025. Epub 2015 Nov 3. PubMed PMID: 26795472

[154] - Hensen SM, Pruijn GJ. *Methods for the detection of peptidylarginine deiminase (PAD) activity and protein citrullination*. Mol Cell Proteomics. 2014; 13(2):388-96. doi: 10.1074/mcp.R113.033746. PubMed PMID: 24298040

[155] - Nicholas AP, Whitaker JN. *Preparation of a monoclonal antibody to citrullinated epitopes: its characterization and some applications to immunohistochemistry in human brain*. Glia. 2002; 37(4): 328-36. PubMed PMID: 11870872.

[156] - Sambandam T, Belousova M, Accaviti-Loper MA, Blanquicett C, Guercello V, Raijmakers R, Nicholas AP. *Increased peptidylarginine deiminase type II in hypoxic astrocytes*. Biochem Biophys Res Commun. 2004; 325(4):1324-9. PubMed PMID: 15555572

[157] - Kholia S, Jorfi S, Thompson PR, Causey CP, Nicholas AP, Inal JM, Lange S. *A novel role for peptidylarginine deiminases in microvesicle release reveals therapeutic potential of PAD inhibition in sensitizing prostate cancer cells to chemotherapy*. J Extracell Vesicles. 2015; 4:26192. doi:10.3402/jev.v4.26192. PubMed PMID: 26095379

[158] - Pritzker LB, Moscarello MA. *A novel microtubule independent effect of paclitaxel: the inhibition of peptidylarginine deiminase from bovine brain*. Biochim Biophys Acta. 1998; 1388(1):154-60. PubMed PMID: 9774721

[159] - Cao L, Sun D, Cruz T, Moscarello MA, Ludwin SK, Whitaker JN. *Inhibition of experimental allergic encephalomyelitis in the Lewis rat by paclitaxel.* J Neuroimmunol. 2000; 108(1-2):103-11. PubMed PMID: 10900343

[160] - Stone EM, Schaller TH, Bianchi H, Person MD, Fast W. *Inactivation of two diverse enzymes in the amidinotransferase superfamily by 2-chloroacetamidine: dimethylargininase and peptidylarginine deiminase.* Biochemistry. 2005; 44(42):13744-52. PubMed PMID: 16229464

[161] - Luo Y, Arita K, Bhatia M, Knuckley B, Lee YH, Stallcup MR, Sato M, Thompson PR. *Inhibitors and inactivators of protein arginine deiminase 4: functional and structural characterization.* Biochemistry. 2006; 45(39):11727-36. PubMed PMID: 17002273

[162] - Chumanevich AA, Causey CP, Knuckley BA, Jones JE, Poudyal D, Chumanevich AP, Davis T, Matesic LE, Thompson PR, Hofseth LJ. *Suppression of colitis in mice by Cl-amidine: a novel peptidylarginine deiminase inhibitor*. Am J Physiol Gastrointest Liver Physiol. 2011; 300(6):G929-38. doi: 10.1152/ajpgi.00435.2010. Epub 2011 Mar 17. PubMed PMID: 21415415

[163] - Lange S, Rocha-Ferreira E, Thei L, Mawjee P, Bennett K, Thompson PR, Subramanian V, Nicholas AP, Peebles D, Hristova M, Raivich G. *Peptidylarginine deiminases: novel drug targets for prevention of neuronal damage following hypoxic ischemic insult (HI) in neonates*. J Neurochem. 2014; 130(4):555-62. doi: 10.1111/jnc.12744. Epub 2014 May 24. PubMed PMID: 24762056

[164] - Cui X, Witalison EE, Chumanevich AP, Chumanevich AA, Poudyal D, Subramanian V, Schetter AJ, Harris CC, Thompson PR, Hofseth LJ. *The induction of microRNA-16 in colon cancer cells by protein arginine deiminase inhibition causes a p53-dependent cell cycle arrest*. PLoS One. 2013;8(1):e53791. doi: 10.1371/journal.pone.0053791. Epub 2013 Jan 7. PubMed PMID: 23308284

[165] - Slack JL, Causey CP, Thompson PR. *Protein arginine deiminase 4: a target for an epigenetic cancer therapy*. Cell Mol Life Sci. 2011; 68(4):709-20. doi: 10.1007/s00018-010-0480-x. Epub 2010 Aug 13. PubMed PMID: 20706768

[166] - McElwee JL, Mohanan S, Griffith OL, Breuer HC, Anguish LJ, Cherrington BD, Palmer AM, Howe LR, Subramanian V, Causey CP, Thompson PR, Gray JW, Coonrod SA. *Identification of PADI2 as a potential breast cancer biomarker and therapeutic target.* BMC Cancer. 2012; 12:500. doi: 10.1186/1471-2407-12-500. PubMed PMID: 23110523

[167] - Knuckley B, Causey CP, Jones JE, Bhatia M, Dreyton CJ, Osborne TC, Takahara H, Thompson PR. *Substrate specificity and kinetic studies of PADs 1, 3, and 4 identify potent and selective inhibitors of protein arginine deiminase 3*. Biochemistry. 2010; 49(23):4852-63. doi: 10.1021/bi100363t. PubMed PMID: 20469888

[168] - Knuckley B, Jones JE, Bachovchin DA, Slack J, Causey CP, Brown SJ, Rosen H, Cravatt BF, Thompson PR. *A fluopol-ABPP HTS assay to identify PAD inhibitors*. Chem Commun (Camb). 2010; 46(38):7175-7. doi: 10.1039/c0cc02634d. Epub 2010 Aug 25. PubMed PMID: 20740228

[169] - Dreyton CJ, Anderson ED, Subramanian V, Boger DL, Thompson PR. *Insights into the mechanism of streptonigrin-induced protein arginine deiminase inactivation*. Bioorg Med Chem. 2014; 22(4):1362-9. doi: 10.1016/j.bmc.2013.12.064. PubMed PMID: 24440480

[170] - Bolzán AD, Bianchi MS. *Genotoxicity of streptonigrin: a review*. Mutat Res. 2001; 488(1):25-37. Review. PubMed PMID: 11223403

[171] - Pekny M, Pekna M. *Astrocyte reactivity and reactive astrogliosis: costs and benefits*. Physiol Rev. 2014; 94(4):1077-98. doi: 10.1152/physrev.00041.2013. Review. PubMed PMID: 25287860.

[172] - Sofroniew MV. *Molecular dissection of reactive astrogliosis and glial scar formation*. Trends Neurosci. 2009; 32(12):638-47. doi: 10.1016/j.tins.2009.08.002. Epub 2009 Sep 24. Review. PubMed PMID: 19782411

[173] - Petrukhin K. *New therapeutic targets in atrophic age-related macular degeneration*. Expert Opin Ther Targets. 2007 May;11(5):625-39. Review. PubMed PMID: 17465722.

[174] - Wu KH, Madigan MC, Billson FA, Penfold PL. *Differential expression of GFAP in early v late AMD: a quantitative analysis*. Br J Ophthalmol. 2003; 87(9):1159-66. PubMed PMID: 12928288;

[175] - Joshi M, Agrawal S, Christoforidis JB. *Inflammatory mechanisms of idiopathic epiretinal membrane formation.* Mediators Inflamm. 2013;2013:192582. doi: 10.1155/2013/192582. Epub 2013 Nov 11. Review. PubMed PMID: 24324293;

[176] - Lewis GP, Fisher SK. *Müller cell outgrowth after retinal detachment: association with cone photoreceptors.* Invest Ophthalmol Vis Sci. 2000; 41(6):1542-5. PubMed PMID: 10798674.

[177] - Gandorfer A, Haritoglou C, Scheler R, Schumann R, Zhao F, Kampik A. *Residual cellular proliferation on the internal limiting membrane in macular pucker surgery*. Retina. 2012; 32(3):477-85. doi: 10.1097/IAE.0b013e3182246e2a. PubMed PMID: 22068175.

[178] - Pekny M, Johansson CB, Eliasson C, Stakeberg J, Wallén A, Perlmann T, Lendahl U, Betsholtz C, Berthold CH, Frisén J. *Abnormal reaction to central nervous system injury in mice lacking glial fibrillary acidic protein and vimentin*. J Cell Biol. 1999; 145(3):503-14. PubMed PMID: 10225952

[179] - Ralton JE, Lu X, Hutcheson AM, Quinlan RA. *Identification of two N-terminal non-alpha-helical domain motifs important in the assembly of glial fibrillary acidic protein*. J Cell Sci. 1994; 107 (Pt 7):1935-48. PubMed PMID: 7983160.

[180] - Inagaki M, Nishi Y, Nishizawa K, Matsuyama M, Sato C. *Site-specific phosphorylation induces disassembly of vimentin filaments in vitro*. Nature. 1987; 328(6131):649-52. PubMed PMID: 3039376.

[181] - Korolainen MA, Auriola S, Nyman TA, Alafuzoff I, Pirttilä T. *Proteomic analysis of glial fibrillary acidic protein in Alzheimer's disease and aging brain*. Neurobiol Dis. 2005; 20(3):858-70. Epub 2005 Jun 27. PubMed PMID: 15979880.

[182] - Nicholas AP, King JL, Sambandam T, Echols JD, Gupta KB, McInnis C, Whitaker JN. *Immunohistochemical localization of citrullinated proteins in adult rat brain*. J Comp Neurol. 2003; 459(3):251-66. PubMed PMID: 12655508.

[183] - Algeciras ME, Takahara H, Bhattacharya SK. *Mechanical stretching elevates peptidyl arginine deiminase 2 expression in astrocytes*. Curr Eye Res. 2008; 33(11):994-1001. doi: 10.1080/02713680802447113. PubMed PMID: 19085382

[184] - Powell C, Grant AR, Cornblath E, Goldman D. *Analysis of DNA methylation reveals a partial reprogramming of the Müller glia genome during retina regeneration*. Proc Natl Acad Sci U S A. 2013; 110(49):19814-9. doi: 10.1073/pnas.1312009110. Epub 2013 Nov 18. PubMed PMID: 24248357

[185] - Galan A, Dergham P, Escoll P, de-la-Hera A, D'Onofrio PM, Magharious MM, Koeberle PD, Frade JM, Saragovi HU. *Neuronal injury external to the retina rapidly activates retinal glia, followed by elevation of markers for cell cycle re-entry and death in retinal ganglion cells*. PLoS One. 2014; 9(7):e101349. doi: 10.1371/journal.pone.0101349. eCollection 2014. PubMed PMID: 24983470

[186] - Tackenberg MA, Tucker BA, Swift JS, Jiang C, Redenti S, Greenberg KP, Flannery JG, Reichenbach A, Young MJ. *Müller cell activation, proliferation and migration following laser injury*. Mol Vis. 2009; 15:1886-96. PubMed PMID: 19768129

[187] - Lange S, Gögel S, Leung KY, Vernay B, Nicholas AP, Causey CP, Thompson PR, Greene ND, Ferretti P. *Protein deiminases: new players in the developmentally regulated loss of neural regenerative ability*. Dev Biol. 2011; 355(2):205-14. doi: 10.1016/j.ydbio.2011.04.015. Epub 2011 Apr 22. PubMed PMID: 21539830

[188] - Traub P, Vorgias CE. *Differential effect of arginine modification with 1,2-cyclohexanedione on the capacity of vimentin and desmin to assemble into intermediate filaments and to bind to nucleic acids*. J Cell Sci. 1984; 65:1-20. PubMed PMID: 6325477.

[189] - Miyazaki K, Okada Y, Yamanaka O, Kitano A, Ikeda K, Kon S, Uede T, Rittling SR, Denhardt DT, Kao WW, Saika S. *Corneal wound healing in an osteopontin-deficient mouse*. Invest Ophthalmol Vis Sci. 2008; 49(4):1367-75. doi: 10.1167/iovs.07-1007. PubMed PMID: 18385052.

[190] - Tuft SJ, Shortt AJ. *Surgical rehabilitation following severe ocular burns*. Eye (Lond). 2009; 23(10):1966-71. doi: 10.1038/eye.2008.414. Epub 2009 Jan 23. PubMed PMID: 19169226.

[191] - Luna G, Lewis GP, Banna CD, Skalli O, Fisher SK. *Expression profiles of nestin and synemin in reactive astrocytes and Müller cells following retinal injury: a comparison with glial fibrillary acidic protein and vimentin*. Mol Vis. 2010; 16:2511-23. PubMed PMID: 21139996

[192] - Cade F, Paschalis EI, Regatieri CV, Vavvas DG, Dana R, Dohlman CH. *Alkali burn to the eye: protection using TNF-α inhibition*. Cornea. 2014; 33(4):382-9. doi: 10.1097/ICO.0000000000000071. PubMed PMID: 24488127.

[193] - Herskowitz JH, Seyfried NT, Duong DM, Xia Q, Rees HD, Gearing M, Peng J, Lah JJ, Levey AI. *Phosphoproteomic analysis reveals site-specific changes in GFAP and NDRG2 phosphorylation in frontotemporal lobar degeneration*. J Proteome Res. 2010; 9(12):6368-79. doi: 10.1021/pr100666c. Epub 2010 Oct 22. PubMed PMID: 20886841

[194] - Puro DG. *Stretch-activated channels in human retinal Muller cells*. Glia. 1991; 4(5):456-60. PubMed PMID: 1718863.

[195] - Liu B, Hunter DJ, Rooker S, Chan A, Paulus YM, Leucht P, Nusse Y, Nomoto H, Helms JA. Wnt signaling promotes Müller cell proliferation and survival after injury. Invest Ophthalmol Vis Sci. 2013 Jan 17;54(1):444-53. doi: 10.1167/iovs.12-10774. PubMed PMID: 23154457.

[196] - Giani A, Thanos A, Roh MI, Connolly E, Trichonas G, Kim I, Gragoudas E, Vavvas D, Miller JW. *In vivo evaluation of laser-induced choroidal neovascularization using spectral-domain optical coherence tomography.* Invest Ophthalmol Vis Sci. 2011; 52(6):3880-7. doi: 10.1167/iovs.10-6266. PubMed PMID: 21296820.

[197] - Bhattacharya SK, Bhat MB, Takahara H. *Modulation of peptidyl arginine deiminase 2 and implication for neurodegeneration*. Curr Eye Res. 2006; 31(12):1063-71. PubMed PMID: 17169845.

[198] - Chirivi RGS, Jenniskens GJ, Raats JMH. *Anti-Citrullinated protein antibodies as novel therapeutic drugs in Rheumatoid Arthritis.* J Clin Cell Immunol 2013; S6 doi: 10.4172/2155-9899.S6-006

[199] - Pekny M, Nilsson M. *Astrocyte activation and reactive gliosis*. Glia. 2005; 50(4):427-34. Review. PubMed PMID: 15846805.

[200] - Sofroniew MV. *Reactive astrocytes in neural repair and protection*. Neuroscientist. 2005; 11(5):400-7. Review. PubMed PMID: 16151042.

[201] - Hippert C, Graca AB, Barber AC, West EL, Smith AJ, Ali RR, Pearson RA. *Müller glia activation in response to inherited retinal degeneration is highly varied and disease-specific.* PLoS One. 2015; 10(3):e0120415. doi: 10.1371/journal.pone.0120415. eCollection 2015. PubMed PMID: 25793273.

[202] - Bringmann A, Iandiev I, Pannicke T, Wurm A, Hollborn M, Wiedemann P, Osborne NN, Reichenbach A. *Cellular signaling and factors involved in Müller cell gliosis: neuroprotective and detrimental effects*. Prog Retin Eye Res. 2009; 28(6):423-51. doi: 10.1016/j.preteyeres.2009.07.001. Epub 2009 Aug 4. Review. PubMed PMID: 19660572.

[203] - Mastronardi FG, Wood DD, Mei J, Raijmakers R, Tseveleki V, Dosch HM, Probert L, Casaccia-Bonnefil P, Moscarello MA. *Increased citrullination of histone H3 in multiple sclerosis brain and animal models of demyelination: a role for tumor necrosis factor-induced peptidylarginine deiminase 4 translocation.* J Neurosci. 2006; 26(44):11387-96. PubMed PMID: 17079667.

[204] - Andrade F, Darrah E, Gucek M, Cole RN, Rosen A, Zhu X. *Autocitrullination of human peptidyl arginine deiminase type 4 regulates protein citrullination during cell activation*. Arthritis Rheum. 2010; 62(6):1630-40. doi: 10.1002/art.27439. PubMed PMID: 20201080.

[205] - Molnár T, Yarishkin O, Iuso A, Barabas P, Jones B, Marc RE, Phuong TT, Križaj D. *Store-Operated Calcium Entry in Müller Glia Is Controlled by Synergistic Activation of TRPC and Orai Channels.* J Neurosci. 2016; 36(11):3184-98. doi: 10.1523/JNEUROSCI.4069-15.2016. PubMed PMID: 26985029

[206] - Keirstead SA, Miller RF. *Calcium waves in dissociated retinal glial (Müller) cells are evoked by release of calcium from intracellular stores.* Glia. 1995; 14(1):14-22. PubMed PMID: 7615342.

[207] - Lindqvist N, Liu Q, Zajadacz J, Franze K, Reichenbach A. *Retinal glial (Müller) cells: sensing and responding to tissue stretch.* Invest Ophthalmol Vis Sci. 2010; 51(3):1683-90. doi: 10.1167/iovs.09-4159. Epub 2009 Nov 5. PubMed PMID: 19892866.

[208] - Ceelen PW, Lockridge A, Newman EA. *Electrical coupling between glial cells in the rat retina*. Glia. 2001 Jul;35(1):1-13. PubMed PMID: 11424187

[209] - Zahs KR, Newman EA. *Asymmetric gap junctional coupling between glial cells in the rat retina*. Glia. 1997; 20(1):10-22. PubMed PMID: 9145301.

[210] - Newman EA. *Propagation of intercellular calcium waves in retinal astrocytes and Müller cells*. J Neurosci. 2001; 21(7):2215-23. PubMed PMID: 11264297

[211] - Lewis HD, Liddle J, Coote JE, Atkinson SJ, Barker MD, Bax BD, Bicker KL, Bingham RP, Campbell M, Chen YH, Chung CW, Craggs PD, Davis RP, Eberhard D, Joberty G, Lind KE, Locke K, Maller C, Martinod K, Patten C, Polyakova O, Rise CE, Rüdiger M, Sheppard RJ, Slade DJ, Thomas P, Thorpe J, Yao G, Drewes G, Wagner DD, Thompson PR, Prinjha RK, Wilson DM. *Inhibition of PAD4 activity is sufficient to disrupt mouse and human NET formation*. Nat Chem Biol. 2015; 11(3):189-91. doi: 10.1038/nchembio.1735. Epub 2015 Jan 26. PubMed PMID: 25622091

[212] - Nakashima K, Hagiwara T, Yamada M. *Nuclear localization of peptidylarginine deiminase V and histone deimination in granulocytes*. J Biol Chem. 2002; 277(51):49562-8. Epub 2002 Oct 18. PubMed PMID: 12393868.

[213] - Highman VN. *Early rise in intraocular pressure after ammonia burns*. Br Med J. 1969; 1(5640):359-60. PubMed PMID: 5762840

[214] - Cohen LP, Pasquale LR. *Clinical characteristics and current treatment of glaucoma.* Cold Spring Harb Perspect Med. 2014; 4(6). pii: a017236. doi: 10.1101/cshperspect.a017236. Review. PubMed PMID: 24890835;

[215] - Gordon IO, Agrawal N, Goldblum JR, Fiocchi C, Rieder F. *Fibrosis in ulcerative colitis: mechanisms, features, and consequences of a neglected problem*. Inflamm Bowel Dis. 2014; 20(11):2198-206. doi: 10.1097/MIB.0000000000000080. Review. PubMed PMID: 24892966.

[216] - Falke LL, Gholizadeh S, Goldschmeding R, Kok RJ, Nguyen TQ. *Diverse origins of the myofibroblast—implications for kidney fibrosis.* Nat Rev Nephrol. 2015; 11(4):233-44. doi: 10.1038/nrneph.2014.246. Epub 2015 Jan 13. Review. PubMed PMID: 25584804.

[217] - Lovicu FJ, Shin EH, McAvoy JW. *Fibrosis in the lens. Sprouty regulation of TGFβ-signaling prevents lens EMT leading to cataract.* Exp Eye Res. 2016 Jan;142:92-101. doi: 10.1016/j.exer.2015.02.004. Epub 2015 May 21. Review. PubMed PMID: 26003864

[218] - Brehar FM, Arsene D, Brinduse LA, Gorgan MR. *Immunohistochemical analysis of GFAP-δ and nestin in cerebral astrocytomas.* Brain Tumor Pathol. 2015; 32(2):90-8. doi: 10.1007/s10014-014-0199-8. Epub 2014 Sep 2. PubMed PMID: 25178519.

[219] - Guérin CJ, Hu L, Scicli G, Scicli AG. *Transforming growth factor beta in experimentally detached retina and periretinal membranes.* Exp Eye Res. 2001; 73(6):753-64. PubMed PMID: 11846507.

[220] - Close JL, Gumuscu B, Reh TA. *Retinal neurons regulate proliferation of postnatal progenitors and Müller glia in the rat retina via TGF beta signaling*. Development. 2005; 132(13):3015-26. PubMed PMID: 15944186.

[221] - Vossenaar ER, Després N, Lapointe E, van der Heijden A, Lora M, Senshu T, van Venrooij WJ, Ménard HA. *Rheumatoid arthritis specific anti-Sa antibodies target citrullinated vimentin*. Arthritis Res Ther. 2004; 6(2):R142-50. Epub 2004 Feb 5. PubMed PMID: 15059278;

[222] - Yoshida T, Nakagawa M. *Clinical aspects and pathology of Alexander disease, and morphological and functional alteration of astrocytes induced by GFAP mutation.* Neuropathology. 2012;

32(4):440-6. doi: 10.1111/j.1440-1789.2011.01268.x. Epub 2011 Nov 28. Review. PubMed PMID: 22118268.

[223] - Rogers RS, Dharsee M, Ackloo S, Sivak JM, Flanagan JG. *Proteomics analyses of human optic nerve head astrocytes following biomechanical strain*. Mol Cell Proteomics. 2012; 11(2):M111.012302. doi: 10.1074/mcp.M111.012302. Epub 2011 Nov 29. PubMed PMID: 22126795

[224] - Mohamed BM, Verma NK, Davies AM, McGowan A, Crosbie-Staunton K, Prina-Mello A, Kelleher D, Botting CH, Causey CP, Thompson PR, Pruijn GJ, Kisin ER, Tkach AV, Shvedova AA, Volkov Y. *Citrullination of proteins: a common post-translational modification pathway induced by different nanoparticles in vitro and in vivo*. Nanomedicine (Lond). 2012; 7(8):1181-95. doi: 10.2217/nnm.11.177. Epub 2012 May 25. PubMed PMID: 22625207;

[225] - Cho W, Messing A. *Properties of astrocytes cultured from GFAP over-expressing and GFAP mutant mice*. Exp Cell Res. 2009; 315(7):1260-72. doi: 10.1016/j.yexcr.2008.12.012. Epub 2008 Dec 29. PubMed PMID: 19146851

[226] - Löffler K, Schäfer P, Völkner M, Holdt T, Karl MO. *Age-dependent Müller glia neurogenic competence in the mouse retina.* Glia. 2015; 63(10):1809-24. doi: 10.1002/glia.22846. Epub 2015 May 6. PubMed PMID: 25943952.

[227] - Ramachandran R, Fausett BV, Goldman D. *Ascl1a regulates Müller glia dedifferentiation and retinal regeneration through a Lin-28-dependent, let-7 microRNA signalling pathway*. Nat Cell Biol. 2010; 12(11):1101-7. doi: 10.1038/ncb2115. Epub 2010 Oct 10. Erratum in: Nat Cell Biol. 2015 Apr;17(4):532. PubMed PMID: 20935637;

[228] - Schneider M, Fuchshofer R. *The role of astrocytes in optic nerve head fibrosis in glaucoma*. Exp Eye Res. 2016; 142:49-55. doi: 10.1016/j.exer.2015.08.014. Epub 2015 Aug 29. Review. PubMed PMID: 26321510.

[229] 17074320 - Reichstein D, Ren L, Filippopoulos T, Mittag T, Danias J. *Apoptotic retinal ganglion cell death in the DBA/2 mouse model of glaucoma.* Exp Eye Res. 2007; 84(1):13-21. Epub 2006 Oct 30. PubMed PMID: 17074320.